US Army Corps of Engineers

(2)

TECHNICAL REPORT HL-91-11

MORNING GLORY INLET AND MANIFOLD OUTLET STRUCTURE, McCOOK RESERVOIR CHICAGO, ILLINOIS

Hydraulic Model Investigation

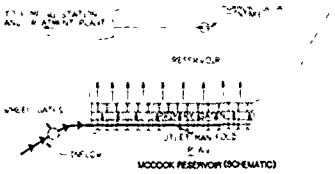

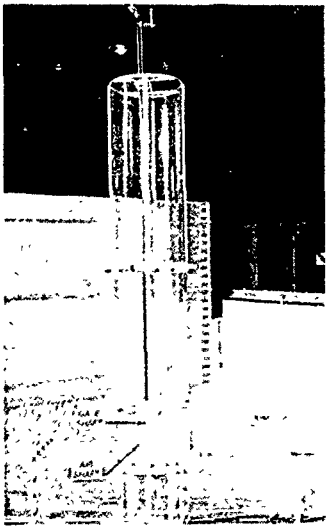

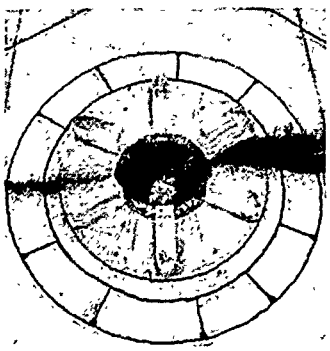

by

Bobby P. Fletcher

Hydraulics Laboratory

DEPARTMENT OF THE ARMY
Waterways Experiment Station, Corps of Engineers
3909 Halls Ferry Road, Vicksburg, Mississippi 39180-6199

June 1991
Final Report

HYDRAULICS LABORATORY

Prepared for US Army Engineer District, Chicago
Chicago, Illinois 60606-7206

Destroy this report when no longer needed. Do not return it to the originator.

The findings in this report are not to be construed as an official Department of the Army position unless so designated by other authorized documents.

The contents of this report are not to be used for advertising, publication, or promotional purposes. Citation of trade names does not constitute an official endorsement or approval of the use of such commercial products.

REPORT DOCUMENTATION PAGE

Form Approved
OMB No. 0704-0188

1. AGENCY USE ONLY (Leave blank)	2. REPORT DATE	3. REPORT TYPE AND DATES COVERED
	June 1991	Final Report

4. TITLE AND SUBTITLE
Morning Glory Inlet and Manifold Outlet Structure, McCook Reservoir, Chicago, Illinois; Hydraulic Model Investigation

5. FUNDING NUMBERS

6. AUTHOR(S)
Bobby P. Fletcher

7. PERFORMING ORGANIZATION NAME(S) AND ADDRESS(ES)
USAE Waterways Experiment Station, Hydraulics Laboratory, 3909 Halls Ferry Road, Vicksburg, MS 39180-6199

8. PERFORMING ORGANIZATION REPORT NUMBER
Technical Report HL-91-11

9. SPONSORING/MONITORING AGENCY NAME(S) AND ADDRESS(ES)
USAED, Chicago, 111 N. Canal Street, Chicago, IL 60606-7206

10. SPONSORING/MONITORING AGENCY REPORT NUMBER

11. SUPPLEMENTARY NOTES
Available from National Technical Information Service, 5285 Port Royal Road, Springfield, VA 22161.

12a. DISTRIBUTION/AVAILABILITY STATEMENT
Approved for public release; distribution unlimited.

12b. DISTRIBUTION CODE

13. ABSTRACT (Maximum 200 words)

A 1:20.7-scale model of the morning glory intake for the McCook Reservoir Inlet, Chicago, IL, was used to develop and investigate a design that would provide satisfactory hydraulic performance. Tests were conducted to investigate the relationship between discharge, pool elevation, hydraulic gradient, and air entrainment in the discharge conduit. Tests indicated that air entrainment occurred only when the water surface was below the bottom of the cover plate. This air entrainment could be eliminated by reducing the discharge to below 550 cfs. Pressure measurement in the structure enabled the computation of losses and indicated no tendency for cavitation for any anticipated flow condition.

A 1:40-scale model of the manifold outlet permitted evaluation and documentation of flow conditions in the wheel gate structure and manifold.

(Continued)

14. SUBJECT TERMS
Air entrainment (water) — McCook Reservoir, Chicago, IL
Hydraulic models — Flow characteristics
Manifold — Intake structures (Continued)

15. NUMBER OF PAGES
93

16. PRICE CODE

17. SECURITY CLASSIFICATION OF REPORT	18. SECURITY CLASSIFICATION OF THIS PAGE	19. SECURITY CLASSIFICATION OF ABSTRACT	20. LIMITATION OF ABSTRACT
UNCLASSIFIED	UNCLASSIFIED		

13. ABSTRACT (Continued).

Pressure measurements indicated no tendency for cavitation. Manifold loss coefficients for various discharges were obtained. The distribution of flow exiting the manifold via 45 ports and the magnitude and direction of flow in the primary basin were documented.

The models indicated that for any potential flow conditions, satisfactory hydraulic performance should be anticipated.

14. SUBJECT TERMS (Continued).

Shaft spillways
Vortex

PREFACE

The model investigations reported herein were authorized by the Headquarters, US Army Corps of Engineers (HQUSACE), on 30 March 1989 at the request of the US Army Engineer District, Chicago (NCC). The studies were conducted by personnel of the Hydraulics Laboratory (HL) of the US Army Engineer Waterways Experiment Station (WES) during the period April 1989 to April 1990 under the direction of Messrs. F. A. Herrmann, Jr., Chief, HL; and R. A. Sager, Assistant Chief, HL; and under the general supervision of Messrs. G. A. Pickering, Chief, Hydraulic Structures Division (HSD), HL; and N. R. Oswalt, Chief, Spillways and Channels Branch, HSD. Project engineer for the model studies was Mr. B. P. Fletcher, assisted by Messrs. J. R. Rucker, Jr., and E. L. Jefferson, all of HSD. The models were constructed by Mr. M. A. Simmons of the Engineering and Construction Services Division, WES. This report was prepared by Mr. Fletcher, drawings were prepared by Mr. Rucker, and the report was edited by Mrs. M. C. Gay, Information Technology Laboratory, WES.

During the investigation, Messrs. Sam Powell, HQUSACE; Scott Vowinkel, US Army Engineer Division, North-Central; John D'Aniglio, Joseph Jacobazzi, Tom Fogarty, Dave Handwerk, Stephen Garbaciak, John Morgan, and Bruce Halverson, NCC; and Dr. Anreek Paintel, Metropolitan Water Reclamation District of Greater Chicago, visited WES to discuss the program of model tests and observe the models in operation.

Commander and Director of WES during preparation of this report was COL Larry B. Fulton, EN. Technical Director was Dr. Robert W. Whalin.

CONTENTS

	Page
PREFACE	1
CONVERSION FACTORS, NON-SI TO SI (METRIC) UNITS OF MEASUREMENT	3
PART I: INTRODUCTION	4
Background	4
The Prototype	7
Purpose and Scope of the Model Studies	9
PART II: THE MODELS	11
Description	11
Scale Relations	15
PART III: TESTS AND RESULTS	17
Morning Glory Intake	17
Manifold Outlet	21
PART IV: SUMMARY AND DISCUSSION	25
TABLES 1–7	
PHOTOS 1–13	
PLATES 1–17	

CONVERSION FACTORS, NON-SI TO SI (METRIC) UNITS OF MEASUREMENT

Non-SI units of measurement used in this report can be converted to SI (metric) units as follows:

Multiply	By	To Obtain
acre-feet	1,233.489	cubic metres
cubic feet	0.02831685	cubic metres
degrees (angle)	0.01745329	radians
feet	0.3048	metres
gallons (US liquid)	0.003785412	cubic metres
inches	25.4	millimetres
miles (US statute)	1.609347	kilometres

MORNING GLORY INLET AND MANIFOLD OUTLET STRUCTURE
MCCOOK RESERVOIR, CHICAGO, ILLINOIS

Hydraulic Model Investigation

PART I: INTRODUCTION

Background

1. The first combined sewers (storm runoff and sewage) in the city of Chicago were constructed in 1834. Beginning in the early 1890's, the increase in construction of buildings, hard pavements, and sidewalks began to cause greater storm runoff than had been allowed for in the original sewer designs. This resulted in overloading the combined sewer system and flooding of basements in the 1890's.

2. Presently, the primary flooding problem in the combined sewer area is basement flooding due to sewer backup. Over 500,000 housing structures are potentially subject to basement flooding and more than 170,000 structures are flooded to varying degrees on an average annual basis. The associated average annual flood damages are estimated to be in excess of $140 million. Additional damage is caused by combined sewer overflows to the area watercourse. Figure 1 illustrates how the combined sewer system works and the flooding problem that occurs when the sewer outfalls become submerged. Figure 2 illustrates additional features of a typical combined sewer system. This type of system transports both sanitary wastewater and storm water runoff in a single pipe. Sanitary water, foundation drainage, and roof runoff from an individual house are carried by the house drain to the lateral sewer located in the street. Storm water from the streets enters the lateral sewer through a catch drain basin. Under normal dry weather conditions, the sewer flow moves from the lateral sewer through the submain and main sewers into the interceptor sewer, which conveys the flow to a waste treatment plant. When the capacity of the interceptor sewer or treatment plant is exceeded by combined sewer and storm flow, the excess runoff overflows, untreated, directly into the local watercourse (Figure 2).

3. The Tunnel and Reservoir Plan, or TARP, has been proposed to reduce the flooding and pollution problems associated with the combined sewer system.

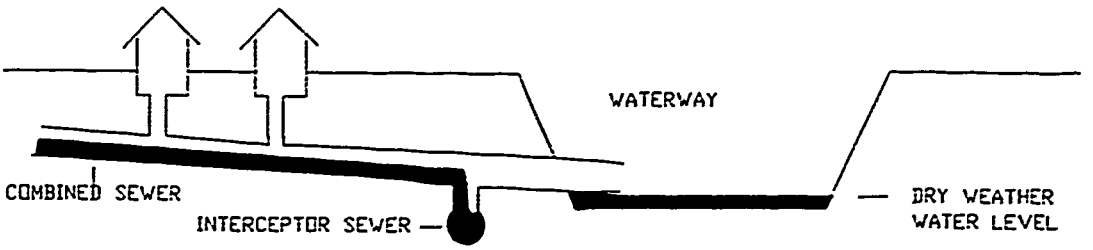

a. Operation of existing outfall, dry weather condition

Under dry weather conditions, the combined sewer system carries sanitary sewage to treatment plants via interceptor sewers. The system has sufficient capacity to handle dry weather flow without backup into basements or discharge into streams.

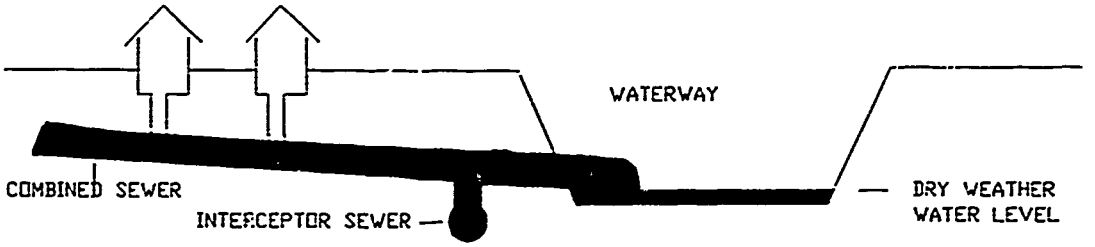

b. Outfall in operation after interceptor capacity is exceeded

At the beginning of a storm period, river levels are low. As rain continues, the sewer system fills up. To relieve pressure in the sewer system, a mixture of storm runoff and sanitary sewage is discharged, untreated, from sewer outfalls into streams.

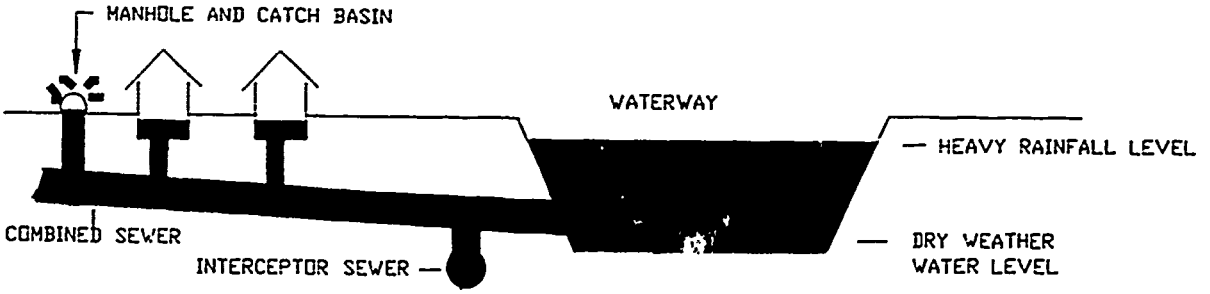

c. Operation of existing outfall, heavy rain condition

During periods of continuing rainfall, river levels rise, submerging the relief outfalls. Pressure then builds up within the sewer system, causing storm water mixed with raw sewage to back up from the sewers into basements and streets.

Figure 1. Combined sewer outfall submergence

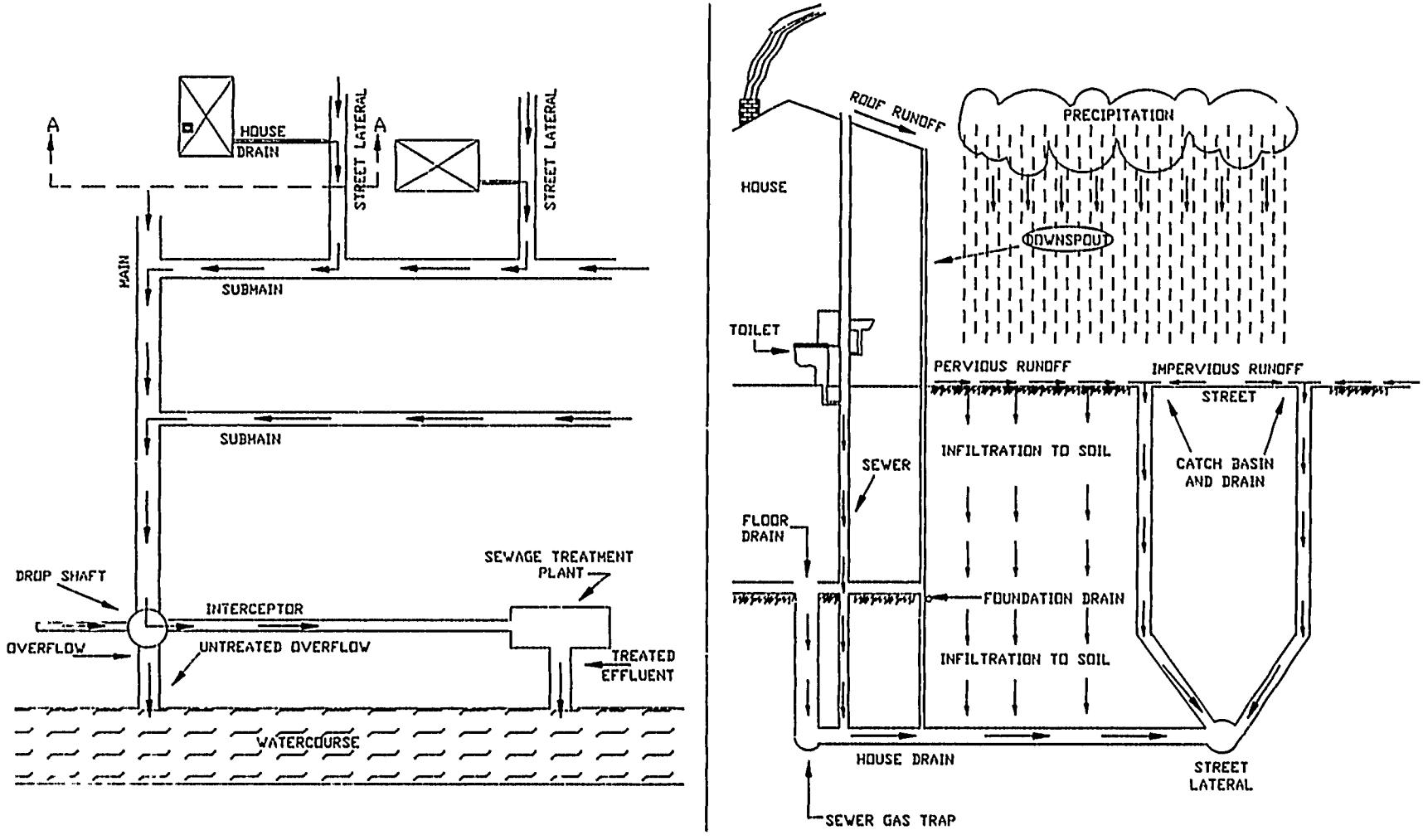

a. Drainage into local watercourse

b. Drainage from an individual house (section A-A)

Figure 2. Typical combined sewer system

TARP, as originally formulated, included near surface collector and drop shaft systems, 132 miles* of tunnels located 200 to 300 ft underground, and five reservoirs. TARP would permit storm water runoff to be collected from the local sewer systems and moved to the tunnels by the collector and drop shaft system. The tunnels would convey the storm water to the reservoirs, which would store the runoff until it could be discharged to the watercourses without causing flooding.

4. In 1974, TARP was divided into two parts by agreement between the Office of Management and Budget and the US Environmental Protection Agency. The Phase 1 features were identified as being related primarily to water quality enhancement. Phase 2 included those features associated mainly with flood damage reduction. Phase 1 includes about 110 miles of tunnels, collector and drop shaft systems which connect the sewers to the tunnels, and upgraded treatment works. Approximately 50 miles of Phase 1 tunnels and two large pumping stations have been constructed and are in operation. Phase 2 includes 22 miles of tunnels and five reservoirs, which would provide 127,000 acre-ft or about 40 billion gallons of floodwater storage. Construction of Phase 2 has not been started.

The Prototype

5. The project plan provides for use of a rock quarry (McCook Reservoir) as a 32,100-acre-ft (10.43 billion gallons) reservoir that would provide temporary storage for combined sewer and storm flow runoff. The storage system would be sufficient to capture the runoff from a 30-year, 24-hour storm event. When the reservoir is filled to its maximum design capacity, the water-surface elevation will be at -70**, or between 90 and 140 ft below the ground surface elevation.

6. The proposed McCook Reservoir will be located in the city of McCook, IL (Figure 3). The proposed reservoir will be located east of East Avenue, west of the Indiana Harbor Belt Railroad, and south of 55th Street within the communities of McCook and Hodgkins, IL, as shown in Plate 1.

---

* A table of factors for converting non-SI units of measurement to SI (metric) units is found on page 3.

** All elevations (el) cited in this report are in feet referenced to Chicago City Datum (CCD).

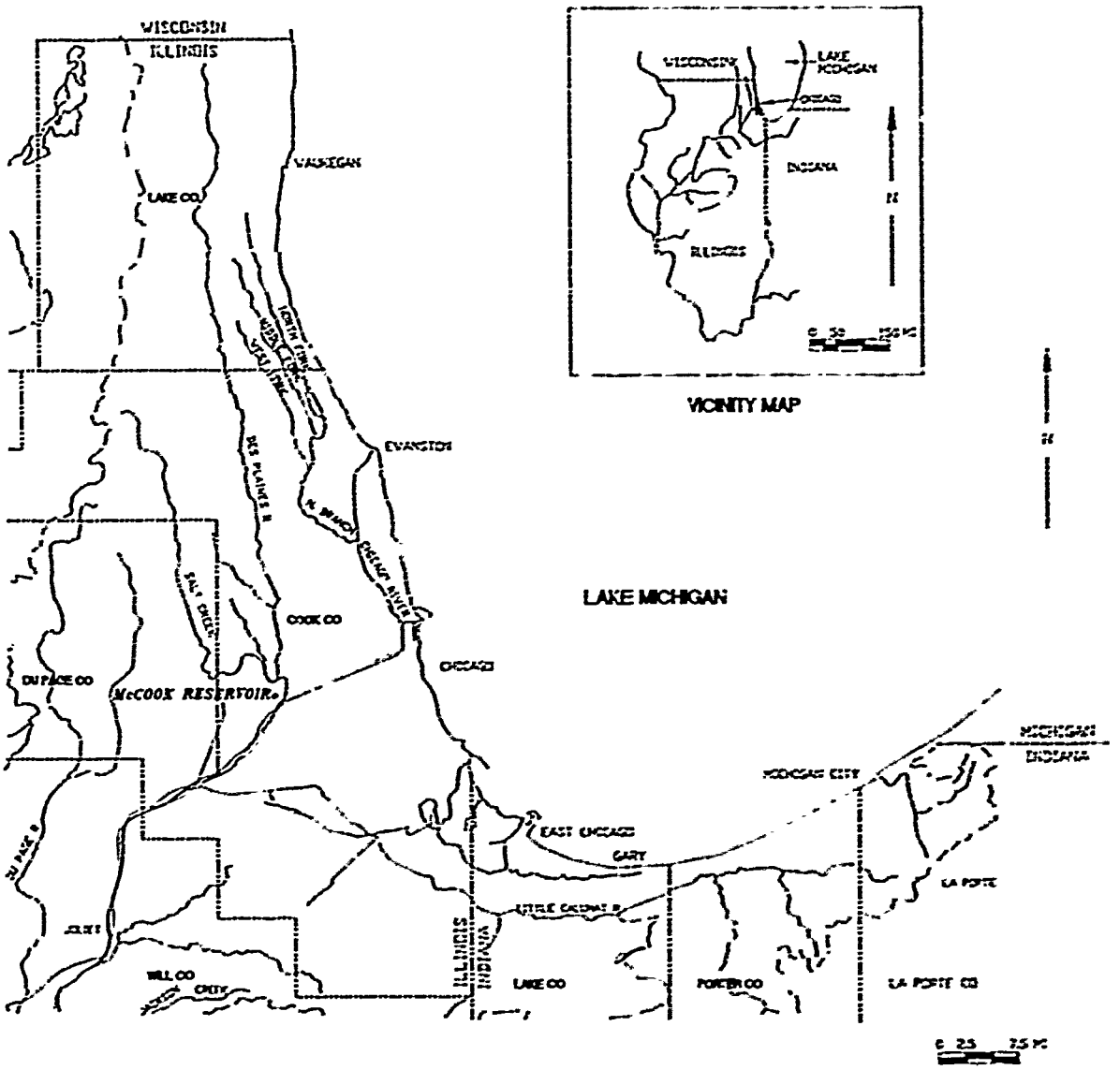

Figure 3. Vicinity and location maps

7. Sewage and storm water in the tunnels would flow by gravity to the McCook Reservoir for temporary storage. Flows from the tunnels as high as 85,000 cfs would discharge into the reservoir (Figure 4) through 45 outlet ports 5.75 ft square evenly spaced every 65 ft in a 2,910-ft-long manifold (Plates 2 and 3). The outlet manifold dimensions will be approximately 37 ft high and 37 ft wide at the upstream end and taper to 25 ft high and 15 ft wide at the downstream end. The invert elevation of the outlet manifold will be -265.5. The outlet manifold will be directly connected to the tunnel with a wheel gate structure/surge chamber (Figure 4) located in the tunnel about 500 ft upstream of the manifold. The wheel gate structure is designed to

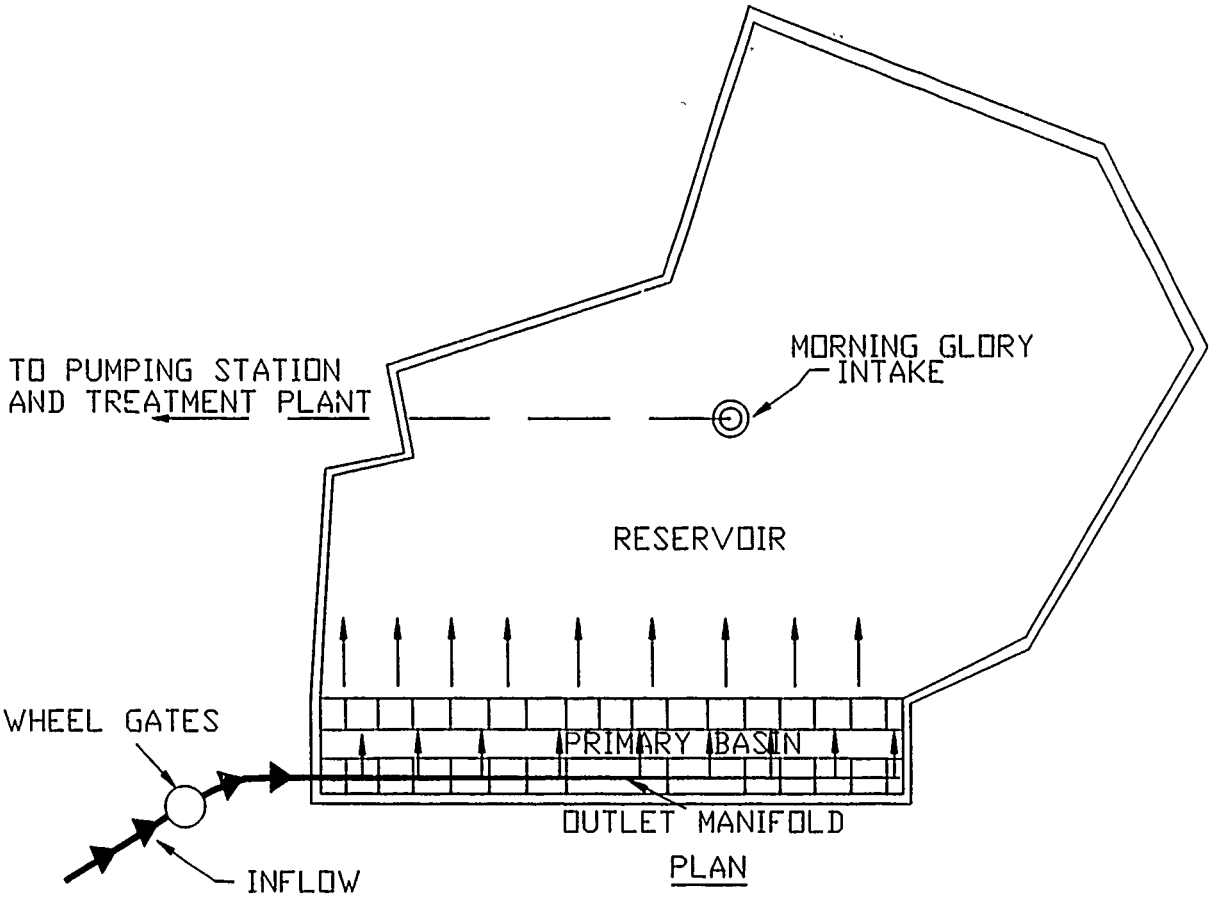

Figure 4. McCook Reservoir (schematic)

permit closure of the gates to prevent flow from the tunnel to the reservoir or to prevent backflow from the reservoir to the tunnel.

8. As the capacity of the West-Southwest Treatment Plant permits, the TARP Mainstream Pumping Station in Hodgkins, IL, will pump sewage and storm water from the McCook Reservoir to the West-Southwest Treatment Plant. The treated effluent will be discharged into the area watercourse. Flow pumped from the reservoir will exit through a morning glory intake structure (Figure 4) located approximately in the bottom of the reservoir.

Purpose and Scope of the Model Studies

9. The model studies were conducted to evaluate the hydraulic characteristics of the morning glory inlet and the manifold outlet structures and develop modifications, if needed, for satisfactory designs. Information desired from operation of the model of the morning glory spillway included

evaluation of head loss, air entrainment, vortices, flow patterns, pressures, and areas of potential cavitation. The model of the manifold outlet was designed to enable evaluation of head loss, flow patterns, velocities, pressures, flow distribution, and discharge rating curves. Designs developed or verified by the models should ensure the hydraulic integrity of the structures for all anticipated flow conditions.

PART II: THE MODELS

Description

10. The model used to investigate the morning glory spillway (Plate 4) was constructed to a linear scale of 1:20.7 and reproduced a 207- by 207-ft area of the reservoir topography. The morning glory spillway was located in the center of the flume (Figure 5). The model simulated the morning glory intake, the vertical shaft, elbow, and a 700-ft length of discharge conduit. Satisfactory flow distribution to the reservoir was provided through ports located around the periphery of the simulated portion of the reservoir (Plate 4). A butterfly valve was located at the downstream end of the conduit (Plate 4) to permit simulation of various hydraulic gradients. The model was capable of simulating discharges as high as 2,000 cfs and water-surface elevations as high as -70. The model was designed to enable calibration of the intake, determination of losses through the structure, detection of areas of potential cavitation, and detection of vortices.

11. Computations involving prototype and model conduit friction indicated insignificant differences in the prototype and model conduit head losses for the design discharge of 2,000 cfs. Therefore, there was no need to adjust the model conduit length or slope to compensate for a difference in head loss.

12. The model used to investigate the manifold outlet was constructed to a linear scale of 1:40 (Plate 2). The model simulated the complete structure (Figure 6), including the wheel gates, gate and surge shafts, transition connecting the wheel gate structure to the manifold, and the primary basin. The wheel gate structure viewed from upstream, downstream, and the side is shown in Figure 7. A side view of a section of the manifold showing the outlet ports is shown in Figure 8. The model could simulate discharges as high as 85,000 cfs and water-surface elevations as high as -140.0. The model provided means for calibrating the wheel gates, detecting areas of potential cavitation, evaluating the transition design upstream and downstream of the wheel gates, evaluating the design of the pier separating the two wheel gates, determining head loss in the manifold, and evaluating energy dissipation in the primary basin.

13. The models were constructed of transparent plastic to permit visual observation of internal flow patterns, turbulence, and air ingestion. Water

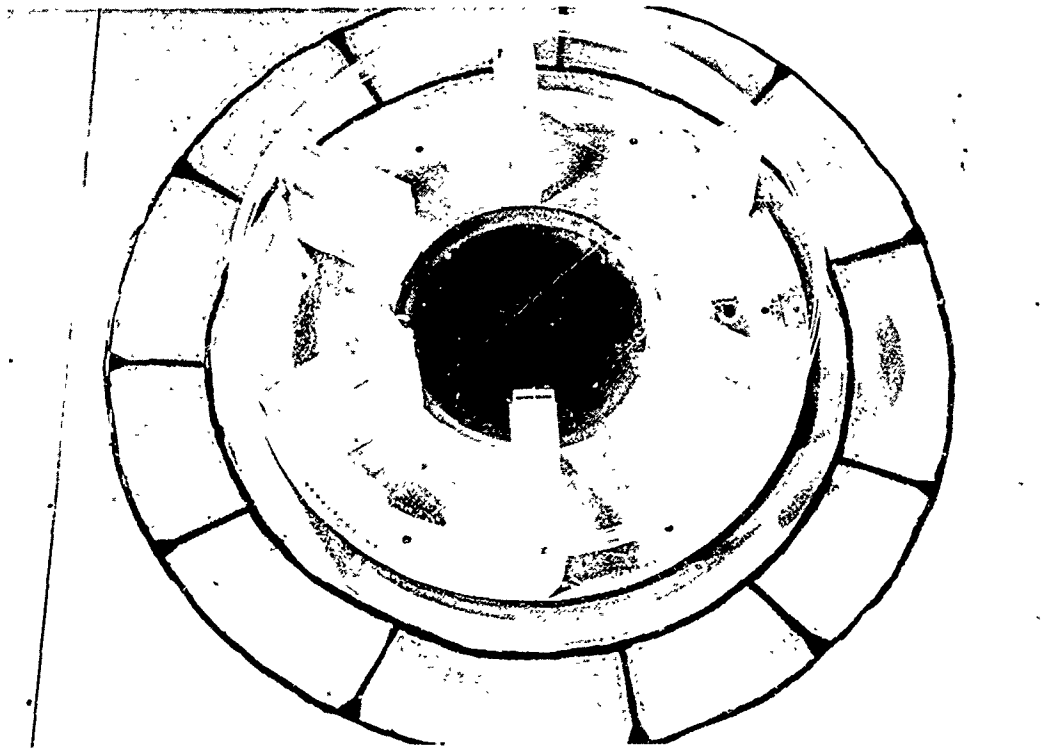

Figure 5. Morning glory intake

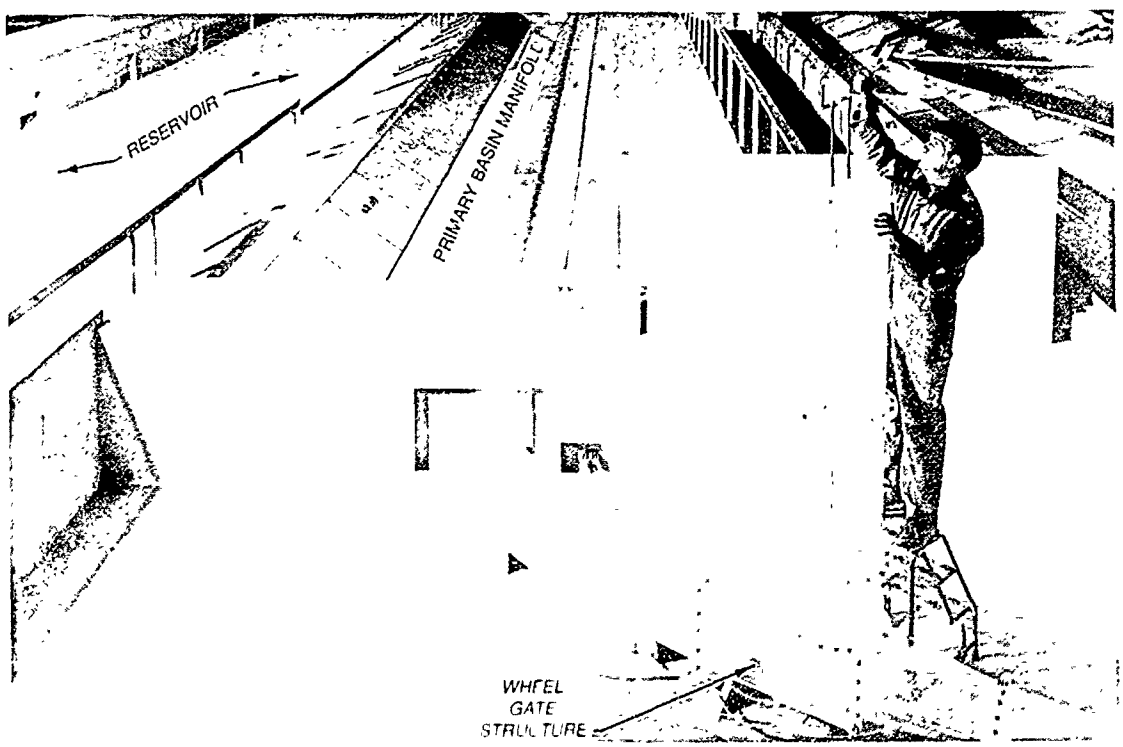

Figure 6. Manifold outlet model

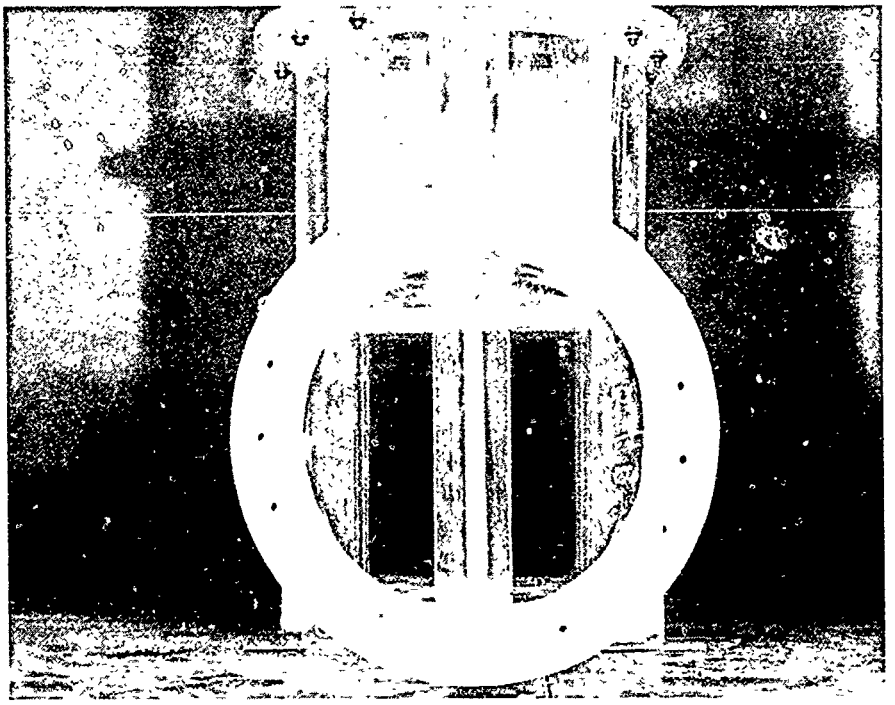

a. Upstream view

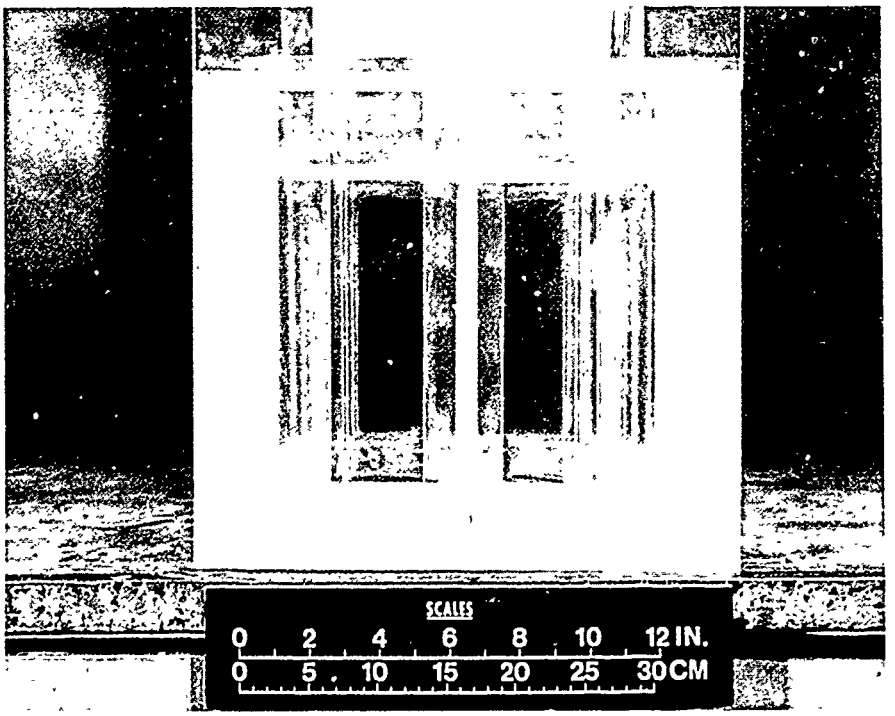

b. Downstream view

Figure 7. Wheel gate structure (Continued)

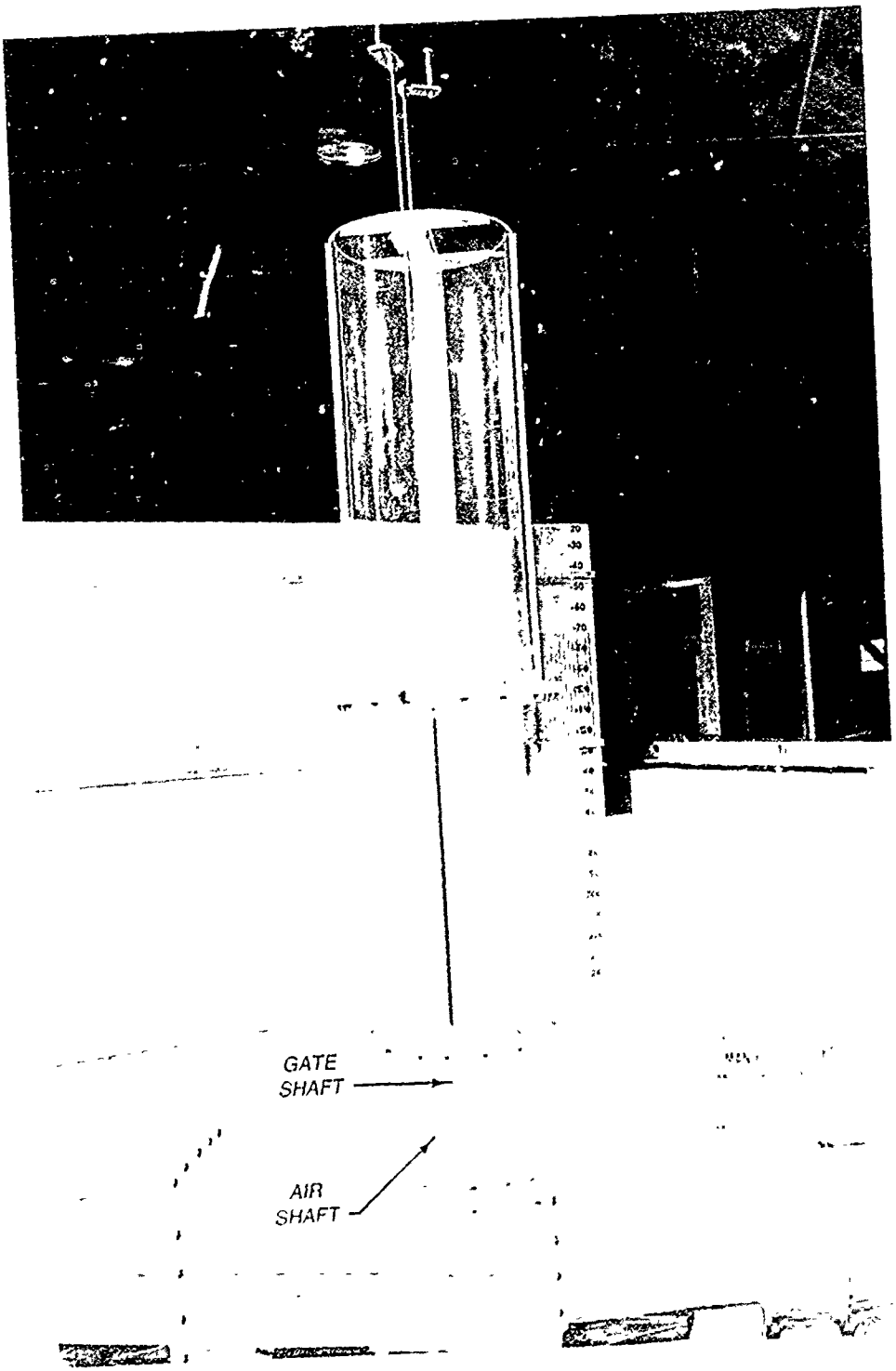

c. Profile

Figure 7. (Concluded)

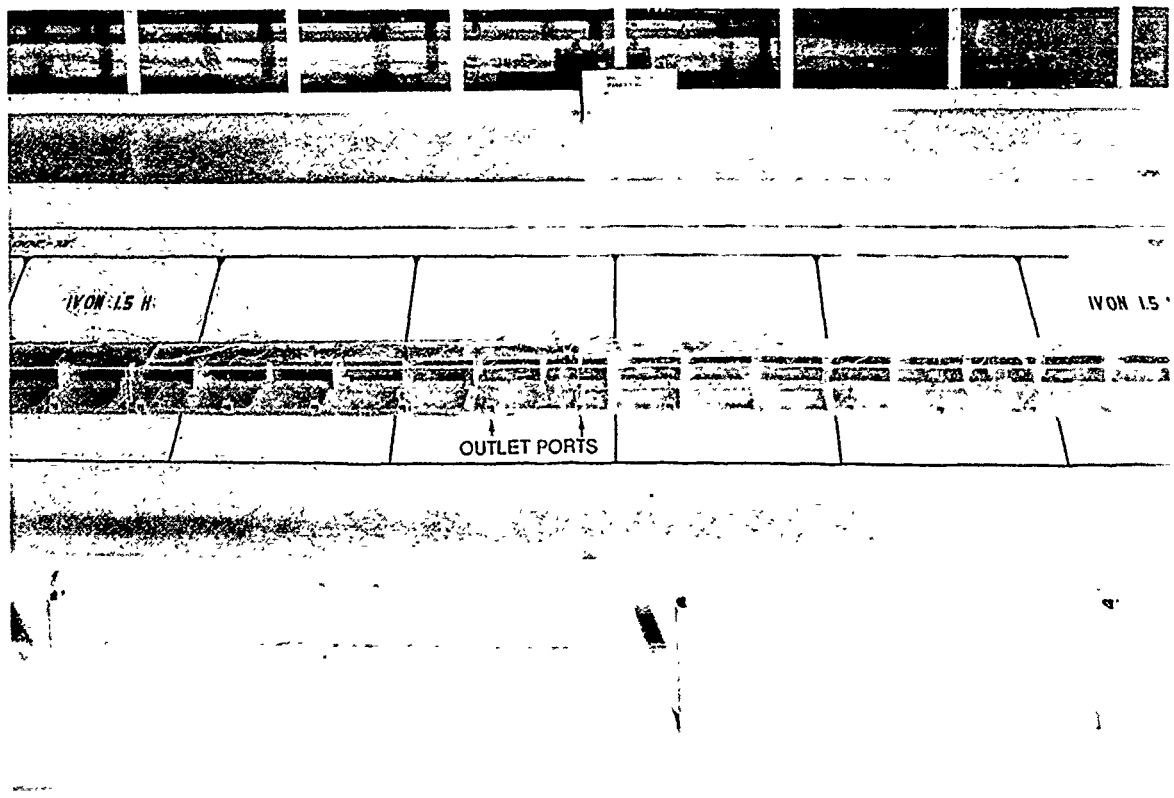

Figure 8. Outlet ports in manifold

used in the models was recycled and discharges were measured with venturi flowmeters. Water-surface elevations were measured with staff and point gages. Velocities were measured with pitot tubes and electronic velocity probes. Current patterns were determined by observation of dye injected into the water and confetti sprinkled on the water surface. Hydrostatic pressures were measured at various locations in the structures with piezometers. Flow conditions were documented by sketches, photographs, and videos.

Scale Relations

14. The accepted equations of hydraulic similitude based on Froude criteria were used to express the mathematical relations between the dimensions and hydraulic quantities of the models and prototypes. The general relations expressed in terms of the model scales or length ratios L_r are presented in the following tabulation:

Characteristic	Dimension*	Scale Relation Model:Prototype	
		Morning Glory Intake	Manifold Outlet
Length	$L_r = L_r$	1:20.7	1:40
Area	$A_r = L_r^2$	1:428.5	1:1,600
Time	$T_r = L_r^{1/2}$	1:4.5	1:6.3
Velocity	$V_r = L_r^{1/2}$	1:4.5	1:6.3
Discharge	$Q_r = L_r^{5/2}$	1:1,949.	1:10,119.3
Pressure	$P_r = L_r$	1:20.7	1:40
Weight	$W_r = L_r^3$	1:8,870	1:64,000

* Dimensions are in terms of length.

PART III: TESTS AND RESULTS

Morning Glory Intake

15. Tests to determine the relationship between discharge, pool elevation, hydraulic gradient, and air entrainment were conducted by setting the hydraulic gradient and discharge and permitting the pool to stabilize. The elevation of the hydraulic gradient was set at a point (piezometer 26) 323 ft downstream from the center line of the shaft (Plate 4). Piezometer 26 was chosen for setting the hydraulic gradient because it was in a hydraulically stable location that was unaffected by turbulence from the elbow and valve located at the downstream end of the conduit. After the pool stabilized, visual observations were made for a period of 20 minutes (prototype) to detect and record the stage of the most severe vortex. Typical stages of vortex development are shown in Figure 9.

16. Evaluation techniques used in the model included documentation of the presence of air in the conduit during either conduit or weir control. During conduit control, if air is drawn into the intake it is by stage D and/or E vortices (Figure 9). Stage D and E vortices generate air entrainment that appears in the form of air bubbles in the conduit as shown in Plate 5. During the transition from weir to conduit or from conduit to weir control, air is entrained by turbulence and is also observed in the conduit as air bubbles. Weir control (Plate 5) occurs when the hydraulic gradient in the shaft is below the weir crest. During weir control, turbulence generated by the plunging nappes induces significant air ingestion in the intake that appears as slug flow in the conduit (Plate 5).

17. Various flow conditions with and without the intake cover plate are shown in Photos 1-7. In some photographs surface currents are depicted by confetti and bottom currents are depicted by dye.

18. The intake cover plate was removed to permit observation of weir control flow conditions below the elevation of the cover plate and to observe vortices that occur only without the cover plate during conduit control. Photos 1-3 illustrate weir control with discharges of 500, 1,000, and 2,000 cfs, respectively. Flow transitioning from weir to conduit control during a discharge of 2,000 cfs is shown in Photo 4. Surface vortices above the intake with a discharge of 2,000 cfs and pool elevations of -190 and -160 are shown

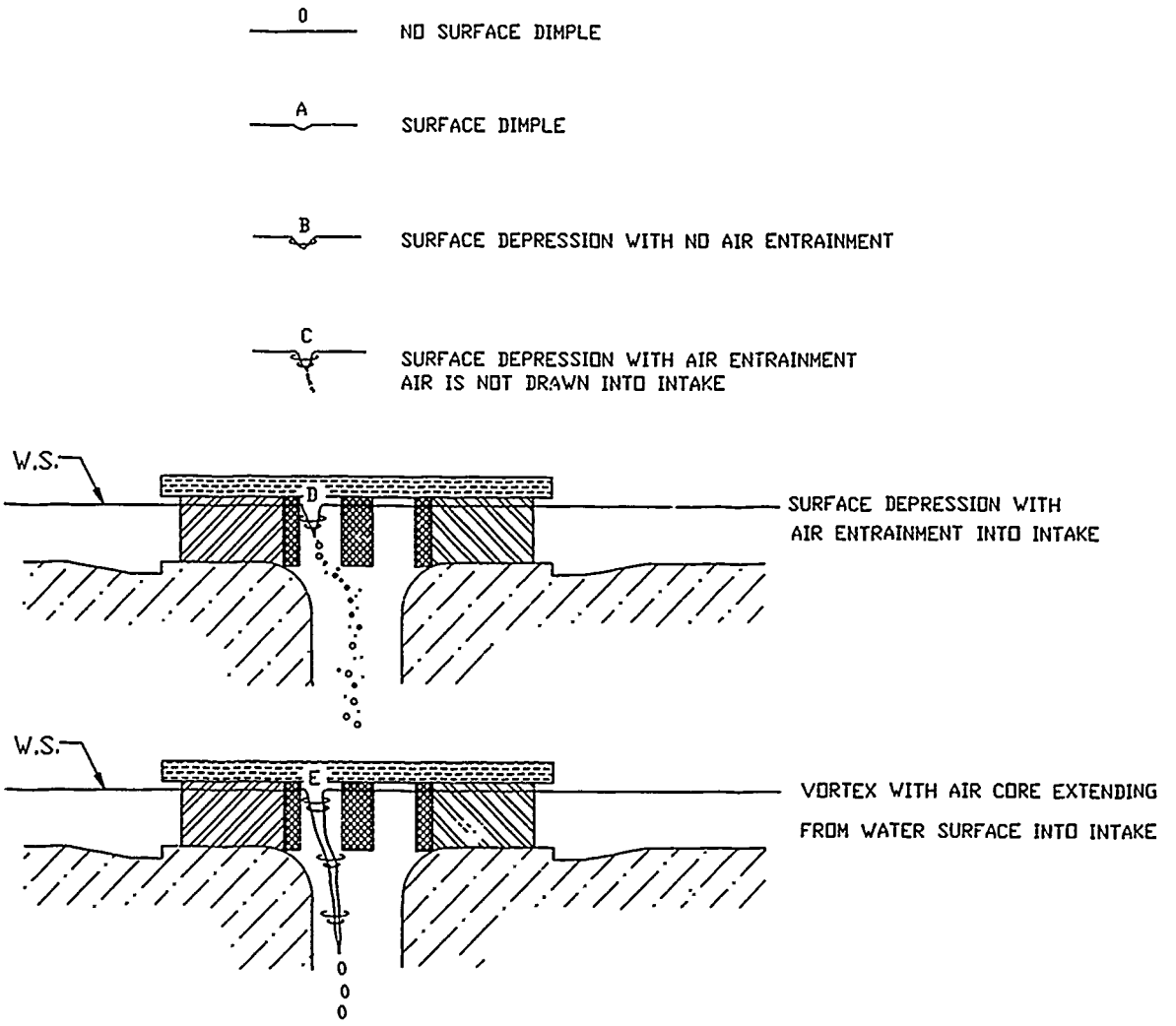

Figure 9. Stages of vortex development

in Photos 5 and 6, respectively. The vortices shown in Photos 5 and 6 were sustained air-entraining vortices that had air cores about 9 in. in diameter (prototype).

19. The cover plate was installed and no significant air-entraining vortices occurred during conduit control. Flow conditions with a discharge of 2,000 cfs and a pool elevation of -190 are shown in Photo 7.

20. The relationship between discharge and pool elevation is presented in Plate 6. Basic data used for development of the plot including flow control and stages of vortex development are tabulated in Table 1. During conduit control, pool characteristics ranged from hydraulic conditions having no vortices to stage E vortices. Since air entrainment in the conduit during conduit control is caused by stage D and E vortices (Figure 9), only the

conditions that are conducive to stage D and E vortices are highlighted in Plate 6. The plot indicates that D and E vortices occurred only when the water surface was below the bottom of the vortex suppressor (cover) plate (el -212). However, even with the water surface below the bottom of the cover plate, stage D and E vortices did not occur during discharges less than 550 cfs.

21. As the hydraulic gradient in the shaft fell below the weir crest el -220, weir control developed. During weir control, the nappe plunges into the shaft, intersects the water surface at the elevation of the hydraulic gradient in the shaft, and ingests air into the shaft. For discharges above 800 cfs (Plate 6), inges d air appeared in the conduit as slug flow (Plate 5). Weir flow with discharges between 550 and 800 cfs (Plate 6) generated only air bubbles in the conduit (Plate 5) similar to those produced by stage D and E vortices. Weir control with discharges below 550 cfs entrained air in the shaft, but the low velocity in the shaft permitted the entrained air to rise to the water surface in the shaft.

22. Pressures for various anticipated flow conditions were measured in the structure with piezometers located as shown in Plates 7 and 8 (type 1 intake). Hydraulic gradient elevations and pressures are tabulated in Table 2. No tendency for cavitation was indicated as pressures were stable (amplitude of pressure fluctuations less than 0.2 ft) and positive for all flow conditions.

23. Entrance losses were obtained from the model data for various flow conditions as foll ws. Energy gradients in the conduit were determined from the pressures indicated by piezometers 18 to 36 (Plate 7) as shown in the following equation:

$$EG = HG + \frac{V^2}{2g} \qquad (1)$$

where

EG = energy gradient

HG = hydraulic gradient

V = average velocity in the conduit, ft/sec

g = acceleration due to gravity, ft/sec^2

Pressures measured with piezometers 18 t. 36 indicated that they were within a

region relatively free from the effects of boundary layer development and acceleration of flow at the entrance and the butterfly valve in the conduit. The conduit resistance coefficients determined were approximately the same as those indicated by the smooth pipe curve of a Moody diagram for appropriate Reynolds numbers. Using piezometers 18 to 36 as a reference, the hydraulic gradients in the conduit were projected to sta 0+23, the conduit entrance. Pressures measured by means of piezometers 6a and 6b (Plate 8) were used to determine the elevation of the energy gradient in the shaft at el -253.4. Separate entrance losses were determined from the elevation of the energy gradient at the conduit entrance, the shaft at el -253.4, and the pool. The separate entrance losses for a discharge of 2,000 cfs and a pool elevation of -190.0 are illustrated by the difference in energy gradient elevations in Plate 7. Separate entrance losses and coefficients for discharges ranging from 1,100 to 2,140 cfs are tabulated in Table 3.

24. Tests were conducted to evaluate the feasibility of reducing the vertical distance between the underside of the cover plate and the spillway crest by lowering the cover plate 2.5 ft to el -214.5 (type 2 intake). A sketch of the type 2 intake is shown in Plate 9.

25. Observation of various flow conditions indicated no tendency for air-entraining vortices. Flow conditions during weir and conduit control were considered similar to those observed in the type 1 intake (i.e., cover plate located at el -212.0).

26. Pressures for various flow conditions were measured in the type 2 design with piezometers located as shown in Plates 9 and 10. Piezometers 1a and 1b were added and installed in the underside of the cover plate as shown in Plate 9. Hydraulic gradient elevations and pressures are tabulated in Table 4. Pressures were stable and positive for all flow conditions.

27. Entrance losses with the type 2 design were obtained for various flow conditions. Pressures determined from piezometers 18 to 36 were used as a reference to project the hydraulic gradients to sta 0+23 (Plate 10), the conduit entrance. Pressures measured by means of piezometers 6a and 6b (Plate 9) were used to determine the elevation of the energy gradient in the shaft at el -253.4. Separate entrance losses were determined from the elevation of the energy gradient at the conduit entrance, the shaft at el -253.4, and the pool. Separate entrance losses and coefficients for various flow conditions are tabulated in Table 5. A comparison with the type 1 design

(test results presented in Table 3) indicates that the average value of the loss coefficient K_e between the pool and the shaft at el -253.4 was insignificantly higher with the type 2 design. Test results indicate that lowering the cover plate 2.5 ft will not have a significant effect on hydraulic performance.

Manifold Outlet

28. The model of the manifold outlet was designed, primarily, to measure pressures in the wheel gate structure and manifold, to determine loss coefficients in the manifold, and to determine flow distribution in the manifold outlet ports and primary basin. Hydraulic performance in the wheel gate structure and manifold (Plate 2) was documented by photographs. Various gate openings and flow conditions in the wheel gate structure (Plate 11) are shown in Photos 8-10. Flow conditions with various water-surface elevations and flows exiting the outlet ports in the manifold are shown in Photos 11-13. Some of the flow conditions were photographed with confetti sprinkled on the water surface simulating a 20-sec (prototype) time exposure to depict the magnitude and direction of surface currents.

29. The approach curve, outlet manifold, various cross sections of the manifold, and piezometer locations are shown in Plate 3. Tests to measure hydrostatic pressure were conducted for various discharges with the wheel gates fully open and a reservoir (tailwater) water-surface elevation of -190.0. Additional piezometer locations and the hydraulic gradients determined from piezometers 1-54 in the wheel gate structure and outlet manifold are shown in Plates 12 and 13, respectively. The basic data are tabulated in Table 6. The pressures determined by means of the piezometers were all positive and no tendency for cavitation was indicated.

30. Computations for a discharge of 50,000 cfs and a velocity V_e of 36.5 ft/sec to determine the total head loss H_e and the loss coefficient K_e for the outlet manifold based on the energy gradient elevations at the upstream end of the outlet manifold are illustrated in Plate 14. Values of head loss and loss coefficients determined from the hydraulic gradients in Plate 13 are tabulated in Table 7.

31. Tests were conducted to investigate for potential areas of cavitation by measuring hydrostatic pressures in one of the manifold outlet ports.

Velocity measurements at the manifold port outlets indicated that the discharge exiting the manifold is almost uniformly distributed among the 45 ports. Also, observations aided by dye injection indicated similar flow patterns exiting each port.

32. Based on the velocity measurements and observations, port 18 (Plate 14) was arbitrarily selected for installation of piezometers and measurement of pressures. Piezometer locations in port 18 are shown in the plan and profile views in Plate 15. Pressures measured for a reservoir water-surface elevation of -190.0 and various discharges are shown in Plate 15. Analysis of the data indicates positive pressures; therefore, there should be no tendency for cavitation in the prototype structure.

33. Tests were conducted to document the magnitude and direction of velocities generated by discharges of 30,000 and 85,000 cfs exiting the 45 ports in the manifold. Pressure and velocity measurements indicated that discharges exiting the ports were approximately evenly distributed among the 45 ports. For a discharge of 85,000 cfs, flow through the upstream port (port 1) exited at an angle of 60 deg from the longitudinal center line of the manifold (Figure 10). Flow from port 44 exited at an angle of 80 deg (Figure 10). As flow successively exited ports 1-45, the angle of the exiting flow became more normal to the manifold because the flow rate and thus the longitudinal component of velocity inside the manifold progressively decreased. Flow from port 45, the port farthest downstream, exited normal to the longitudinal center line of the manifold (Figure 10) because port 45 was offset 10 ft from the downstream end of the manifold. The 10-ft offset permitted flow inside the manifold to approach the port from a direction essentially normal to the port.

34. The direction of flow exiting the manifold gradually became more normal to the manifold as discharges were reduced below 85,000 cfs. For a discharge of 10,000 cfs, the angle of flow exiting ports 1-44 increased by about 10 deg relative to the flow direction measured with a discharge of 85,000 cfs (Figure 10). Flow exiting port 45 remained normal to the manifold, regardless of the discharge.

35. Currents and velocities generated in the primary basin by discharges of 30,000 and 85,000 cfs are shown in Plates 16 and 17, respectively. Typical flow patterns and velocities in the primary basin in cross-section views are also shown in Plates 16 and 17. The currents and velocities shown in the plan

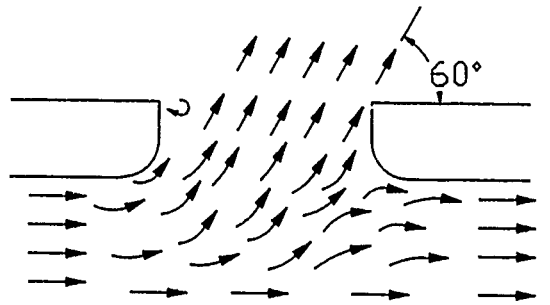

a. Port 1

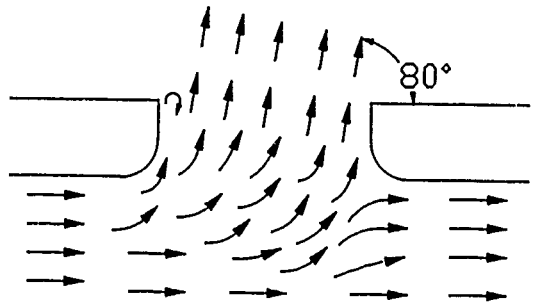

b. Port 44

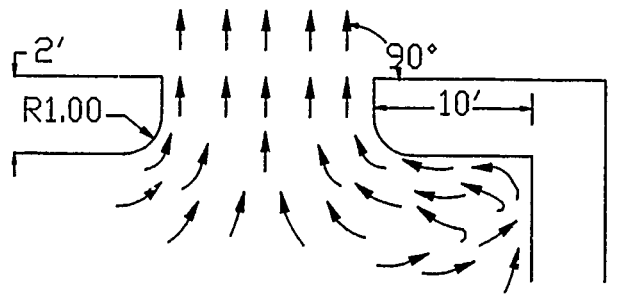

c. Port 45

Figure 10. Typical flow patterns for flow exiting manifold ports at a discharge of 85,000 cfs

views were measured 2 ft above the bottom. Angular flow exiting the manifold ports contributed to eddies at the upstream and downstream ends of the primary basin (Plates 16 and 17). No significant surface waves were generated. The energy in the flow exiting the manifold ports was satisfactorily dissipated in the primary basin.

PART IV: SUMMARY AND DISCUSSION

36. Tests were conducted in two separate models to investigate hydraulic performance in the morning glory intake and manifold outlet.

37. The model of the morning glory intake was designed to permit evaluation of head loss, flow patterns, vortices, and areas of potential cavitation. Tests indicated that the cover plate was needed to prevent the formation of air-entraining vortices during conduit control. Subsequent tests indicated that the elevation of the cover plate could be lowered 2.5 ft without adversely affecting hydraulic performance.

38. Tests were conducted to determine the relationship between discharge, pool elevation, hydraulic gradient, and air entrainment. Air entrainment (vortices) during conduit control normally occurred when the water surface was below the underside of the cover plate during the transition from conduit to weir control. The test results indicated that air entrainment could be prevented by reducing the discharge to 550 cfs or less. During weir control, the nappe plunged into the shaft and ingested air into the shaft. For discharges above 800 cfs, ingested air appeared in the conduit as slug flow. Weir flow with discharges between 550 and 800 cfs generated only air bubbles in the conduit. Weir control with discharges below 550 cfs did entrain air in the shaft, but the low velocity in the shaft permitted the entrained air to rise to the water surface in the shaft.

39. Pressures measured for various flow conditions indicated no tendency for cavitation. Entrance losses in the morning glory intake were obtained for various flow conditions by measuring pressures in the shaft and conduit. The pressures in the conduit were used to establish the elevation of the hydraulic gradient at the conduit entrance. Additional piezometers located in the intake and shaft were used to determine the separate losses in the structure.

40. The model of the manifold outlet permitted evaluation and documentation of flow conditions in the wheel gate structure and manifold. Hydrostatic pressure in the wheel gate structure and manifold was measured by means of piezometers for various discharges. The pressures were all positive and no tendency for cavitation was indicated. Loss coefficients based on the elevation of the hydraulic gradient at the upstream end of the manifold were determined for various discharges.

41. Pressures measured at a manifold outlet port that had typical flow

characteristics indicated no zones of potential cavitation.

42. The magnitude and direction of flow exiting the 45 ports was measured in the primary basin. Discharge exiting the manifold was evenly distributed among the 45 ports. The energy in the flow exiting the ports was satisfactorily dissipated in the primary basin.

43. Test results obtained from the models of the morning glory intake and the manifold outlet indicate satisfactory hydraulic performance can be expected for any anticipated flow conditions.

Table 1

Discharge Versus Pool Elevation

Type 1 Design

Elevation of Hydraulic Gradient Piezometer 26*	Discharge cfs	Pool El	Flow Control**	Stage of Vortex Development†
-130	220	-129.8	Conduit	0
↓	330	-128.9	↓	↓
	550	-128.2		
	660	-127.3		
	1,100	-124.7		
	1,500	-123.5		
	2,000	-116.5		
	2,200	-114.5		A
↓	2,400	-111.0		0
-160	220	-159.9		
↓	330	-159.6		
	550	-159.0		
	660	-158.8		
	1,100	-156.8		
	1,500	-153.5		
	2,000	-148.5		
	2,200	-145.5		
↓	2,400	-139.5		
-190	220	-190.0		
↓	330	-189.8		
	550	-189.2		
	660	-189.0		
	1,110	-187.7		
	1,500	-185.0		
	2,000	-181.2		
	2,200	-178.8		
↓	2,400	-176.5		
-205	220	-205.0	↓	
↓	330	-204.7		
	550	-203.7		
	660	-203.5		↓
	1,100	-201.7		A
	1,500	-197.8		A
↓	2,000	-195.0	↓	0

(Continued)

* See Plate 4.

** See Plate 5.

† See Figure 9.

Table 1 (Concluded)

Elevation of Hydraulic Gradient Piezometer 26	Discharge cfs	Pool El	Flow Control	Stage of Vortex Development
-205	2,200	-190.5	Conduit	0
-205	2,400	-186.0	Conduit	0
-210	220	-209.9		
	330	-209.5		
	550	-208.9		
	660	-208.5		
	1,100	-207.2		A
	1,500	-203.0		A
	2,000	-196.5		0
	2,200	-194.0		B
-215	220	-214.8		0
	330	-214.8		0
	550	-213.8		C
	660	-213.8		D & E
	1,100	-211.8		0
	1,500	-207.5		A
	2,000	-202.0		0
	2,200	-200.0		B
-220	220	-217.8		C
	330	-217.5		C
	550	-217.0		D & E
	660	-216.5		D & E
	1,110	-215.2		D & E
	1,500	-212.2		D & E
	2,000	-207.5		A
	2,200	-205.5		A
-230	220	-218.0	Weir	C
	330	-217.8		C
	550	-217.0		D & E
	660	-216.8		D & E
	1,100	-216.0		Slug Flow
	1,500	-215.5		Slug Flow
	2,000	-214.6		Slug Flow
	2,200	-214.3		Slug Flow

Table 2

Hydraulic Gradients and Pressures, Type 1 Design

Piezometer No.	Piezometer El	Hydraulic Gradient El	Pressure ft
	Discharge 1,100 cfs, Pool El -190.1		
1	-220.00	-190.0	30.0
2	-220.00	-190.0	30.0
3	-221.24	-190.3	30.9
4	-223.31	-190.6	32.7
5	-226.21	-191.0	35.2
6	-229.32	-191.9	37.4
6a	-253.40	-192.2	61.2
6b	-253.40	-192.2	61.2
7	-283.25	-193.2	90.1
8	-283.25	-191.9	91.4
9	-289.88	-193.0	96.9
10	-298.50	-193.0	105.5
11	-310.00	-193.0	117.0
12	-304.30	-192.2	112.1
13	-304.35	-193.2	111.2
14	-304.40	-193.0	111.4
15	-304.45	-193.2	111.3
16	-304.50	-193.2	111.3
17	-304.55	-193.2	111.4
18	-304.60	-193.3	111.3
19	-304.65	-193.4	111.3
20	-304.70	-193.3	111.4
21	-304.75	-193.3	111.5
22	-304.80	-193.5	111.3
23	-304.85	-193.5	111.4
24	-304.90	-193.6	111.3
25	-304.95	-193.7	111.3
26	-305.00	-193.8	111.2
27	-305.05	-193.8	111.3
28	-305.10	-193.9	111.2
29	-305.15	-193.9	111.3
30	-305.20	-194.1	111.1
31	-305.25	-194.2	111.1
32	-305.30	-194.3	111.0
33	-305.35	-194.4	111.0
34	-305.40	-194.6	110.8
35	-305.45	-194.6	110.9
36	-305.50	-194.6	110.9
37	-305.55	-194.8	110.8
38	-305.60	-194.7	110.9

(Continued)

Table 2 (Continued)

Piezometer No.	Piezometer El	Hydraulic Gradient El	Pressure ft
39	-305.65	-195.0	110.7
40	-305.70	-195.0	110.7
41	-305.75	-195.0	110.8
42	-305.80	-195.2	110.6
43	-305.85	-195.2	110.7
	Discharge 1,300 cfs, Pool El -189.9		
1	-220.00	-190.0	30.0
2	-220.00	-190.0	30.0
3	-221.24	-190.5	31.7
4	-223.31	-190.8	32.5
5	-226.21	-191.5	34.7
6	-229.32	-192.5	36.8
6a	-253.40	-192.8	60.6
6b	-253.40	-192.8	60.6
7	-283.25	-194.2	89.1
8	-283.25	-192.5	90.8
9	-289.88	-194.5	95.4
10	-298.50	-193.0	105.5
11	-310.00	-192.9	117.1
12	-304.30	-194.3	110.1
13	-304.35	-194.3	110.1
14	-304.40	-194.4	110.0
15	-304.45	-194.6	109.9
16	-304.50	-194.7	109.8
17	-304.55	-194.7	109.9
18	-304.60	-194.8	109.8
19	-304.65	-194.9	109.8
20	-304.70	-194.9	109.8
21	-304.75	-195.0	109.8
22	-304.80	-195.0	109.8
23	-304.85	-195.0	109.9
24	-304.90	-195.2	109.7
25	-304.95	-195.0	110.0
26	-305.00	-195.4	109.6
27	-305.05	-195.5	109.6
28	-305.10	-195.6	109.4
29	-305.15	-195.6	109.6
30	-305.20	-195.7	109.5
31	-305.25	-195.8	109.5
32	-305.30	-195.8	109.5
33	-305.35	-195.8	109.6
34	-305.40	-195.9	109.5

(Continued)

Table 2 (Continued)

Piezometer No.	Piezometer El	Hydraulic Gradient El	Pressure ft
35	-305.45	-196.0	109.5
36	-305.50	-196.0	109.5
37	-305.55	-196.3	109.3
38	-305.60	-196.2	109.4
39	-305.65	-196.4	109.3
40	-305.70	-196.4	109.4
41	-305.75	-196.4	109.4
42	-305.80	-196.6	109.2
43	-305.85	-196.6	109.3
	Discharge 1,500 cfs, Pool El -190.2		
1	-220.00	-190.0	30.0
2	-220.00	-190.0	30.0
3	-221.24	-190.6	31.6
4	-223.31	-191.3	32.0
5	-226.21	-192.4	33.8
6	-229.32	-193.9	35.4
6a	-253.40	-194.1	59.3
6b	-253.40	-194.1	59.3
7	-283.25	-196.5	86.8
8	-283.25	-193.8	90.5
9	-289.88	-197.0	92.9
10	-298.50	-195.9	102.6
11	-310.00	-194.5	116.5
12	-304.)	-196.1	108.2
13	-304.35	-196.6	107.8
14	-304.40	-196.7	108.7
15	-304.45	-196.7	108.8
16	-304.50	-196.7	108.9
17	-304.55	-197.0	107.6
18	-304.60	-197.2	108.4
19	-304.65	-197.5	107.2
20	-304.70	-197.5	107.2
21	-304.75	-197.7	107.1
22	-304.80	-197.8	107.0
23	-304.85	-197.8	107.1
24	-304.90	-197.8	107.1
25	-304.95	-197.5	107.5
26	-305.00	-198.3	106.7
27	-305.05	-198.4	106.7
28	-305.10	-198.5	106.6
29	-305.15	-198.4	106.8
30	-305.20	-198.6	106.6

(Continued)

Table 2 (Continued)

Piezometer No.	Piezometer El	Hydraulic Gradient El	Pressure ft
31	-305.25	-198.6	106.7
32	-305.30	-198.6	106.7
33	-305.35	-198.6	106.8
34	-305.40	-198.8	106.6
35	-305.45	-199.2	106.3
36	-305.50	-199.2	106.3
37	-305.55	-199.4	106.2
38	-305.60	-199.4	106.2
39	-305.65	-199.6	106.1
40	-305.70	-199.6	106.1
41	-305.75	-199.7	106.1
42	-305.80	-199.9	105.9
43	-305.85	-200.0	105.9
	Discharge 1,750 cfs, Pool El -189.7		
1	-220.00	-190.0	30.0
2	-220.00	-190.2	30.8
3	-221.24	-191.0	30.2
4	-223.31	-191.4	31.9
5	-226.21	-192.8	33.4
6	-229.32	-194.8	34.5
6a	-253.40	-195.0	58.4
6b	-253.40	-195.0	58.4
7	-283.25	-197.7	85.6
8	-283.25	-194.8	88.5
9	-289.88	-198.2	91.7
10	-298.50	-196.4	102.1
11	-310.00	-195.3	115.7
12	-304.30	-197.4	106.9
13	-304.35	-197.8	106.6
14	-304.40	-197.9	106.5
15	-304.45	-197.9	106.6
16	-304.50	-197.9	106.6
17	-304.55	-198.0	106.6
18	-304.60	-198.2	106.4
19	-304.65	-198.4	106.3
20	-304.70	-198.6	106.1
21	-304.75	-198.7	106.1
22	-304.80	-198.8	106.0
23	-304.85	-198.8	106.1
24	-304.90	-198.9	106.0
25	-304.95	-198.9	106.1
26	-305.00	-199.0	106.0

(Continued)

Table 2 (Continued)

Piezometer No.	Piezometer El	Hydraulic Gradient El	Pressure ft
27	-305.05	-199.2	105.9
28	-305.10	-199.3	105.7
29	-305.15	-199.4	105.8
30	-305.20	-199.6	105.6
31	-305.25	-199.7	105.5
32	-305.30	-199.8	105.5
33	-305.35	-199.9	105.5
34	-305.40	-200.1	105.3
35	-305.45	-200.2	105.3
36	-305.50	-200.3	105.2
37	-305.55	-200.4	105.2
38	-305.60	-200.3	105.3
39	-305.65	-200.7	104.1
40	-305.70	-200.8	104.9
41	-305.75	-200.7	105.1
42	-305.80	-201.2	104.6
43	-305.85	-201.3	104.6
	Discharge 2,000 cfs, Pool El -190.0		
1	-220.00	-190.0	30.0
2	-220.00	-190.0	30.0
3	-221.24	-191.2	30.0
4	-223.31	-192.1	31.2
5	-226.21	-194.0	32.2
6	-229.32	-196.5	32.8
6a	-253.40	-196.8	56.6
6b	-253.40	-197.0	56.4
7	-283.25	-200.8	82.6
8	-283.25	-196.5	86.8
9	-289.88	-201.5	88.4
10	-298.50	-199.8	98.7
11	-310.00	-197.2	112.8
12	-304.30	-200.0	104.3
13	-304.35	-201.0	103.4
14	-304.40	-200.5	103.9
15	-304.45	-200.9	103.6
16	-304.50	-201.1	103.4
17	-304.55	-201.2	103.4
18	-304.60	-201.1	103.5
19	-304.65	-201.3	103.4
20	-304.70	-201.5	103.2
21	-304.75	-201.8	103.0
22	-304.80	-201.9	102.9

(Continued)

Table 2 (Continued)

Piezometer No.	Piezometer El	Hydraulic Gradient El	Pressure ft
23	-304.85	-202.0	102.9
24	-304.90	-202.5	102.4
25	-304.95	-201.9	103.1
26	-305.00	-202.5	102.5
27	-305.05	-202.5	102.6
28	-305.10	-202.6	102.5
29	-305.15	-202.7	102.5
30	-305.20	-202.8	102.4
31	-305.25	-203.0	102.3
32	-305.30	-203.5	101.8
33	-305.35	-203.4	102.0
34	-305.40	-203.9	101.5
35	-305.45	-203.9	101.6
36	-305.50	-204.3	101.2
37	-305.55	-204.1	101.5
38	-305.60	-204.3	101.3
39	-305.65	-205.0	100.7
40	-305.70	-206.0	99.7
41	-305.75	-204.1	101.7
42	-305.80	-205.0	100.8
43	-305.85	-205.1	100.8
	Discharge 2,140 cfs, Pool EL -189.0		
1	-220.00	-190.0	30.0
2	-220.00	-189.9	30.1
3	-221.24	-191.2	30.0
4	-223.31	-192.0	31.3
5	-226.21	-194.1	32.1
6	-229.32	-196.8	32.5
6a	-253.40	-196.9	56.5
6b	-253.40	-197.1	56.3
7	-283.25	-201.2	82.1
8	-283.25	-196.5	86.8
9	-289.88	-201.5	88.4
10	-298.50	-200.1	98.4
11	-310.00	-197.9	112.1
12	-304.30	-200.3	104.0
13	-304.35	-201.0	103.4
14	-304.40	-201.0	103.4
15	-304.45	-201.3	103.2
16	-304.50	-201.3	103.2
17	-304.55	-201.5	103.1
18	-304.60	-201.8	102.8

(Continued)

Table 2 (Concluded)

Piezometer No.	Piezometer El	Hydraulic Gradient El	Pressure ft
19	-304.65	-202.1	102.6
20	-304.70	-202.2	102.5
21	-304.75	-202.2	102.6
22	-304.80	-202.5	102.3
23	-304.85	-202.3	102.6
24	-304.90	-202.7	102.2
25	-304.95	-202.4	102.6
26	-305.00	-203.3	101.7
27	-305.05	-203.2	101.9
28	-305.10	-203.3	101.8
29	-305.15	-203.5	101.7
30	-305.20	-203.7	101.5
31	-305.25	-204.2	101.1
32	-305.30	-204.3	101.0
33	-305.35	-204.3	101.1
34	-305.40	-204.6	100.8
35	-305.45	-204.8	100.7
36	-305.50	-204.9	100.6
37	-305.55	-205.2	100.4
38	-305.60	-205.2	100.4
39	-305.65	-205.5	100.2
40	-305.70	-206.4	99.3
41	-305.75	-205.3	100.5
42	-305.80	-205.6	100.2
43	-305.85	-205.8	100.1

Table 3

Separate and Total Losses in Intake

Type 1 Intake

Discharge cfs	Pool El	Energy Gradient* ℄ of Shaft	Energy Gradient** at Sta 0+23	H_c	H_t	H_e	K_c	K_t	K_e
2,140	-189.0	-190.4	-193.8	1.4	3.4	4.8	0.212	0.515	0.727
2,000	-190.0	-191.1	-194.0	1.1	2.9	4.0	0.190	0.500	0.690
1,750	-189.7	-190.6	-193.1	0.9	2.5	3.4	0.205	0.568	0.773
1,500	-190.2	-190.6	-192.9	0.7	2.0	2.7	0.219	0.625	0.844
1,300	-189.9	-190.4	-191.7	0.5	1.3	1.8	0.208	0.542	0.750
1,100	-190.1	-190.5	-191.3	0.4	0.8	1.2	0.235	0.470	0.705
						Average	0.211	0.536	0.747

Note: $H_c = K_c \frac{v^2}{2g}$ = Loss in feet from the water surface to el -253.4 in riser shaft.

$H_t = K_t \frac{v^2}{2g}$ = Loss in feet from el -253.4 to just inside the conduit entrance (sta 0+23).

$H_e = K_e \frac{v^2}{2g}$ = Total entrance loss.

K_c = Entrance loss coefficient.

K_t = Elbow loss coefficient.

K_e = Total loss coefficient.

* Determined from hydraulic gradients based on piezometers located in shaft at sta 0+00 and el -253.4.

** Determined from hydraulic gradients based on piezometers 18-36 extended to sta 0+23.

Table 4

Hydraulic Gradients and Pressures, Type 2 Design

Piezometer No.	Piezometer El	Hydraulic Gradient El	Pressure ft
	Discharge 500 cfs, Pool El -190.7		
1a	-214.50	-190.0	23.5
1b	-214.50	-191.0	23.5
1	-220.00	-190.7	29.3
2	-220.00	-190.9	30.1
3	-221.24	-190.0	31.2
4	-223.31	-190.1	33.2
5	-226.21	-190.2	36.0
6	-229.32	-190.4	38.9
6a	-253.40	-191.1	62.3
6b	-250.40	-191.3	62.4
7	-281.25	-190.9	90.4
8	-281.25	-190.6	90.7
	-289.88	-191.0	98.9
10	-298.50	-191.0	107.5
11*	-310.00	0	0
12	-304.30	-191.0	113.3
13	-304.35	-191.1	113.3
14	-304.40	-191.1	113.3
15	-304.45	-191.2	113.3
16	-304.50	-191.2	113.3
17	-304.55	-191.2	113.4
18	-304.60	-191.3	113.3
19	-304.65	-191.4	113.2
20	-304.70	-191.3	113.4
21	-304.75	-191.4	113.4
22	-304.80	-191.4	113.4
23*	-304.85	0	0
24*	-304.90	0	0
25	-304.95	-191.5	113.4
26	-305.00	-191.5	113.5
27*	-305.05	0	0
28	-305.10	-191.5	113.6
29	-305.15	-191.5	113.6
30	-305.20	-191.5	113.7
31	-305.25	-191.6	113.7
32	-305.30	-191.5	113.8
33	-305.35	-191.5	113.9
34	-305.40	-191.5	113.9

(Continued)

* Piezometer malfunction.

Table 4 (Continued)

Piezometer No.	Piezometer El	Hydraulic Gradient El	Pressure ft
35	-305.45	-191.5	113.9
36	-305.50	-191.5	114.0
37	-305.55	-191.6	114.0
38	-305.60	-191.6	114.0
39	-305.65	-191.7	113.9
40	-305.70	-191.7	114.0
41	-305.75	-191.7	114.1
42	-305.80	-191.8	114.0
43	-305.85	-191.8	114.1
	Discharge 1,100 cfs, Pool El -190.9		
1a	-214.50	-191.8	114.2
1b	-214.50	-191.6	114.5
1	-220.00	-190.9	29.1
2	-220.00	-190.3	29.7
3	-221.24	-190.9	30.3
4	-223.31	-191.2	32.1
5	-226.21	-191.8	34.4
6	-229.32	-192.7	36.6
6a	-253.40	-193.0	60.4
6b	-250.40	-193.0	60.4
7	-281.25	-193.9	87.4
8	-281.25	-192.5	88.8
9	-289.88	-192.3	97.6
10	-298.50	-193.8	104.7
11*	-310.00	0	0
12	-304.30	-193.8	110.5
13	-304.35	-194.3	110.1
14	-304.40	-194.2	110.2
15	-304.45	-194.3	110.1
16	-304.50	-194.4	110.1
17	-304.55	-194.4	110.2
18	-304.60	-194.5	110.1
19	-304.65	-194.5	110.1
20	-304.70	-194.6	110.1
21	-304.75	-194.6	110.2
22	-304.80	-194.6	110.2
23	-304.85	-194.0	110.9
24*	-304.90	0	0
25	-304.95	-194.7	110.3
26	-305.00	-194.8	110.2

(Continued)

* Piezometer malfunction.

Table 4 (Continued)

Piezometer No.	Piezometer El	Hydraulic Gradient El	Pressure ft
27	-305.05	-194.9	110.2
28	-305.10	-195.1	110.0
29	-305.15	-195.2	109.9
30	-305.20	-195.3	109.9
31	-305.25	-195.4	109.9
32	-305.30	-195.4	109.9
33	-305.35	-195.5	109.9
34	-305.40	-195.6	109.8
35	-305.45	-195.7	109.8
36	-305.50	-195.7	109.8
37	-305.55	-195.8	109.8
38	-305.60	-195.9	109.7
39	-305.65	-195.9	109.7
40	-305.70	-195.9	109.8
41	-305.75	-195.9	109.9
42	-305.80	-196.1	109.7
43	-305.85	-196.1	109.8
	Discharge 1,300 cfs, Pool El -190.3		
1a	-214.50	-191.2	23.3
1b	-214.50	-191.1	23.4
1	-220.00	-190.3	29.5
2	-220.00	-190.2	29.8
3	-221.24	-191.1	30.1
4	-223.31	-191.3	32.0
5	-226.21	-192.1	34.1
6	-229.32	-193.2	36.1
6a	-253.40	-193.3	60.1
6b	-250.40	-193.3	60.1
7	-281.25	-194.8	86.4
8	-281.25	-193.1	88.2
9	-289.88	-195.0	94.9
10	-298.50	-193.4	105.1
11*	-310.00	0	0
12	-304.30	-194.6	109.7
13	-304.35	-195.0	109.4
14	-304.40	-195.0	109.4
15	-304.45	-195.0	109.4
16	-304.50	-195.0	109.5
17	-304.55	-195.0	109.6
18	-304.60	-195.1	109.5

(Continued)

* Piezometer malfunction.

Table 4 (Continued)

Piezometer No.	Piezometer El	Hydraulic Gradient El	Pressure ft
19	-304.65	-195.2	109.4
20	-304.70	-195.3	109.4
21	-304.75	-195.3	109.4
22	-304.80	-195.4	109.4
23*	-304.85	0	0
24*	-304.90	0	0
25	-304.95	-195.6	109.4
26	-305.00	-195.8	109.2
27*	-305.05	0	0
28	-305.10	-195.9	109.2
29	-305.15	-195.9	109.2
30	-305.20	-196.0	109.2
31	-305.25	-196.2	109.1
32	-305.30	-196.2	109.1
33	-305.35	-196.2	109.2
34	-305.40	-196.4	109.0
35	-305.45	-196.5	108.9
36	-305.50	-196.6	108.9
37	-305.55	-196.7	108.9
38	-305.60	-196.8	108.8
39	-305.65	-196.8	108.8
40	-305.70	-196.7	109.0
41	-305.75	-196.8	108.9
42	-305.80	-197.0	108.8
43	-305.85	-197.0	108.9
	Discharge 1,500 cfs, Pool El -189.8		
1a	-214.50	-191.2	23.3
1b	-214.50	-191.8	22.7
1*	-220.00	0	0
2	-220.00	-190.2	29.8
3	-221.24	-191.2	30.0
4	-223.31	-191.6	31.7
5	-226.21	-192.8	33.4
6	-229.32	-194.0	35.3
6a	-253.40	-193.8	59.1
6b	-250.40	-193.8	59.1
7	-281.25	-196.2	85.1
8	-281.25	-193.9	87.4
9	-289.88	-196.6	93.3
10	-298.50	-196.1	102.4

(Continued)

* Piezometer malfunction.

Table 4 (Continued)

Piezometer No.	El	Hydraulic Gradient El	Pressure ft
11*	-310.00	0	0
12	-304.30	-195.9	108.4
13	-304.35	-196.1	108.3
14	-304.40	-196.1	108.3
15	-304.45	-196.2	108.3
16	-304.50	-196.2	108.3
17	-304.55	-196.3	108.3
18	-304.60	-196.4	108.2
19	-304.65	-196.8	108.6
20	-304.70	-196.9	107.8
21	-304.75	-196.9	107.9
22	-304.80	-197.0	107.8
23*	-304.85	0	0
24*	-304.90	0	0
25	-304.95	-197.0	107.9
26	-305.00	-197.2	107.8
27*	-305.05	0	0
28	-305.10	-197.3	107.8
29	-305.15	-197.3	107.8
30	-305.20	-197.5	107.7
31	-305.25	-197.7	107.6
32	-305.30	-197.8	107.5
33	-305.35	-197.9	107.5
34	-305.40	-198.0	107.4
35	-305.45	-198.1	107.4
36	-305.50	-198.2	107.3
37	-305.55	-198.3	107.3
38	-305.60	-198.3	107.3
39	-305.65	-198.5	107.1
40	-305.70	-198.5	107.2
41	-305.75	-198.5	107.3
42	-305.80	-198.9	106.9
43	-305.85	-198.9	107.0
	Discharge 1,750 cfs, Pool El -190.5		
1a	-214.50	-191.7	22.8
1b	-214.50	-191.0	23.5
1	-220.00	-190.5	29.7
2	-220.00	-190.8	31.0
3	-221.24	-190.6	30.6
4	-223.31	-191.3	32.0

(Continued)

* Piezometer malfunction.

Table 4 (Continued)

Piezometer No.	Piezometer El	Hydraulic Gradient El	Pressure ft
5	-226.21	-192.7	33.5
6	-229.32	-194.5	34.8
6a	-253.40	-195.9	57.5
6b	-250.40	-195.9	57.5
7	-281.25	-197.6	83.7
8	-281.25	-194.2	87.1
9	-289.88	-197.8	92.1
10	-298.50	-196.4	102.1
11*	-310.00	0	0
12	-304.30	-197.6	106.7
13	-304.35	-198.1	106.3
14	-304.40	-198.1	106.3
15	-304.45	-198.3	106.1
16	-304.50	-198.4	106.1
17	-304.55	-198.5	106.1
18	-304.60	-198.9	105.7
19	-304.65	-199.1	105.5
20	-304.70	-199.2	105.5
21	-304.75	-199.2	105.6
22	-304.80	-199.4	105.4
23*	-304.85	0	0
24*	-304.90	0	0
25	-304.95	-199.6	105.4
26	-305.00	-200.2	104.8
27	-305.05	-200.3	104.8
28	-305.10	-200.5	104.6
29	-305.15	-200.7	104.4
30	-305.20	-200.8	104.4
31	-305.25	-201.1	104.2
32	-305.30	-201.2	104.1
33	-305.35	-201.2	104.2
34	-305.40	-201.6	103.8
35	-305.45	-201.8	103.6
36	-305.50	-201.9	103.6
37	-305.55	-202.1	103.5
38	-305.60	-202.2	103.4
39	-305.65	-202.6	103.0
40	-305.70	-202.7	103.0
41	-305.75	-202.7	103.1
42	-305.80	-203.0	102.8
43	-305.85	-203.1	102.8

(Continued)

* Piezometer malfunction.

Table 4 (Continued)

Piezometer No.	Piezometer El	Hydraulic Gradient El	Pressure ft
	Discharge 2,000 cfs, Pool El -190.1		
1a	-214.50	-190.9	23.6
1b	-214.50	-190.8	23.7
1	-220.00	-190.1	29.9
2	-220.00	-190.0	31.0
3	-221.24	-191.6	29.6
4	-223.31	-192.5	30.8
5	-226.21	-195.0	31.2
6	-229.32	-197.6	31.7
6a	-253.40	-197.0	56.4
6b	-250.40	-197.1	56.3
7	-281.25	-201.9	79.4
8	-281.25	-197.0	84.3
9	-289.88	-202.4	87.5
10	-298.50	-200.0	98.5
11*	-310.00	0	0
12	-304.30	-201.9	102.4
13	-304.35	-201.8	102.6
14	-304.40	-201.7	102.7
15	-304.45	-201.9	102.5
16	-304.50	-201.9	102.6
17	-304.55	-202.1	102.5
18	-304.60	-202.5	102.1
19	-304.65	-202.6	102.0
20	-304.70	-202.9	101.8
21	-304.75	-202.8	101.9
22	-304.80	-203.0	101.8
23*	-304.85	0	0
24*	-304.90	0	0
25	-304.95	-203.7	101.3
26	-305.00	-203.9	101.1
27*	-305.05	0	0
28	-305.10	-204.1	101.0
29	-305.15	-204.0	101.1
30	-305.20	-204.3	100.9
31	-305.25	-204.8	100.4
32	-305.30	-204.7	100.6
33	-305.35	-204.8	100.6
34	-305.40	-205.1	100.3
35	-305.45	-205.2	100.3
36	-305.50	-205.3	100.2

(Continued)

* Piezometer malfunction.

Table 4 (Continued)

Piezometer No.	Piezometer El	Hydraulic Gradient El	Pressure ft
37	-305.55	-205.6	100.0
38	-305.60	-205.6	100.0
39	-305.65	-205.9	99.7
40	-305.70	-205.9	99.8
41	-305.75	-206.0	99.8
42	-305.80	-206.3	99.5
43	-305.85	-206.5	99.4
	Discharge 2,140 cfs, Pool El -189.5		
1a	-214.50	-190.5	24.0
1b	-214.50	-190.0	24.5
1	-220.00	-189.5	29.5
2	-220.00	-189.8	31.2
3	-221.24	-191.0	30.2
4	-223.31	-192.0	31.3
5	-226.21	-194.5	31.7
6	-229.32	-197.3	32.0
6a	-253.40	-197.3	56.1
6b	-250.40	-197.5	55.9
7	-281.25	-201.7	79.6
8	-281.25	-196.7	84.6
9	-289.88	-202.4	87.5
10	-298.50	-200.3	98.2
11*	-310.00	0	0
12	-304.30	-200.8	103.5
13	-304.35	-201.7	102.7
14	-304.40	-201.7	102.7
15	-304.45	-201.8	102.6
16	-304.50	-201.9	102.6
17	-304.55	-202.0	102.6
18	-304.60	-202.6	102.0
19	-304.65	-202.6	102.0
20	-304.70	-203.0	101.7
21	-304.75	-203.1	101.6
22	-304.80	-203.2	101.6
23*	-304.85	0	0
24*	-304.90	0	0
25	-304.95	-204.0	100.9
26	-305.00	-204.5	100.5
27*	-305.05	0	0
28	-305.10	-204.7	100.4

(Continued)

* Piezometer malfunction.

Table 4 (Concluded)

Piezometer No.	Piezometer El	Hydraulic Gradient El	Pressure ft
29	-305.15	-204.8	100.3
30	-305.20	-205.0	100.2
31	-305.25	-205.0	100.3
32	-305.30	-205.2	100.1
33	-305.35	-205.3	100.1
34	-305.40	-205.4	100.0
35	-305.45	-205.9	99.5
36	-305.50	-206.0	99.5
37	-305.55	-206.1	99.5
38	-305.60	-206.3	99.3
39	-305.65	-206.7	98.9
40	-305.70	-206.8	98.9
41	-305.75	-206.9	98.9
42	-305.80	-207.2	98.6
43	-305.85	-207.5	98.4

Table 5

Separate and Total Losses in Intake

Type 2

Discharge cfs	Pool El	Energy Gradient* ℄ of Shaft	Energy Gradient** at Sta 0+23	H_c	H_t	H_e	K_c	K_t	K_e
2,140	-189.5	-190.8	-194.7	1.3	3.9	5.2	0.197	0.591	0.788
2,000	-190.1	-191.3	-195.0	1.2	3.7	4.9	0.208	0.642	0.850
1,750	-190.5	-191.5	-193.4	1.0	1.9	2.9	0.227	0.431	0.658
1,500	-189.8	-190.6	-192.4	0.8	1.8	2.6	0.247	0.556	0.803
1,300	-190.3	-190.9	-192.1	0.6	1.2	1.8	0.247	0.494	0.741
1,100	-190.9	-191.3	-192.3	0.4	1.0	1.4	0.230	0.575	0.805
500	-190.7	-190.8	-191.0	0.1	0.2	0.3	0.270	0.541	0.811
						Average	0.232	0.547	0.779

Note: $H_c = K_c \frac{V^2}{2g}$ = Loss in feet from the water surface to el -253.4 in riser shaft.

$H_t = K_t \frac{V^2}{2g}$ = Loss in feet from el -253.4 to just inside the conduit entrance (sta 0+23).

$H_e = K_e \frac{V^2}{2g}$ = Total entrance loss.

* Determined from hydraulic gradients based on piezometers located in shaft at sta 0+00 and el -253.4.

** Determined from hydraulic gradients based on piezometers 18-36 extended to sta 0+23.

Table 6

Outlet Manifold Hydraulic Gradients

Piezometer No.	Piezometer El	Hydraulic Gradient El	Pressure ft
	Discharge 30,000 cfs, Reservoir Water-Surface El -190.0		
1	-249.00	-165.5	83.5
2	-249.00	-164.5	84.5
3	-265.50	-149.0	116.5
4	-264.70	-183.4	81.3
5	-265.50	-187.5	78.0
6	-265.50	-171.5	94.0
6a	-247.00	-171.0	76.0
6b	-247.00	-173.0	74.0
7	-265.50	-173.0	92.5
8	-265.50	-174.0	91.5
9	-265.50	-174.0	91.5
10	-265.50	-173.5	92.0
11	-265.50	-174.0	91.5
12	-265.50	-174.5	91.0
13	-265.50	-174.0	91.5
14	-265.50	-174.5	91.0
15	-265.50	-174.9	90.6
16	-265.50	-175.0	90.5
17	-265.50	-175.0	90.5
18	-265.50	-175.1	90.4
19	-265.50	-175.1	90.4
20	-265.50	-175.1	90.4
21	-265.50	-175.1	90.4
22	-265.50	-175.1	90.4
23	-265.50	-175.2	90.3
24	-265.50	-175.1	90.1
25	-265.50	175.4	90.1
26	-265.50	-175.4	90.1
27	-265.50	175.2	90.3
28	-265.50	175.3	90.2
29	-265.50	175.4	90.1
30	-265.50	176.0	89.5
31	-265.50	176.0	89.5
32	-265.50	176.0	89.5
33	-265.50	176.0	89.5
34	-265.50	176.0	89.5
35	-265.50	176.1	89.4
36	-265.50	176.3	89.2
37	-265.50	176.3	89.2
38	-265.50	176.4	89.1

(Continued)

Table 6 (Continued)

Piezometer No.	Piezometer El	Hydraulic Gradient El	Pressure ft
39	-265.50	175 0	90.5
40	-265.50	177.2	88.3
41	-265.50	177.0	88.5
42	-265.50	176.7	88.8
43	-265.50	176.2	89.3
44	-265.50	176.0	89.5
45	-265.50	176.0	89.5
46	-265.50	175.5	90.0
47	-265.50	175.3	90.2
48	-265.50	-174.0	91.5
49	-265.50	-173.9	91.6
50	-265.50	-173.8	91.7
51	-265.50	-173.5	92.0
52	-265.50	-173.0	92.5
53	-265.50	-173.0	92.5
54	-265.50	-172.9	92.6
Discharge 50,000 cfs, Reservoir Water-Surface El -190.0			
1	-249.00	-143.0	106.0
2	-249.00	-145.0	104.0
3	-265.50	-115.0	150.5
4	-264.70	-172.0	92.7
5	-265.50	-173.0	92.5
6	-265.50	-145.0	120.5
6a	-247.00	-141.0	106.0
6b	-247.00	-191.2	99.0
7	-265.50	-147.0	118.5
8	-265.50	-152.0	113.5
9	-265.50	-148.0	117.5
10	-265.50	-148.0	117.5
11	-265.50	-149.0	116.5
12	-265.50	-150.0	115.5
13	-265.50	-150.0	115.5
14	-265.50	-150.0	115.5
15	-265.50	-151.0	114.5
16	-265.50	-152.0	113.5
17	-265.50	-152.0	113.5
18	-265.50	-152.0	113.5
19	-265.50	-152.5	113.0
20	-265.50	-153.0	112.5
21	-265.50	-153.0	112.5
22	-265.50	-153.0	112.5
23	-265.50	-153.5	112.0

(Continued)

Table 6 (Continued)

Piezometer No.	Piezometer El	Hydraulic Gradient El	Pressure ft
24	-265.50	-154.0	111.5
25	-265.50	-154.0	111.5
26	-265.50	-154.5	111.0
27	-265.50	-153.5	112.0
28	-265.50	-154.0	111.5
29	-265.50	-154.0	111.5
30	-265.50	-155.0	110.5
31	-265.50	-155.0	110.5
32	-265.50	-155.0	110.5
33	-265.50	-155.0	110.5
34	-265.50	-156.0	109.5
35	-265.50	-156.0	109.5
36	-265.50	-155.0	110.5
37	-265.50	-156.0	109.5
38	-265.50	-155.7	109.8
39	-265.50	-156.0	109.5
40	-265.50	-155.5	110.0
41	-265.50	-155.0	110.5
42	-265.50	-156.0	109.5
43	-265.50	-155.5	110.0
44	-265.50	-155.5	110.0
45	-265.50	-154.5	111.0
46	-265.50	-154.0	111.5
47	-265.50	-154.0	111.5
48	-265.50	-154.7	110.8
49	-265.50	-150.0	115.5
50	-265.50	-152.0	113.5
51	-265.50	-151.0	114.5
52	-265.50	-150.0	115.0
53	-265.50	-150.0	115.0
54	-265.50	-149.0	116.5
Discharge 70,000 cfs, Reservoir Water-Surface El -190.0			
1	-249.00	-108.25	140.7
2	-249.00	-112.75	136.2
3	-265.50	-70.50	195.2
4	-264.70	-160.25	104.4
5	-265.50	-175.0	90.5
6	-265.50	-100.0	165.5
6a	-247.00	-85.0	-180.5
6b	-247.00	-105.0	142.0

(Continued)

* Piezometer malfunction.

Table 6 (Continued)

Piezometer No.	Piezometer El	Hydraulic Gradient El	Pressure ft
7	-265.50	-105.0	160.0
8	-265.50	-103.5	162.0
9	-265.50	-105.5	165.0
10	-265.50	-107.5	158.0
11	-265.50	-109.0	156.5
12	-265.50	-110.0	155.5
13	-265.50	-109.5	156.0
14	-265.50	-110.5	155.0
15	-265.50	-114.5	151.0
16	-265.50	-114.5	151.0
17	-265.50	-115.5	150.0
18	-265.50	-116.0	149.5
19	-265.50	-117.0	148.5
20	-265.50	-116.0	149.5
21	-265.50	-116.5	149.0
22	-265.50	-117.5	148.0
23	-265.50	-118.0	147.5
24	-265.50	-118.5	147.0
25	-265.50	-118.0	147.5
26	-265.50	-117.5	148.0
27	-265.50	-116.5	149.0
28	-265.50	-117.5	148.0
29	-265.50	-117.0	148.5
30	-265.50	-117.5	148.0
31	-265.50	-119.0	146.5
32	-265.50	-119.0	146.5
33	-265.50	-119.0	146.5
34	-265.50	-119.5	146.0
35	-265.50	-119.0	146.5
36	-265.50	-119.0	146.5
37	-265.50	-119.0	146.5
38	-265.50	-119.0	146.5
39	-265.50	-118.5	147.0
40*	-265.50	0	0
41	-265.50	-118.0	147.5
42	-265.50	-117.5	148.0
43	-265.50	-115.5	150.0
44	-265.50	-115.5	150.0
45	-265.50	-115.0	150.5
46	-265.50	-118.0	147.5
47	-265.50	-119.5	146.0

(Continued)

* Piezometer malfunction.

Table 6 (Continued)

Piezometer No.	Piezometer El	Hydraulic Gradient El	Pressure ft
48	-265.50	-118.0	147.5
49	-265.50	-117.0	148.5
50	-265.50	-123.5	142.0
51	-265.50	-116.0	149.5
52	-265.50	-114.0	151.5
53	-265.50	-112.5	153.0
54	-265.50	-111.0	154.5
	Discharge 85,000 cfs, Reservoir Water-Surface El -190.0		
1	-249.00	-90.0	159.0
2	-249.00	-94.0	155.0
3	-265.50	-60.0	189.0
4	-264.70	-185.5	79.2
5	-265.50	-169.0	96.5
6	-265.50	-90.5	175.0
6a	-247.00	-75.0	172.0
6b	-247.00	-96.5	150.5
7	-265.50	-92.0	173.0
8	-265.50	-89.5	176.0
9	-265.50	-90.5	175.0
10	-265.50	-93.0	172.5
11	-265.50	-93.5	172.0
12	-265.50	-94.5	171.0
13	-265.50	-94.0	171.5
14	-265.50	-95.8	169.7
15	-265.50	-97.8	167.7
16	-265.50	-99.0	166.5
17	-265.50	-100.0	165.5
18	-265.50	-99.5	166.0
19	-265.50	-99.0	165.7
20	-265.50	-100.3	165.2
21	-265.50	-101.0	164.5
22	-265.50	-102.0	163.5
23	-265.50	-102.5	163.5
24	-265.50	-103.0	162.5
25	-265.50	-104.5	161.0
26	-265.50	-103.0	162.5
27	-265.50	-102.0	163.5
28	-265.50	-104.0	161.5
29	-265.50	-103.5	162.0
30	-265.50	-104.5	161.0
31	-265.50	-105.0	160.5
32	-265.50	-150.5	160.0

(Continued)

Table 6 (Concluded)

Piezometer No.	El	Hydraulic Gradient El	Pressure ft
33	-265.50	-106.0	159.5
34	-265.50	-106.0	159.5
35	-265.50	-106.5	159.0
36	-265.50	-106.7	158.8
37	-265.50	-105.5	160.0
38	-265.50	-105.5	160.0
39	-265.50	-105.5	160.0
40*	-265.50	0	0
41	-265.50	-104.5	161.0
42	-265.50	-104.7	160.8
43	-265.50	-102.0	163.5
44	-265.50	-104.0	161.5
45	-265.50	-102.0	163.5
46	-265.50	-104.0	161.5
47	-265.50	-104.0	161.5
48	-265.50	-104.0	161.5
49	-265.50	-100.0	165.5
50	-265.50	-97.0	160.5
51	-265.50	-98.5	167.0
52	-265.50	-97.5	168.0
53	-265.50	-96.5	150.5
54	-265.50	-95.5	170.0

* Piezometer malfunction

Table 7

Outlet Manifold Head Loss and Loss Coefficients

Discharge cfs	Reservoir Water-Surface El	Energy Gradient at Upstream End of Manifold*	Head Loss H_e ft of Water	$\frac{V_e^2}{2g}$ ft	Loss Coefficient K_e**
30,000	-190.0	-165.5	24.5	7.5	3.27
50,000	-190.0	-126.3	63.7	20.7	3.08
70,000	-190.0	-60.1	129.9	40.9	3.18
85,000	-190.0	-27.1	162.9	59.9	2.72

* Based on piezometers in manifold (Plate 13).

** Loss coefficient $K_e = \frac{H_e}{V^2/2g}$ where H_e is head loss in ft and $V_e^2/2g$ is velocity head in ft at the upstream end of the manifold (Plate 13).

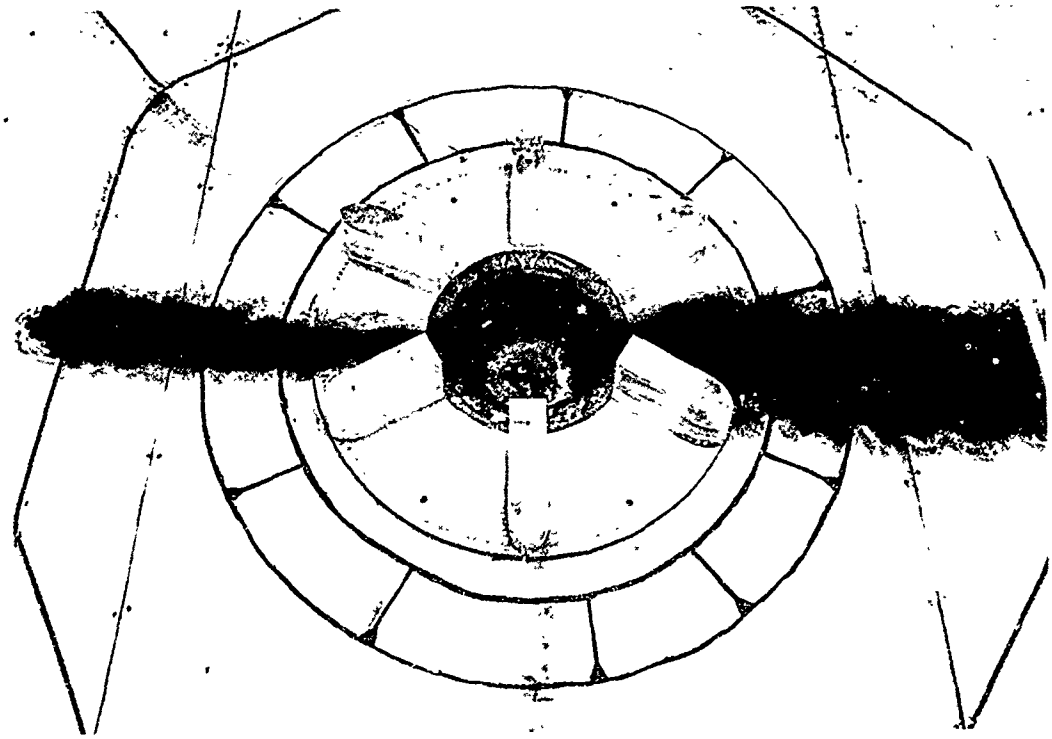

Photo 1. Flow conditions; weir control; no cover plate; discharge 500 cfs, pool el -217.7

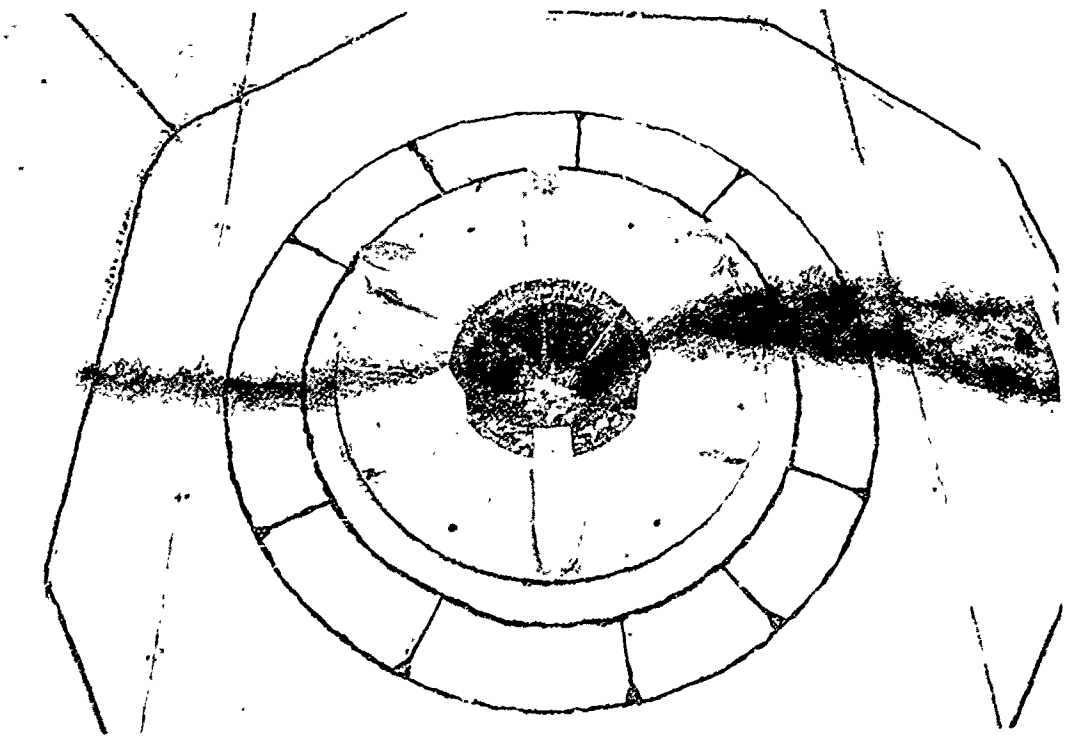

Photo 2. Flow conditions; weir control; no cover plate; discharge 1,000 cfs; pool el -216.1

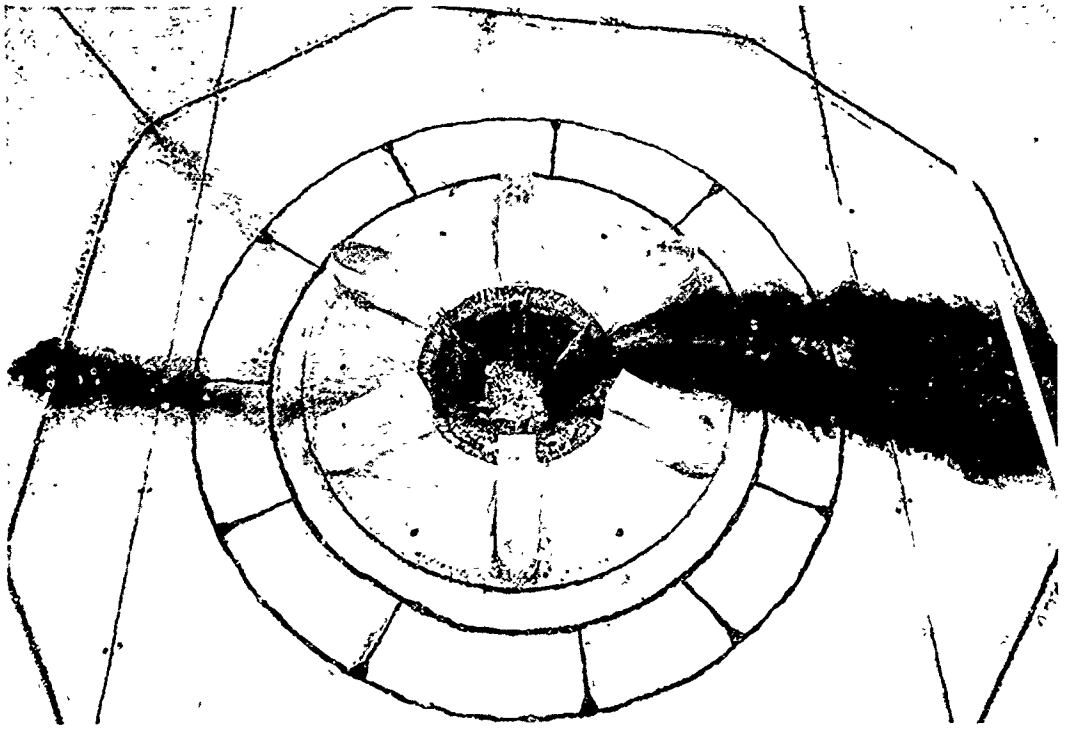

Photo 3. Flow conditions; weir control; no cover plate; discharge 2,000 cfs, pool el -216.1

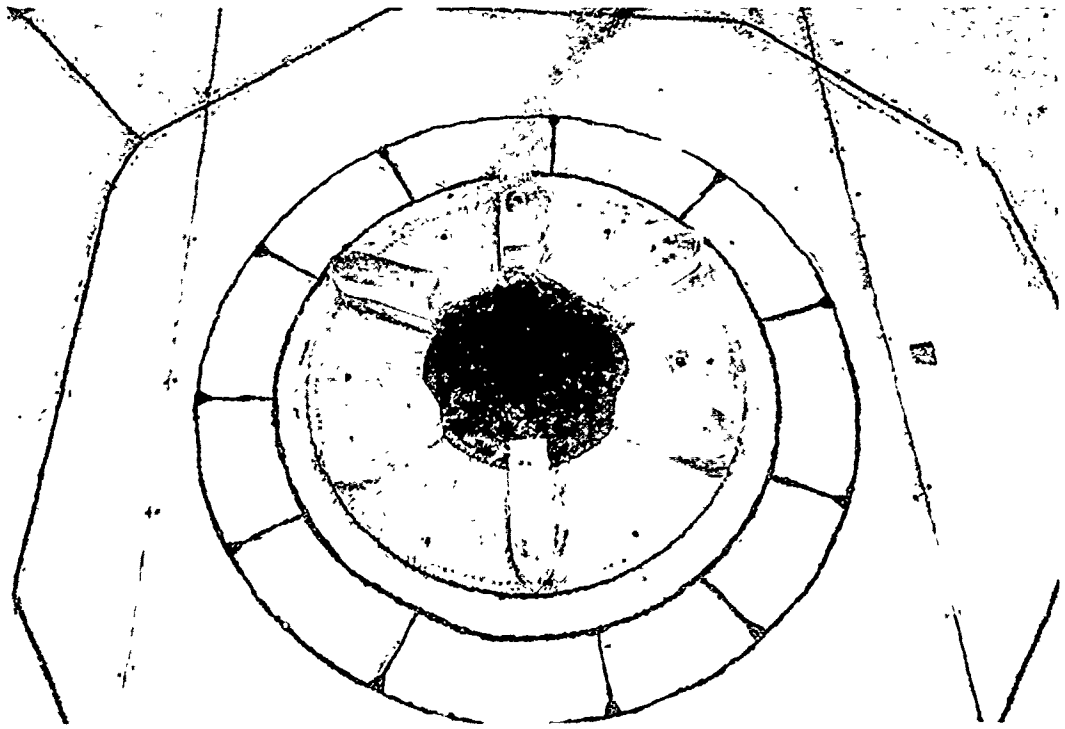

Photo 4. Flow conditions; transition from weir to conduit control; no cover plate; discharge 2,000 cfs, pool el -214.0

Photo 5. Flow conditions; conduit control; no cover plate; discharge 2,000 cfs, pool el -190.0

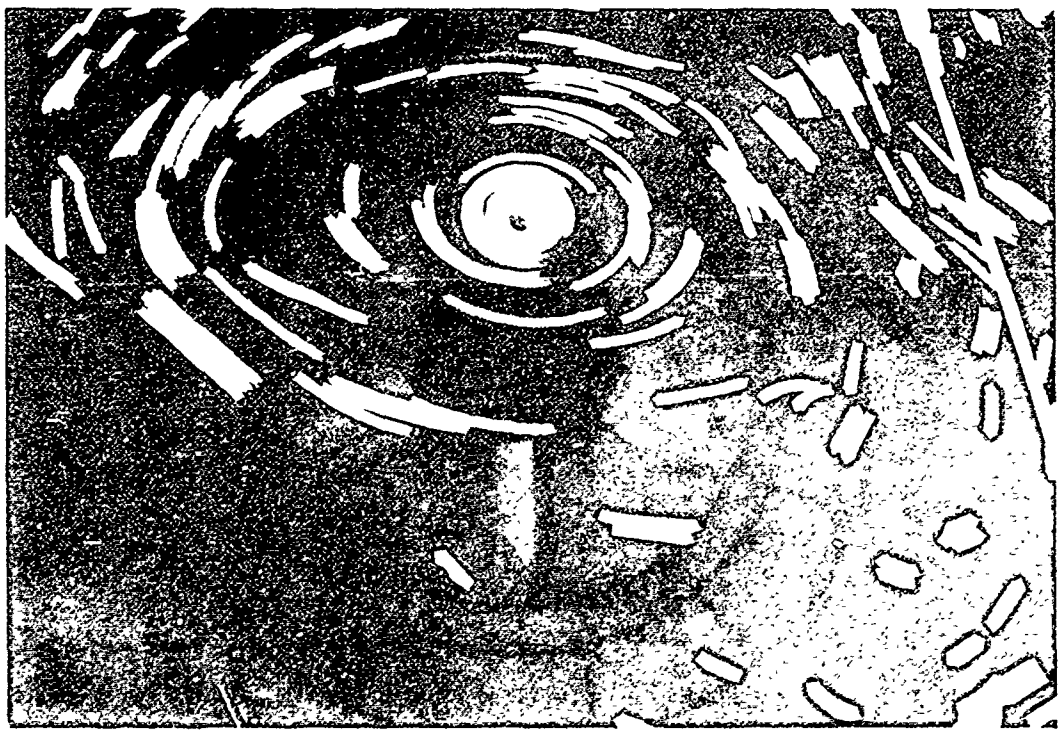

Photo 6. Flow conditions; conduit control; no cover plate; discharge 2,000 cfs, pool el -160.0

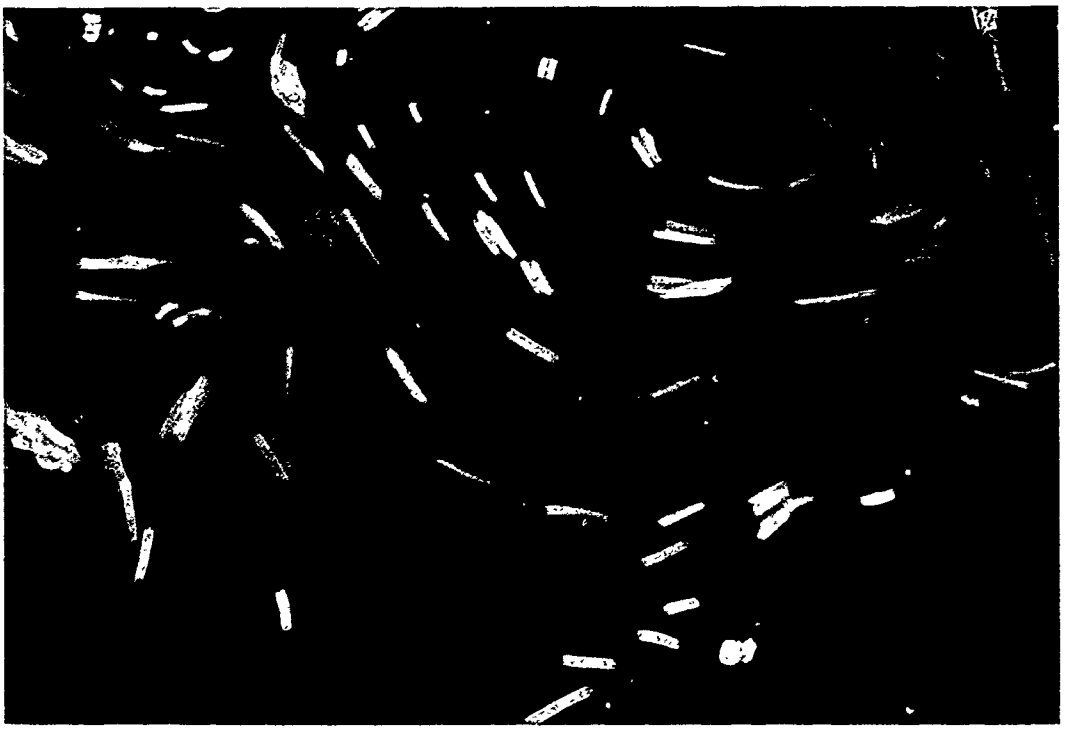

Photo 7. Flow conditions; conduit control; with cover plate; discharge 2,000 cfs, pool el -190.0

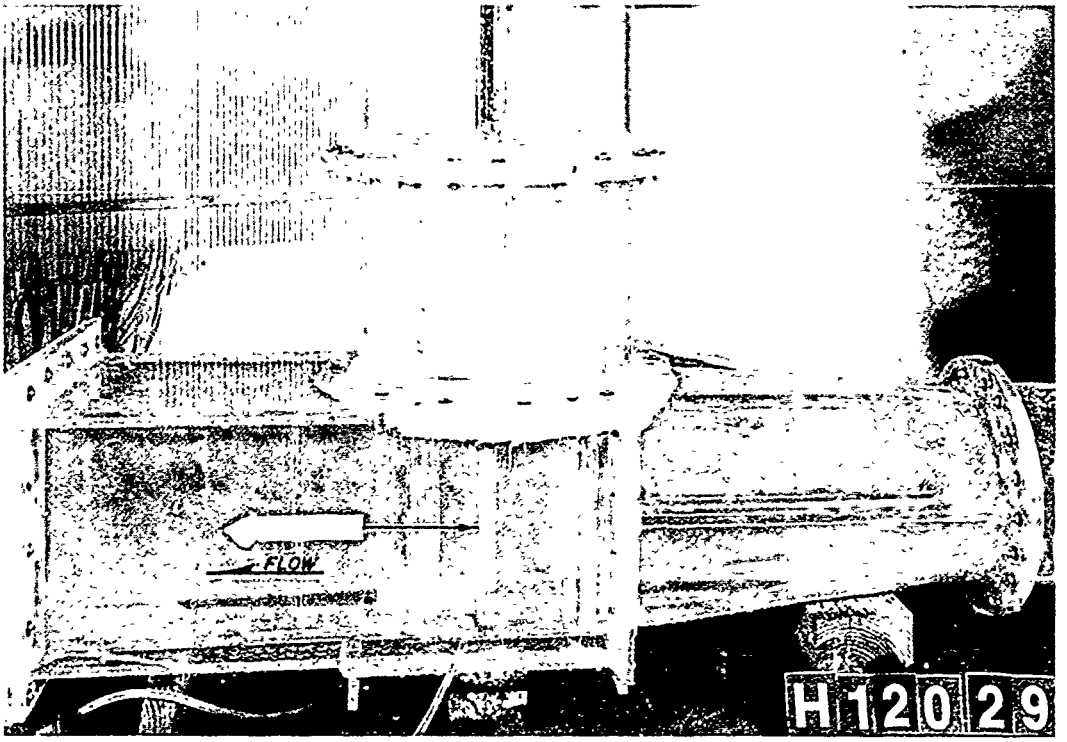

a. Gate 1 fully open, gate 2 fully open

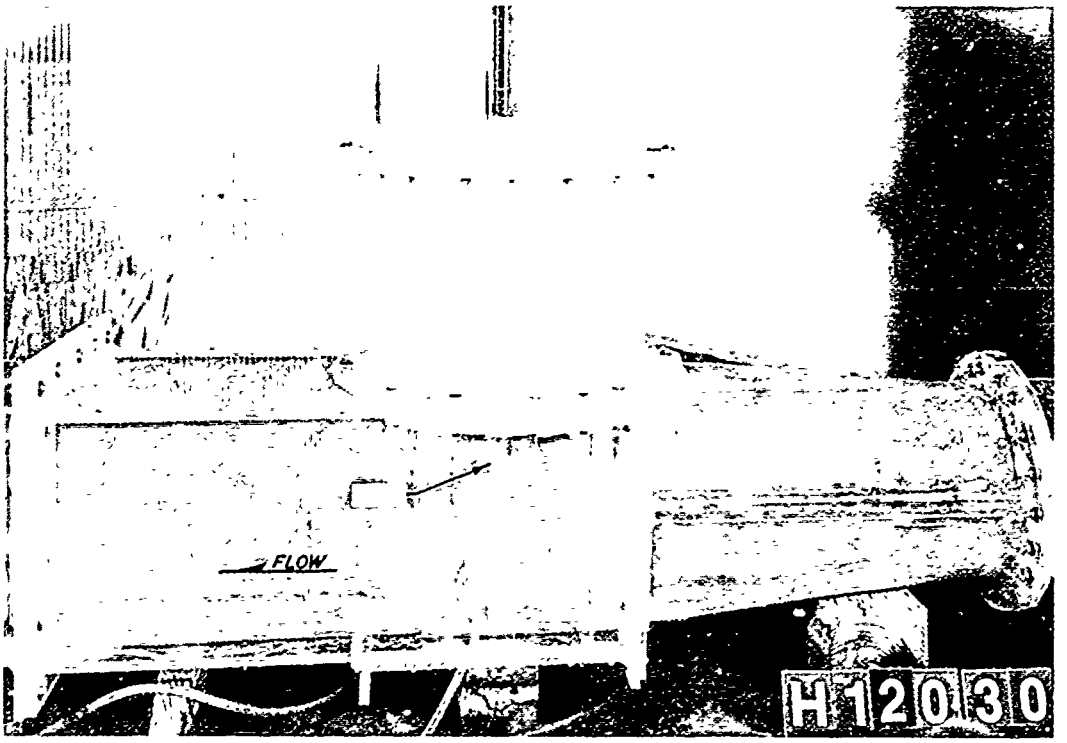

b. Gate 1 fully open, gate 2 three-fourths open

Photo 8. Flow conditions, wheel gate structure; discharge 30,000 cfs; reservoir water-surface el -190.0 (Continued)

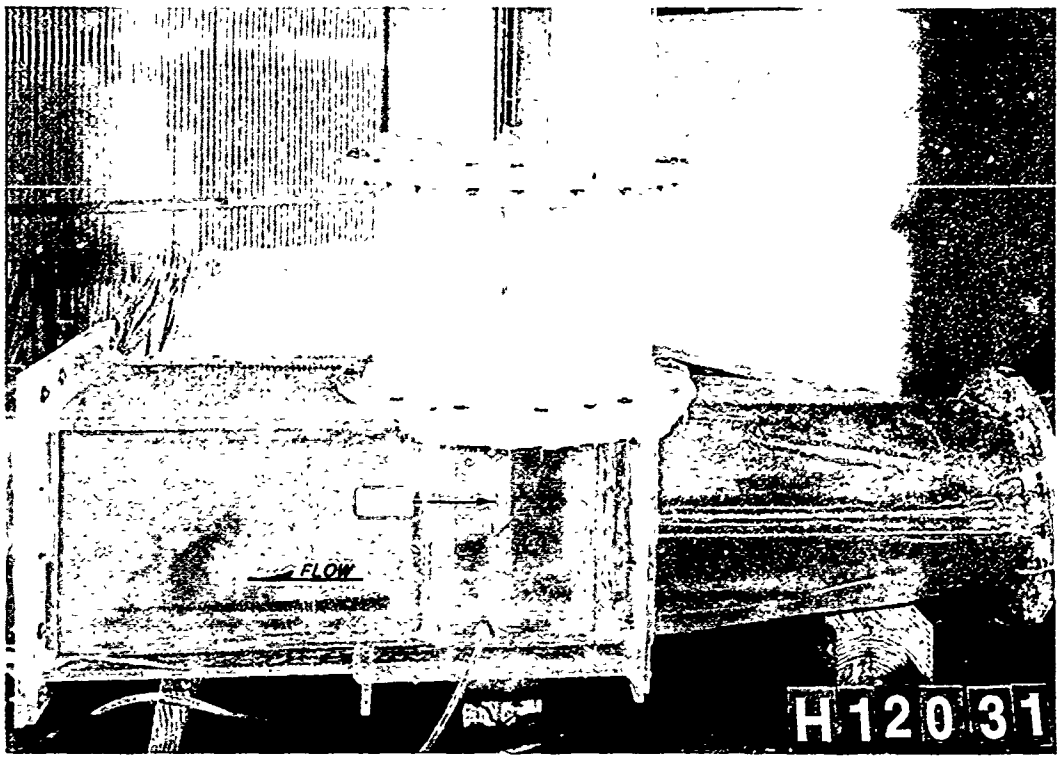

c. Gate 1 fully open, gate 2 half open

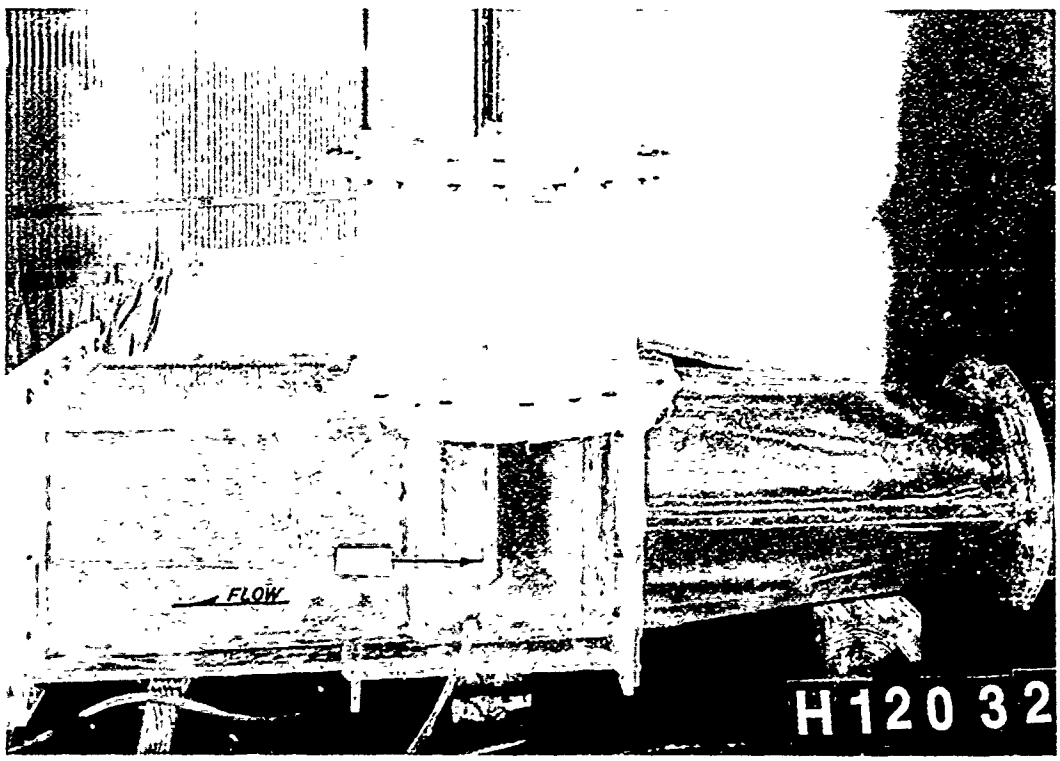

d. Gate 1 fully open, gate 2 one-fourth open

Photo 8. (Concluded)

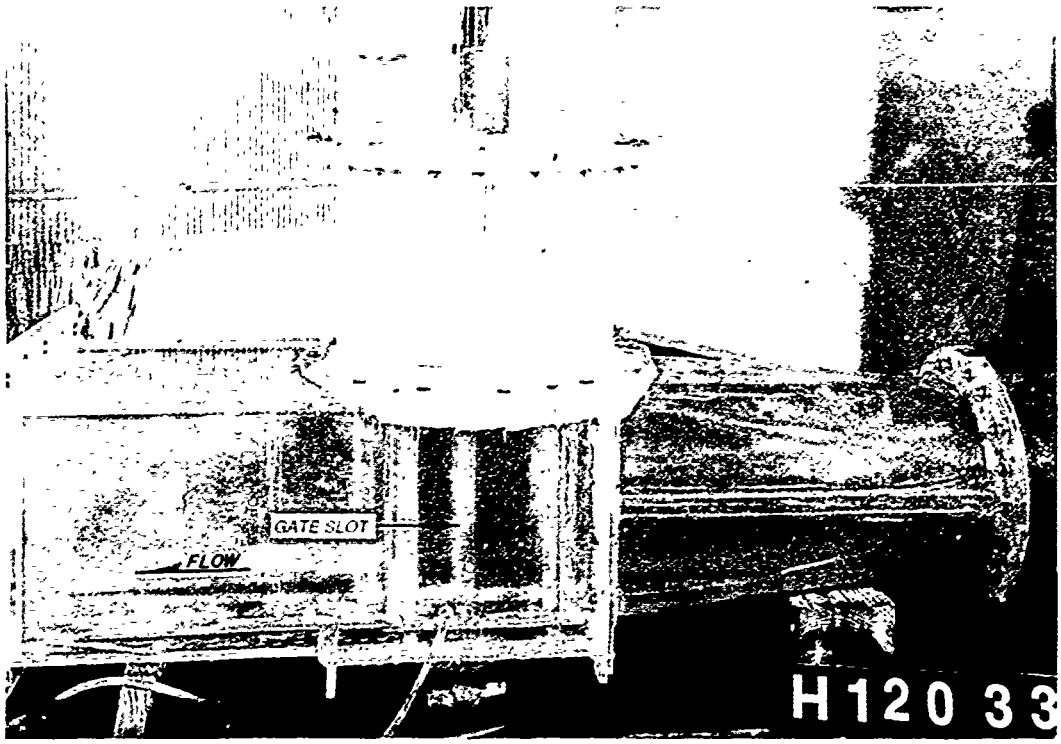

a. Gate 1 fully open, gate 2 fully open

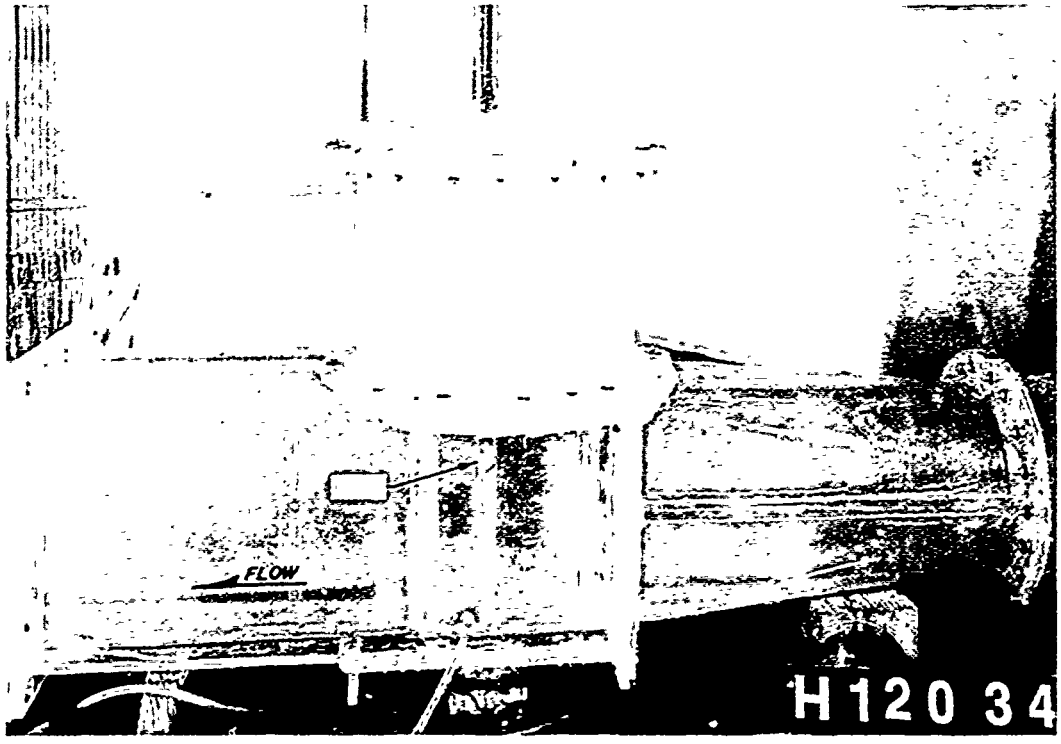

b. Gate 1 fully open, gate 2 three-fourths open

Photo 9. Flow conditions, wheel gate structure; discharge 50,000 cfs; reservoir water-surface el -190.0 (Continued)

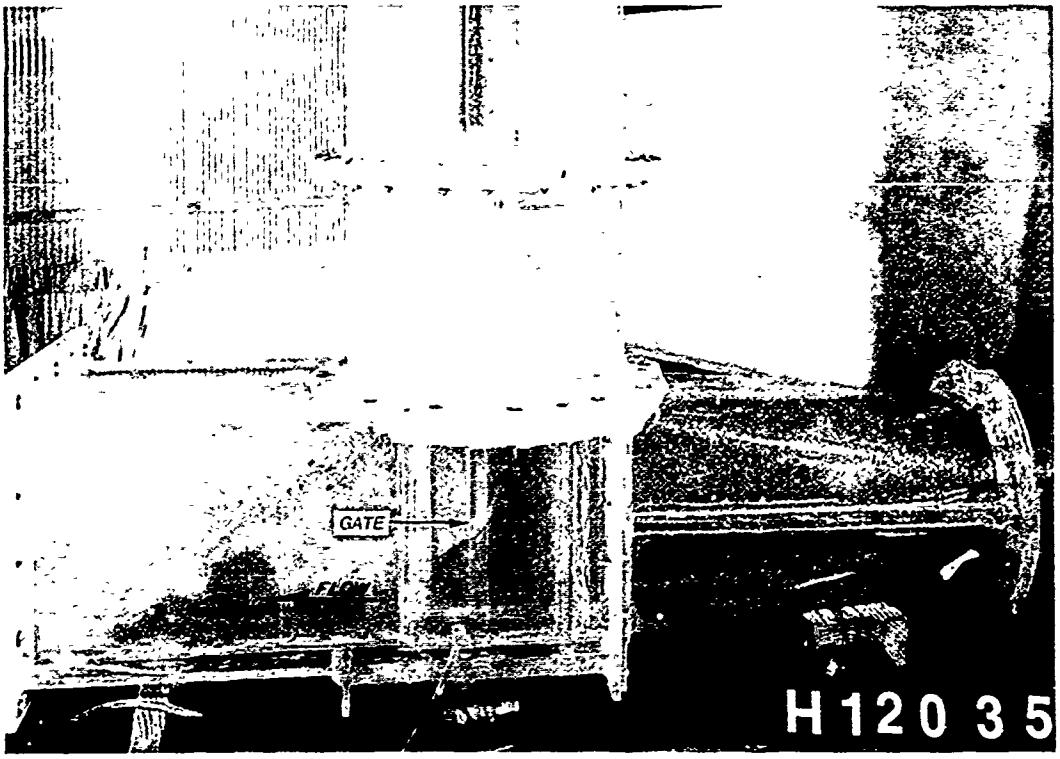

c. Gate 1 fully open, gate 2 half open

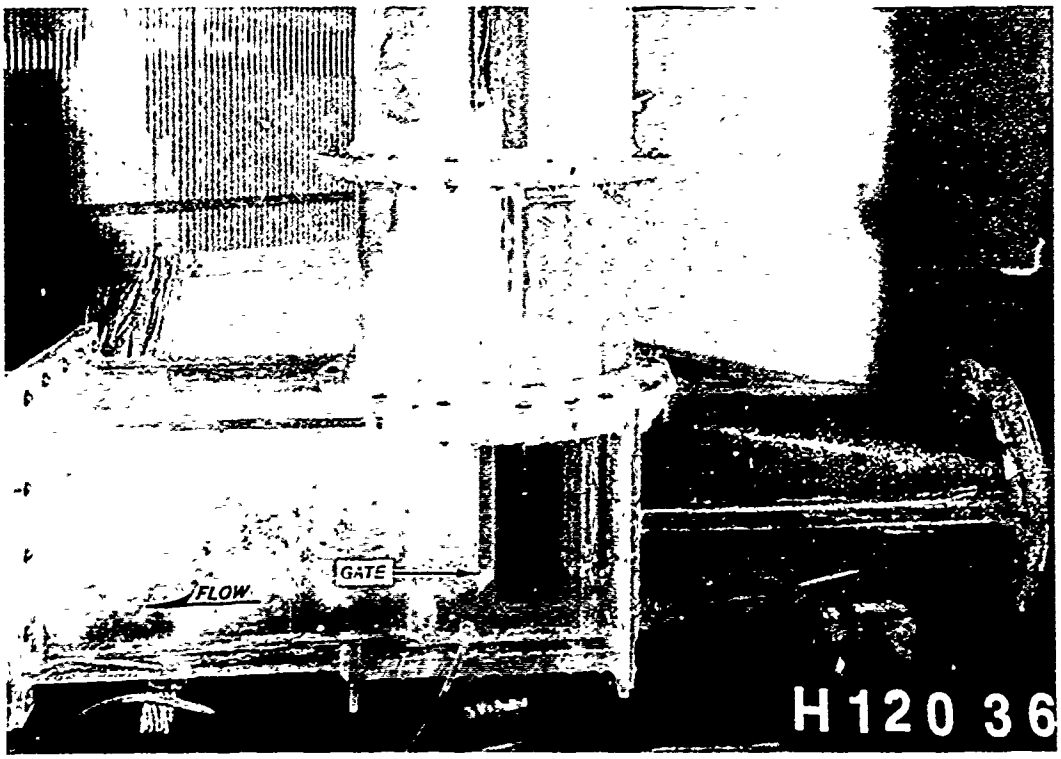

d. Gate 1 fully open, gate 2 one-fourth open

Photo 9. (Concluded)

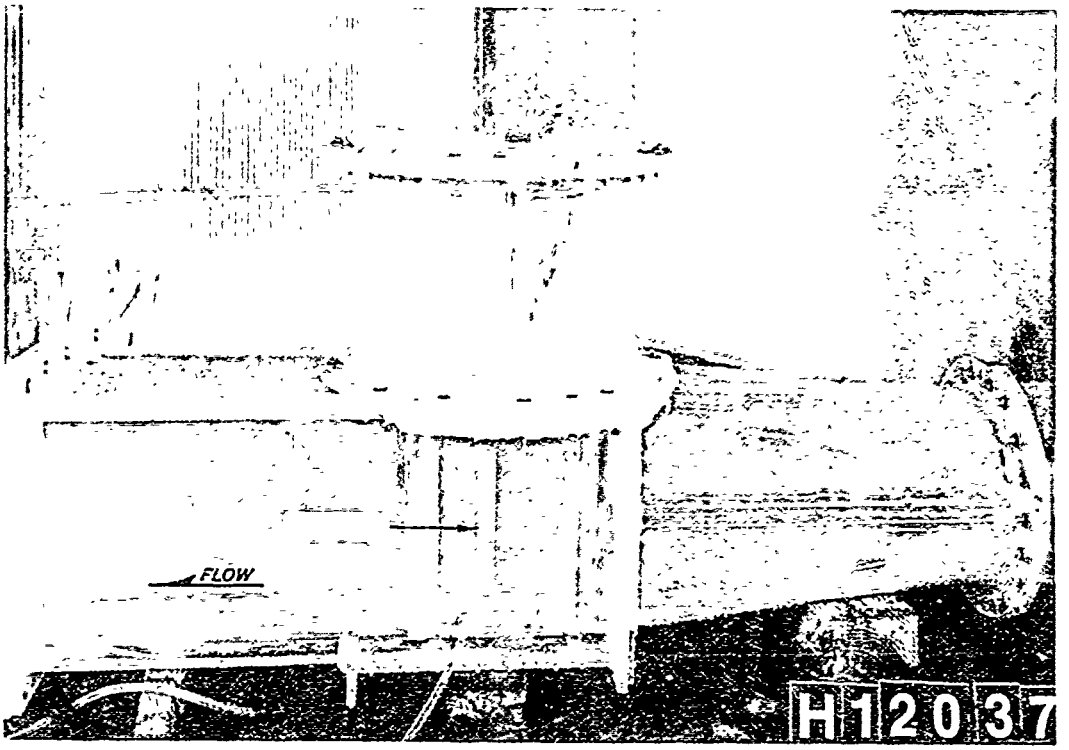

a. Gate 1 fully open, gate 2 fully open

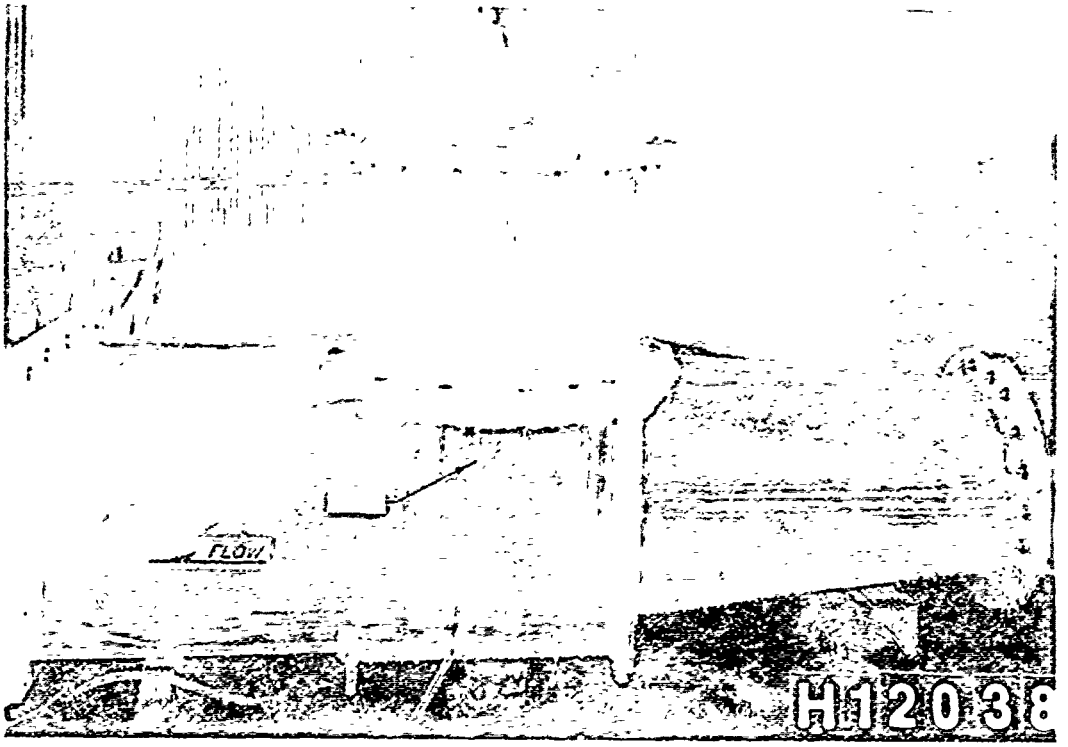

b. Gate 1 fully open, gate 2 fully open

Photo 10 Flow conditions, wheel gate structure, discharge 85,000 cfs, reservoir water surface el 190.0

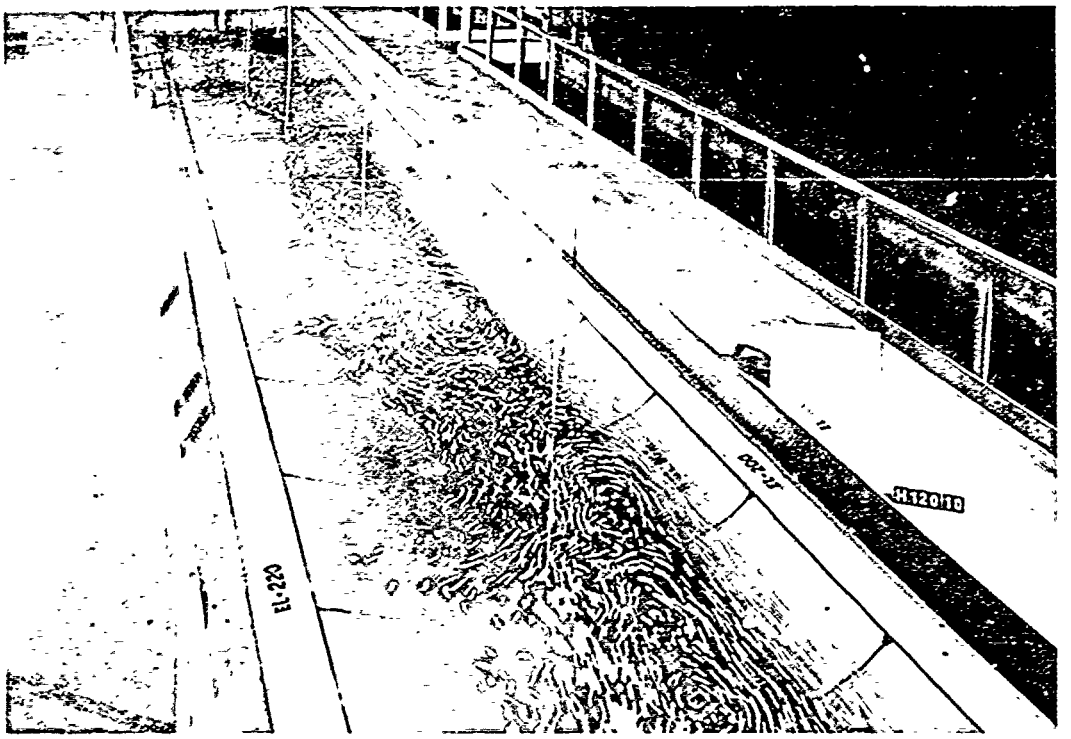

a. Reservoir water-surface el -215.0

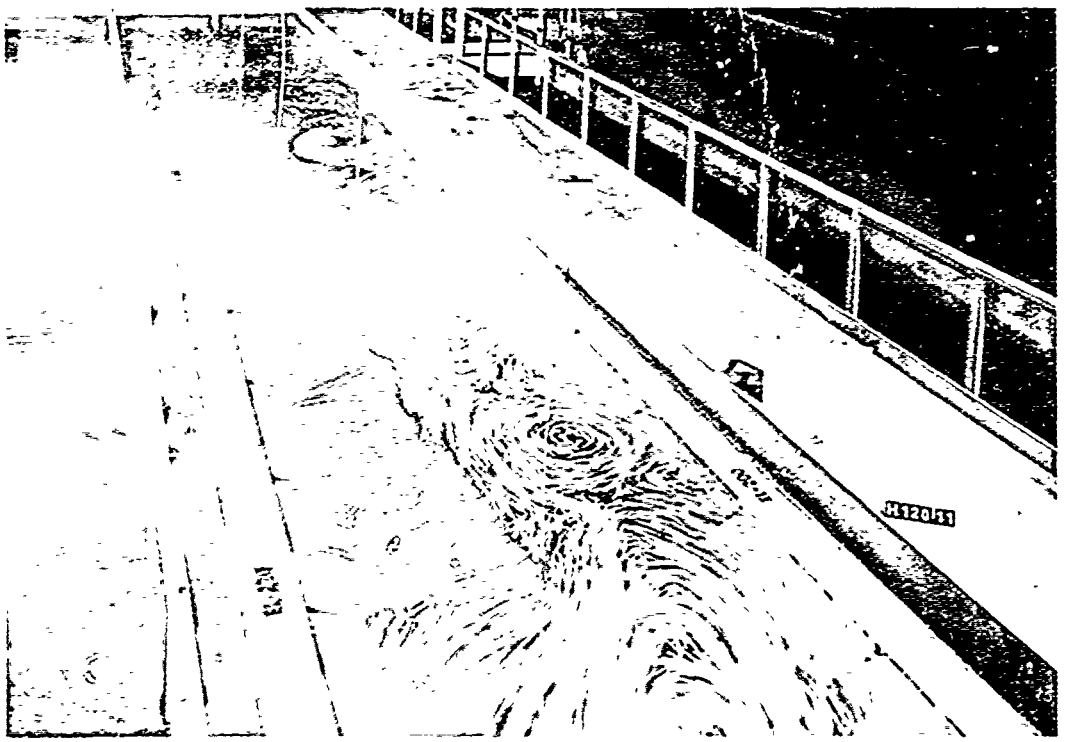

b. Reservoir water-surface el -195.0

Photo 11. Flow conditions, outlet manifold; discharge 10,000 cfs; exposure time 20 sec (prototype) (Continued)

c. Reservoir water-surface el -190.0

Photo 11. (Concluded)

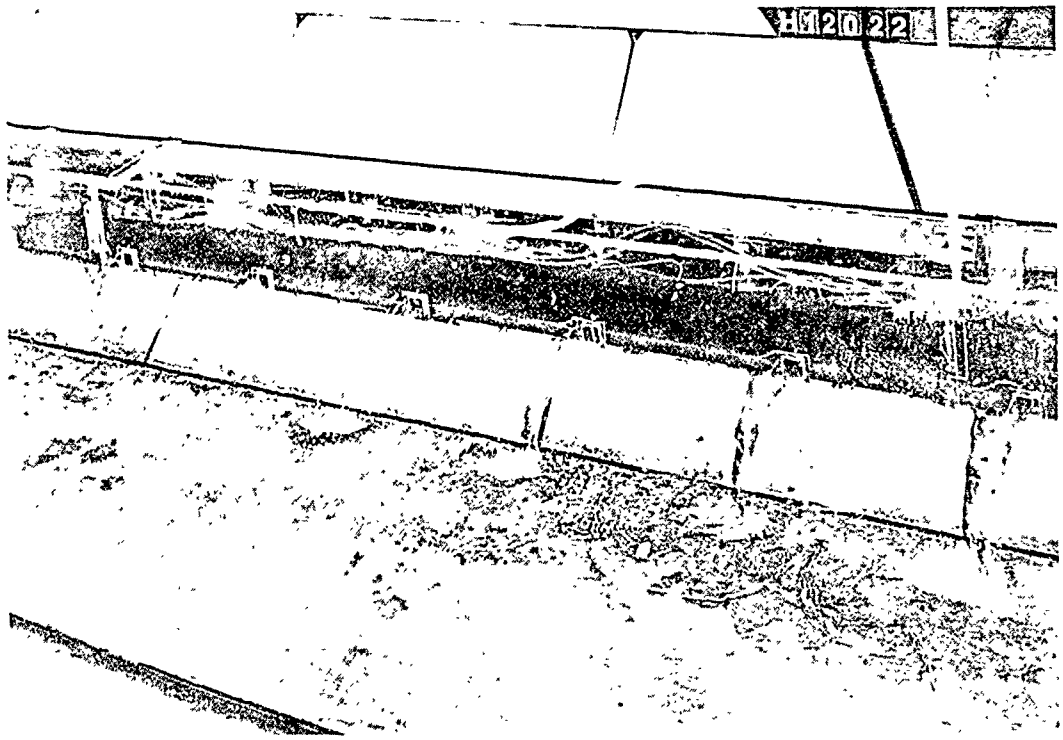

a. Reservoir water-surface el -282.0

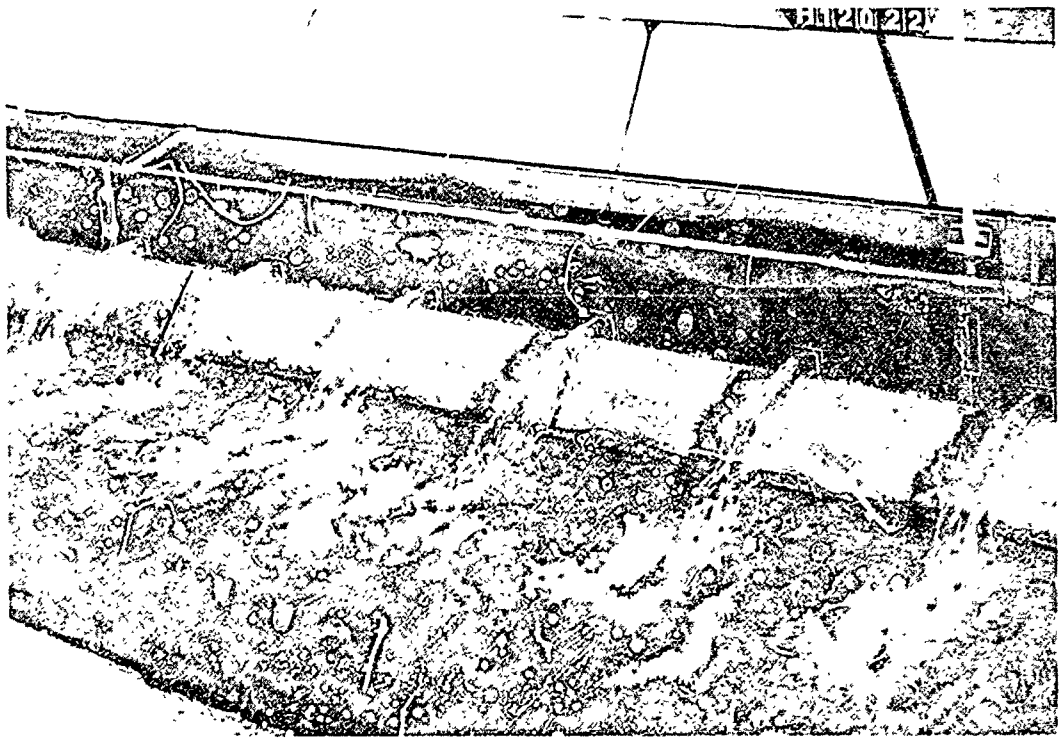

b. Reservoir water-surface el -280.0

Photo 12. Flow conditions, outlet manifold; discharge 30,000 cfs; exposure time 20 sec (prototype) (Sheet 1 of 4)

c. Reservoir water-surface el -265.0

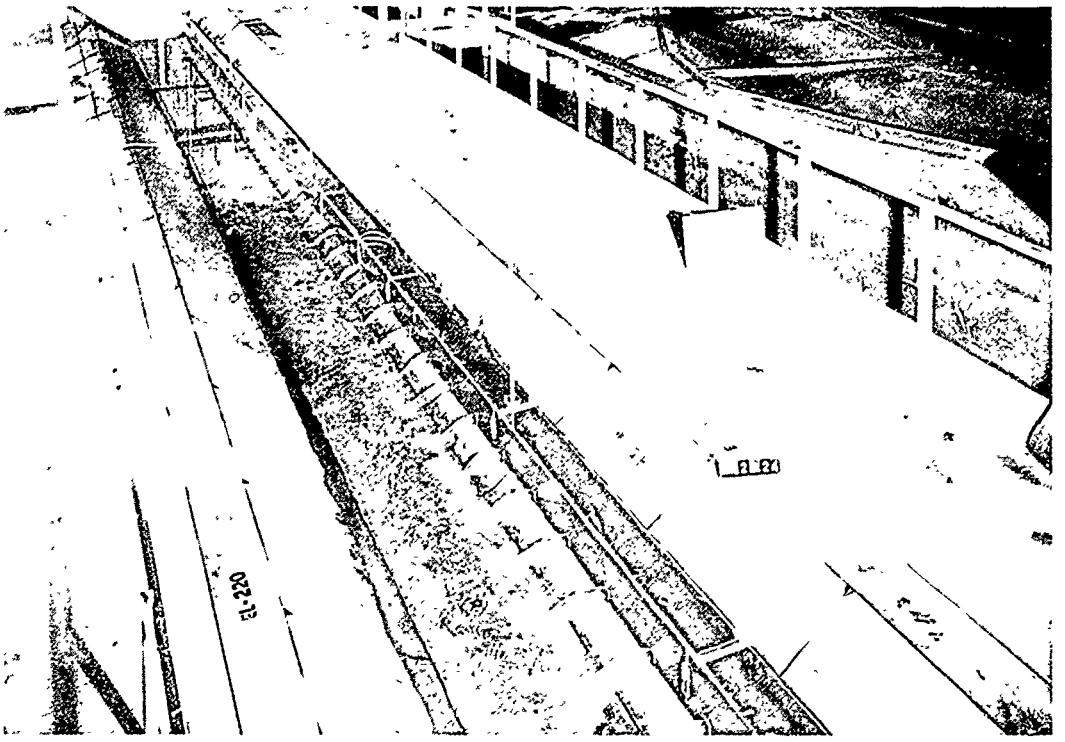

d. Reservoir water-surface el -280.0

Photo 12. (Sheet 2 of 4)

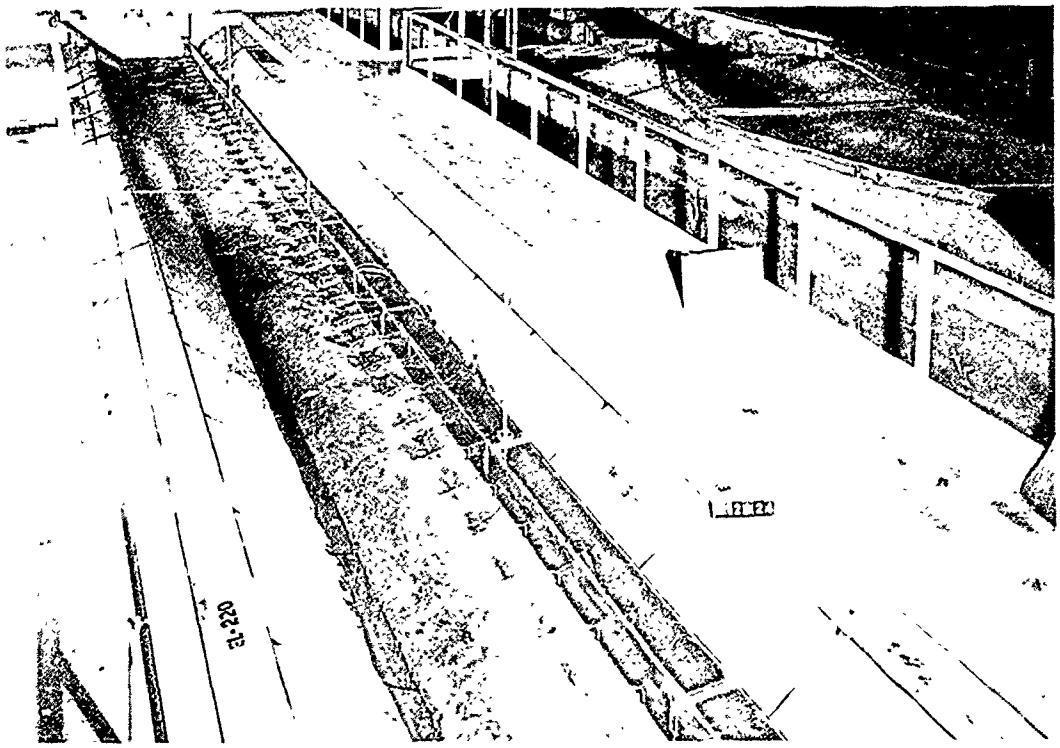

e. Reservoir water-surface el -275.0

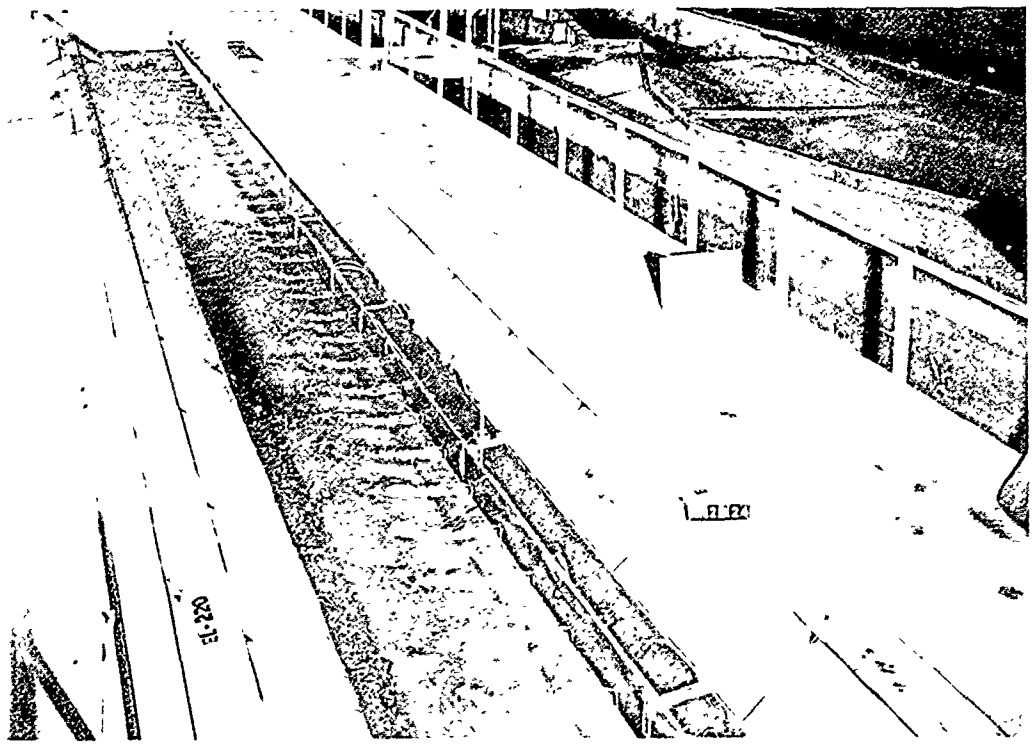

f. Reservoir water-surface el -265.0

Photo 12. (Sheet 3 of 4)

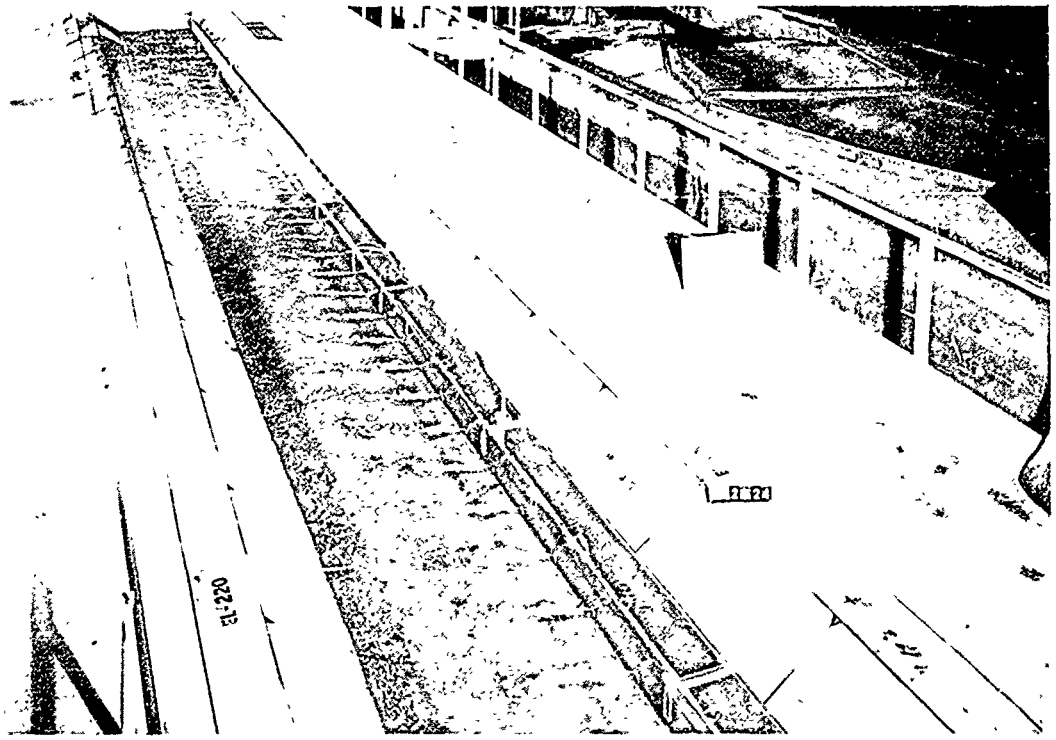

g. Reservoir water-surface el -261.0

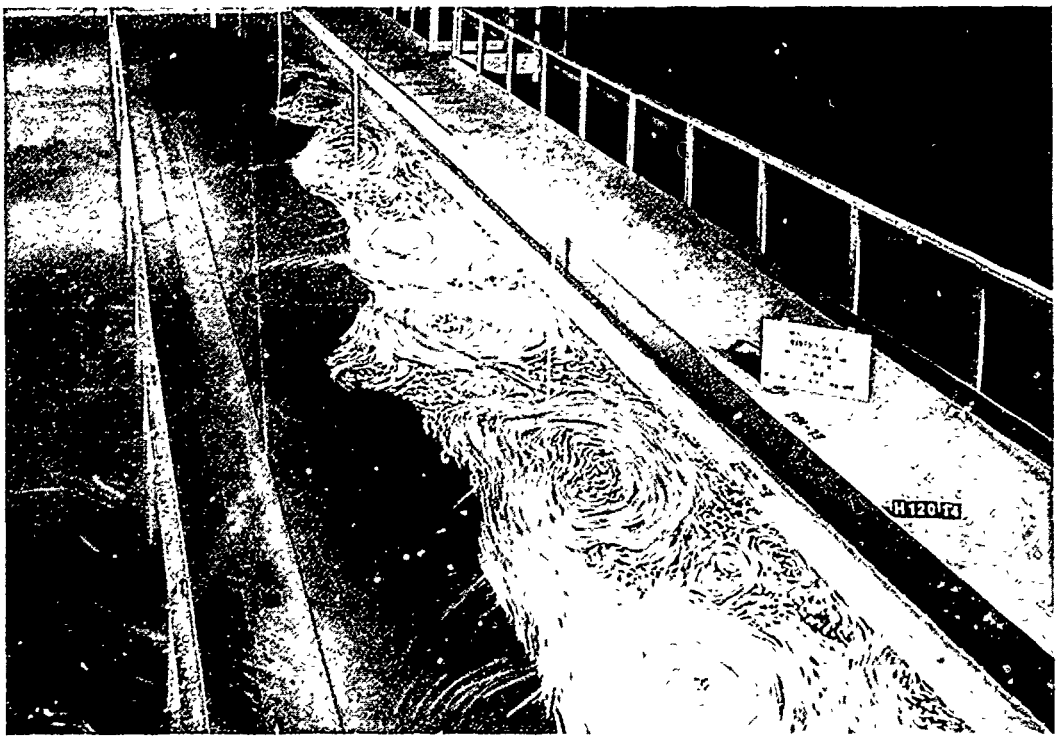

h. Reservoir water-surface el -195.0

Photo 12. (Sheet 4 of 4)

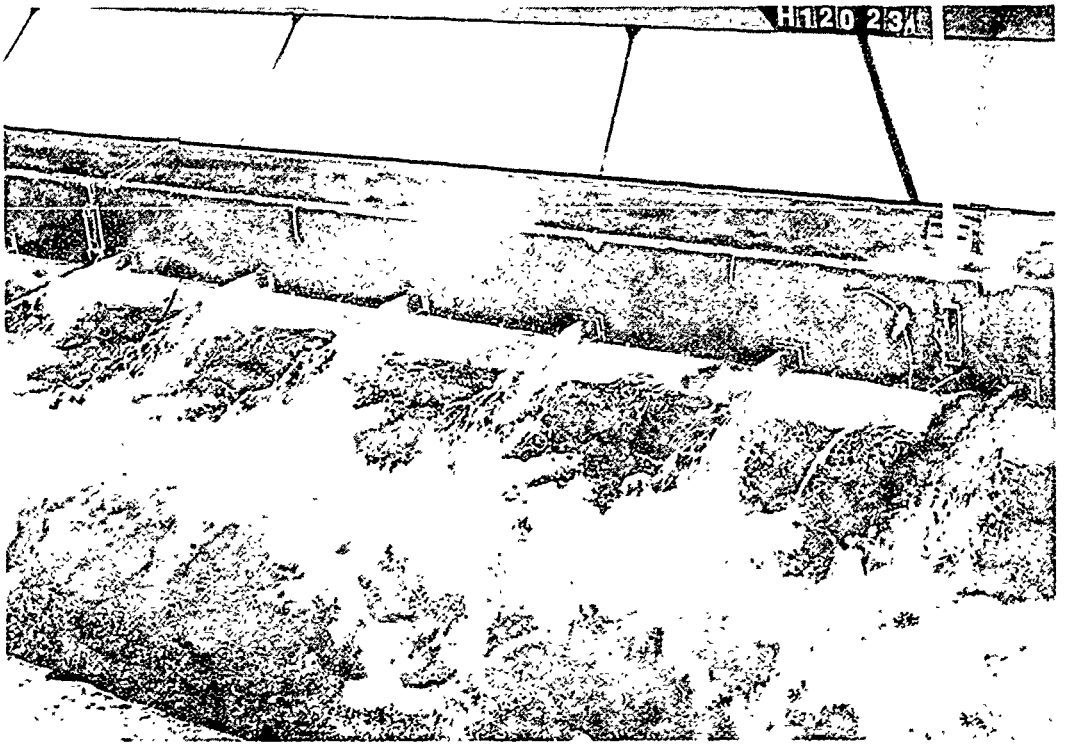

a. Reservoir water-surface el -275.0

b. Reservoir water-surface el -266.0

Photo 13. Flow conditions, outlet manifold; discharge 85,000 cfs; exposure time 20 sec (prototype) (Sheet 1 of 4)

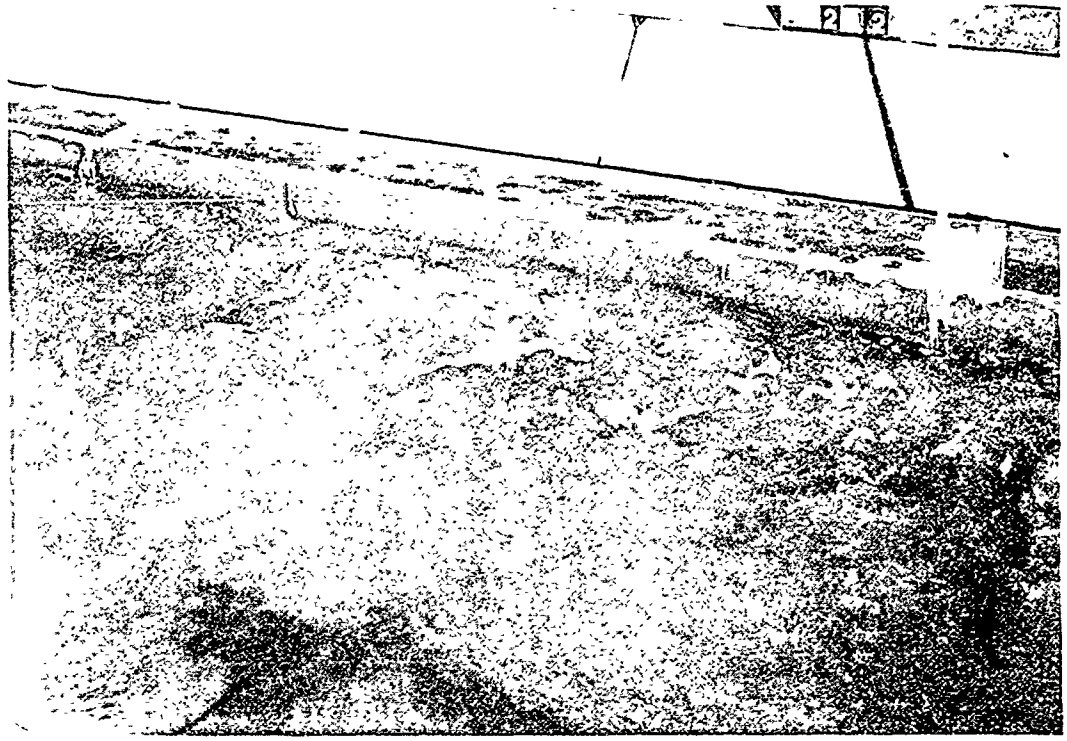

c. Reservoir water-surface el -253.0

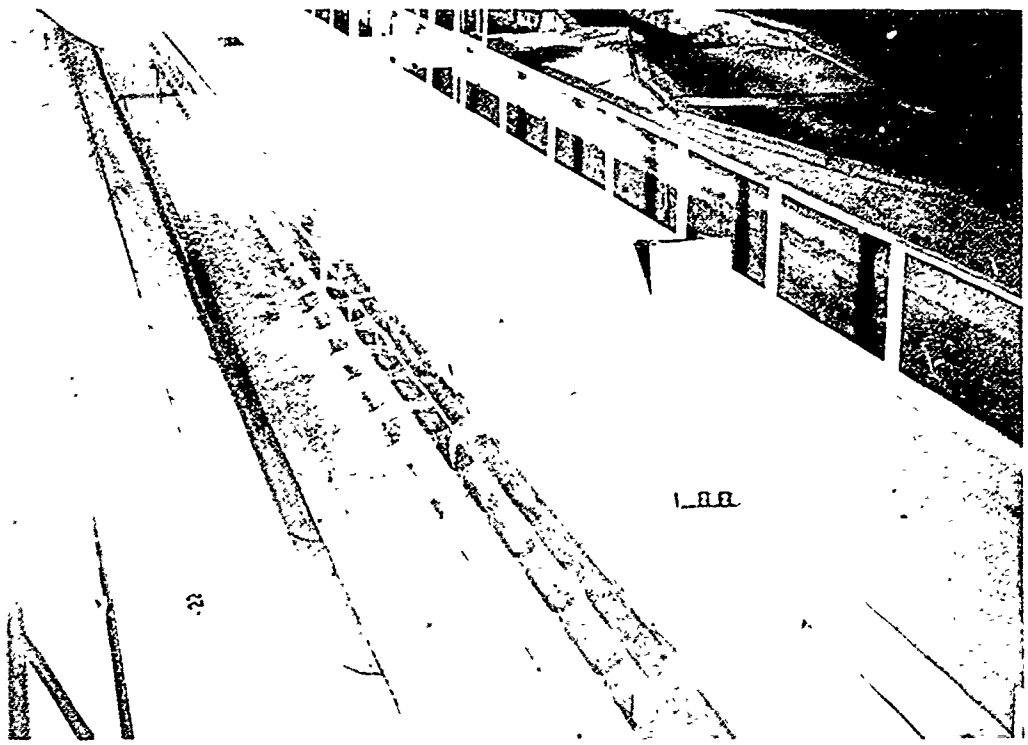

d. Reservoir water-surface el -280.0

Photo 13. (Sheet 2 of 4)

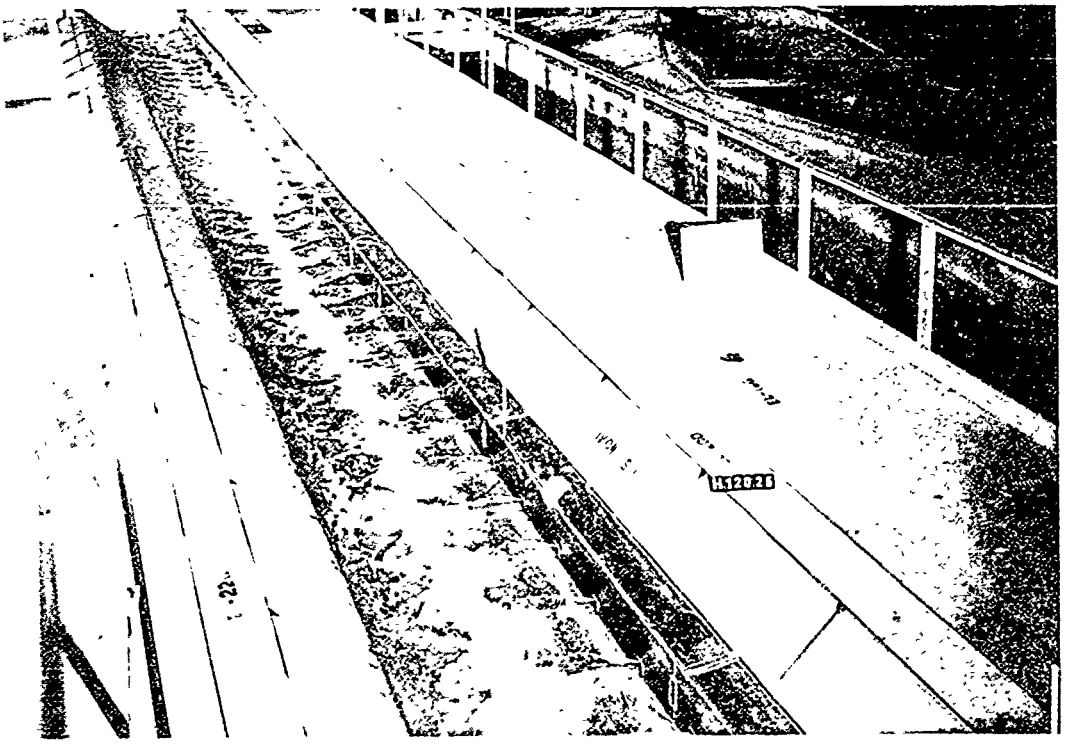

e. Reservoir water-surface el -275.0

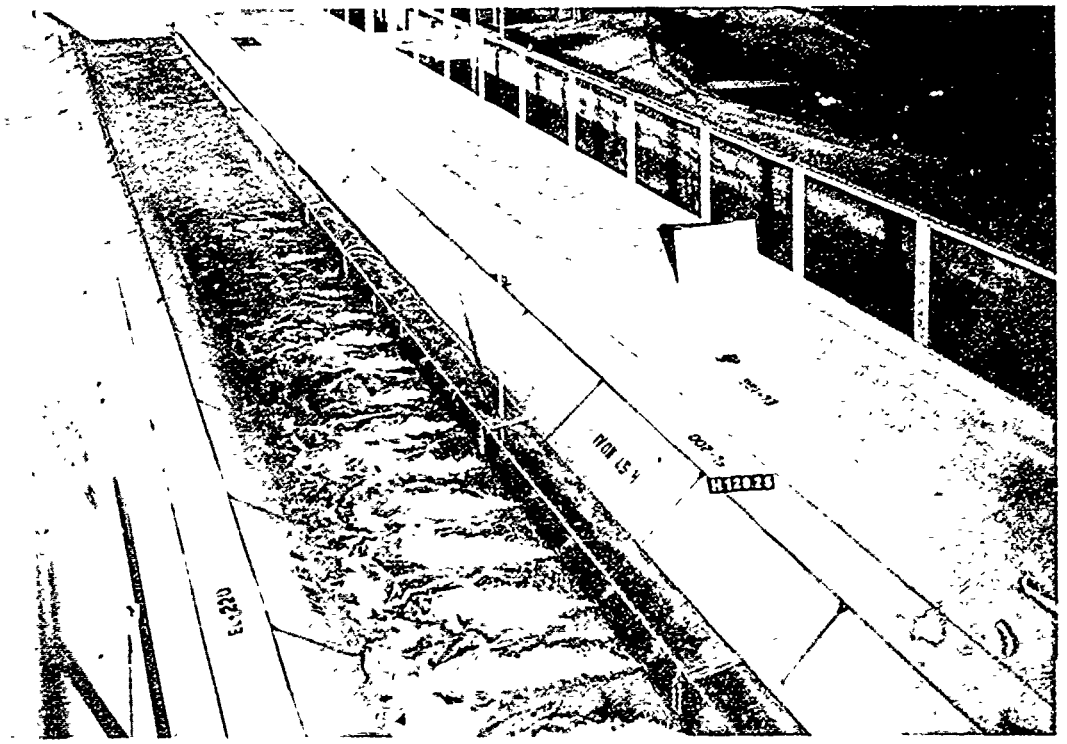

f. Reservoir water-surface el -260.0

Photo 13. (Sheet 3 of 4)

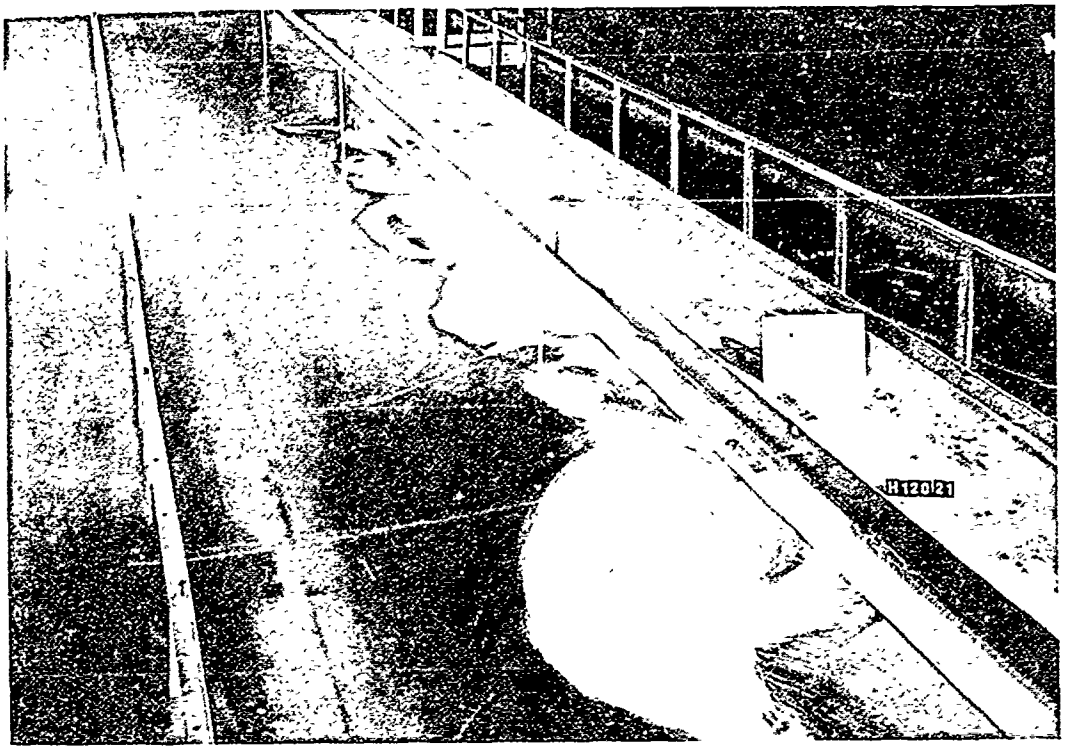

g. Reservoir water-surface el -190.0

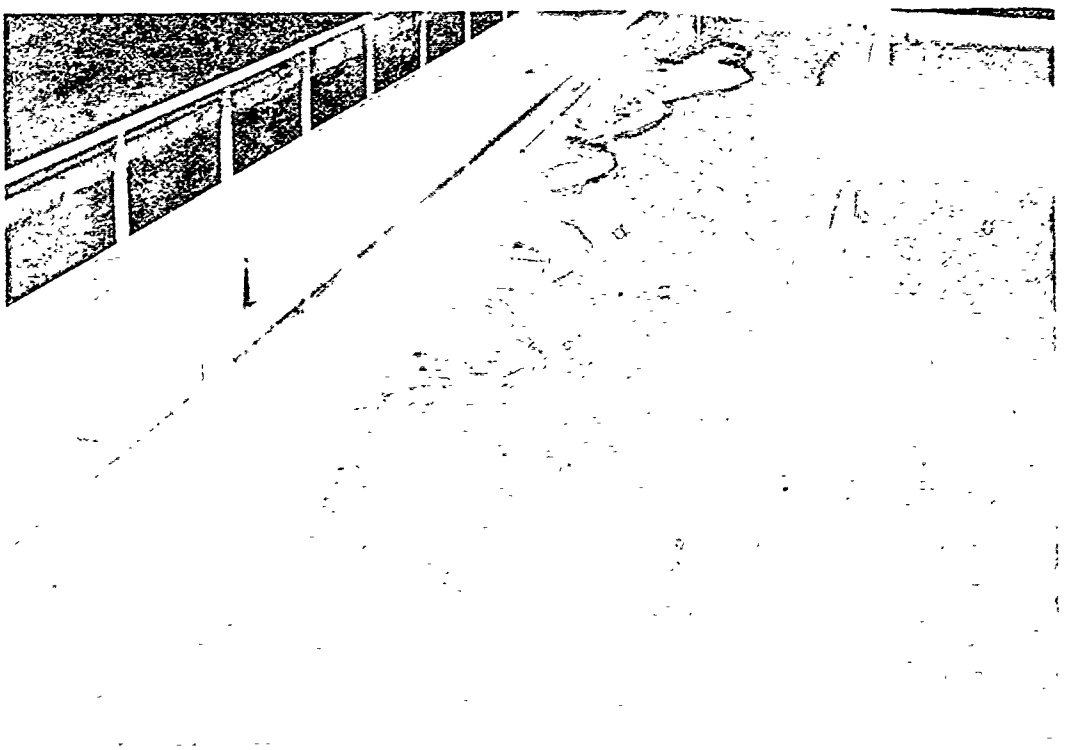

h. Reservoir water surface el -260.0

Photo 13. (Sheet 4 of 4)

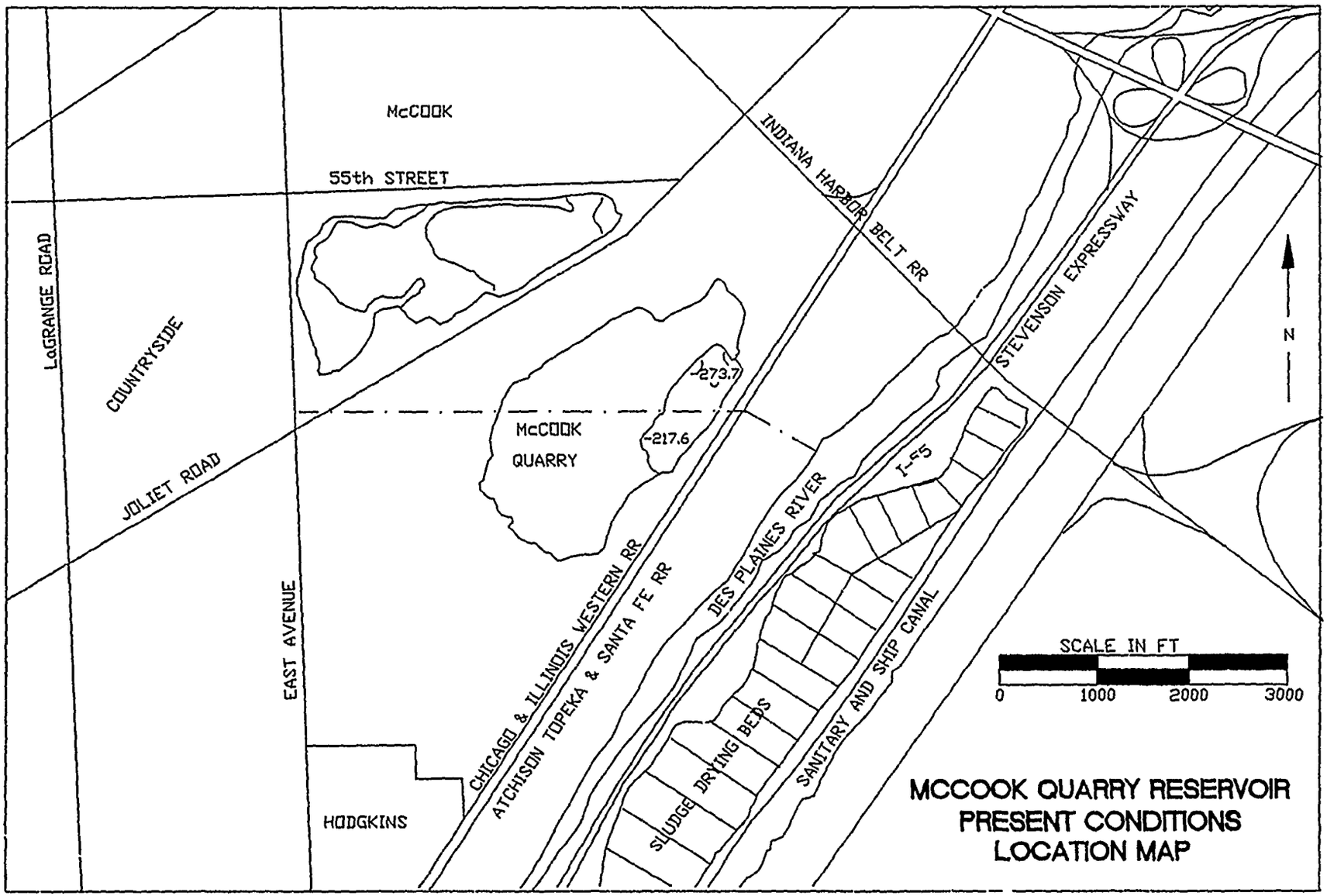

MCCOOK QUARRY RESERVOIR
PRESENT CONDITIONS
LOCATION MAP

PLATE 1

PLATE 2

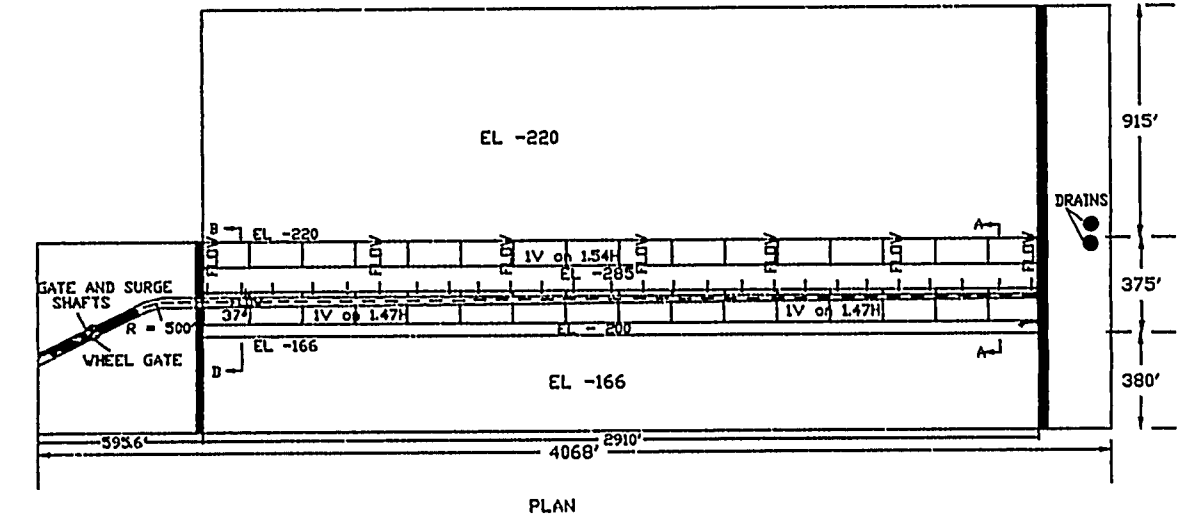

PLAN

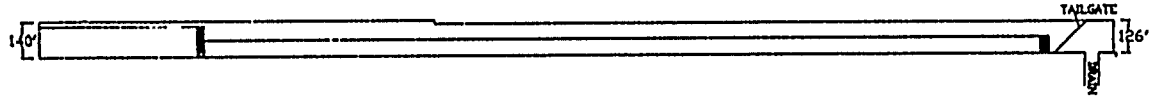

PROFILE

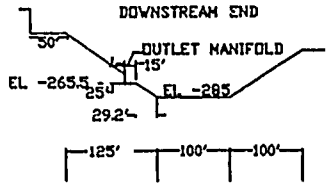

SECTION A-A

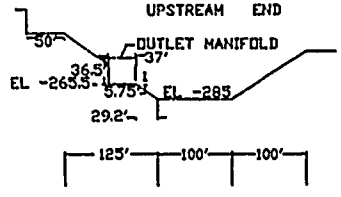

SECTION B-B

MCCOOK MANIFOLD

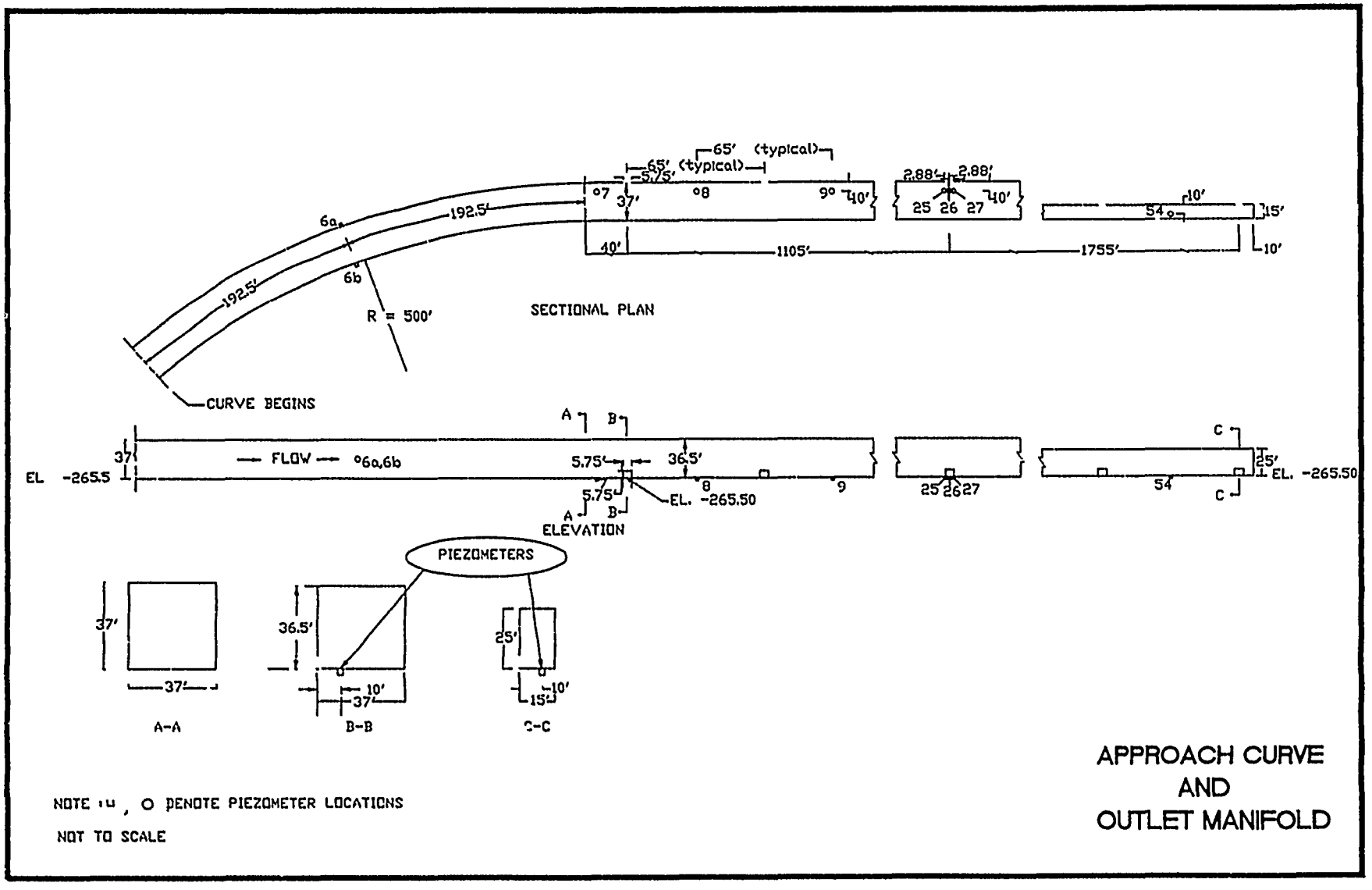
65' (typical)
65' (typical)
5.75'
2.88'
2.88'
10'
15'
10'
1105'
1755'
40'
40'
40'
37'
192.5'
192.5'
6a
6b
R = 500'
SECTIONAL PLAN
CURVE BEGINS
A
B
C
37'
FLOW
5.75'
36.5'
25'
EL. -265.5
EL. -265.50
5.75'
EL. -265.50
ELEVATION
PIEZOMETERS
37'
36.5'
25'
37'
10'
37'
15'
10'
A-A
B-B
C-C
NOTE : ⊔ , O DENOTE PIEZOMETER LOCATIONS
NOT TO SCALE
APPROACH CURVE
AND
OUTLET MANIFOLD

PLATE 3

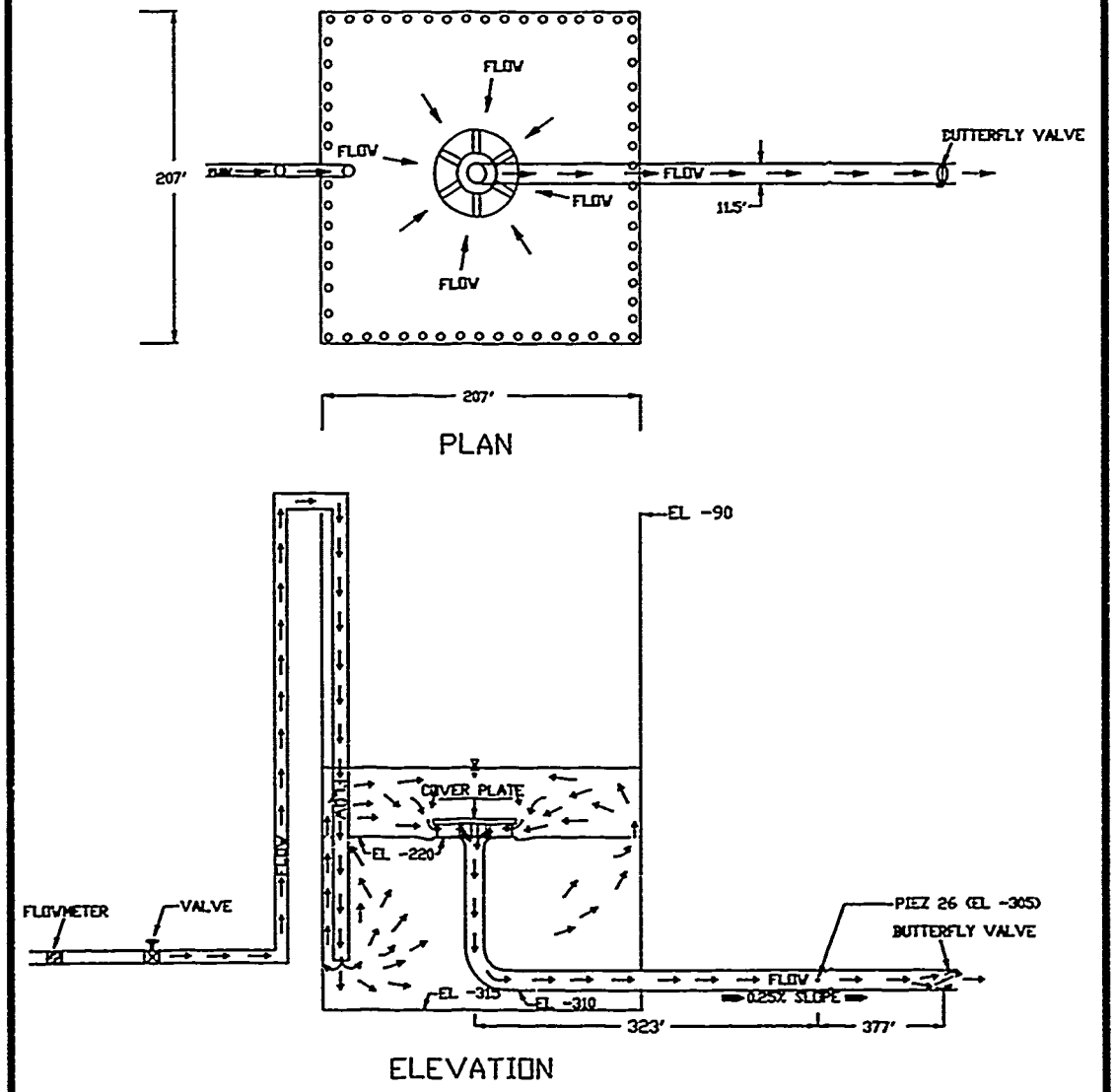

MORNING GLORY INTAKE
PLAN AND ELEVATION

PLATE 4

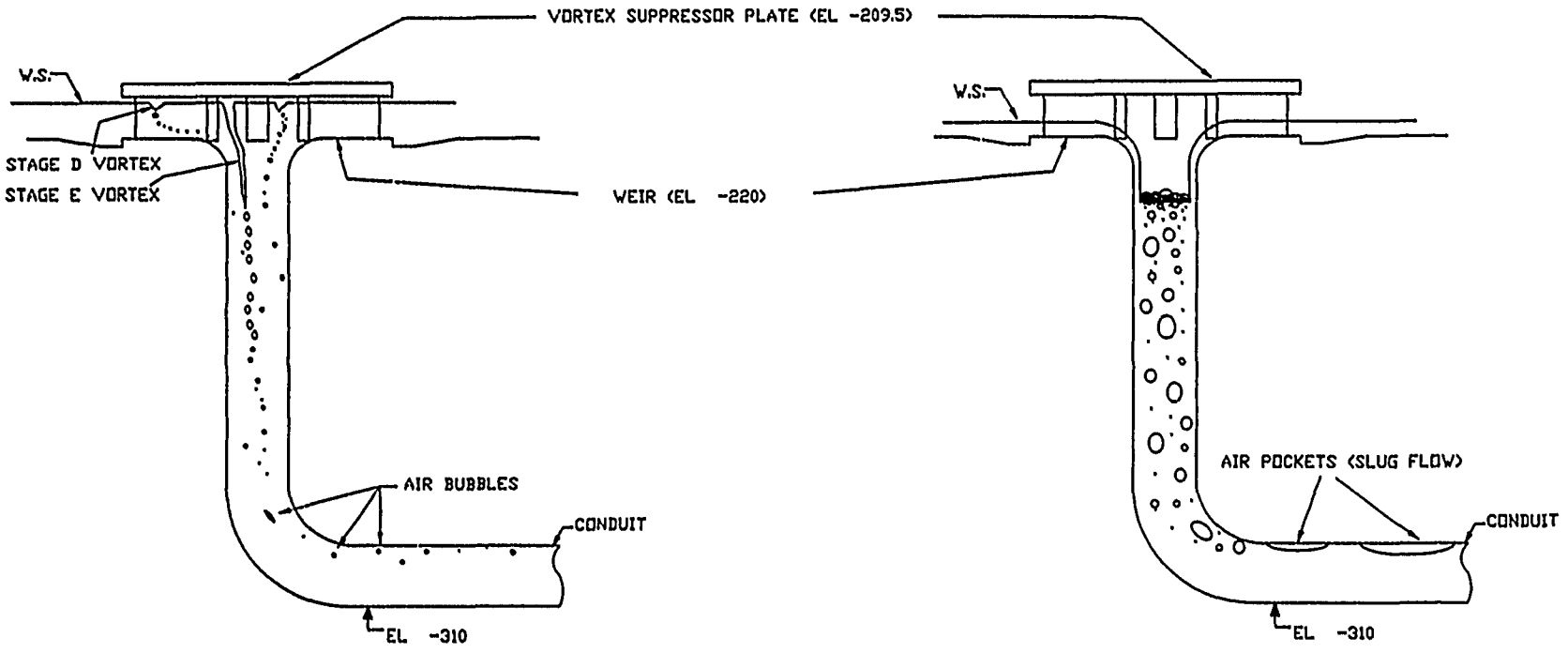

HYDRAULIC CHARACTERISTICS CONDUIT AND WEIR CONTROL

PLATE 5

PLATE 6

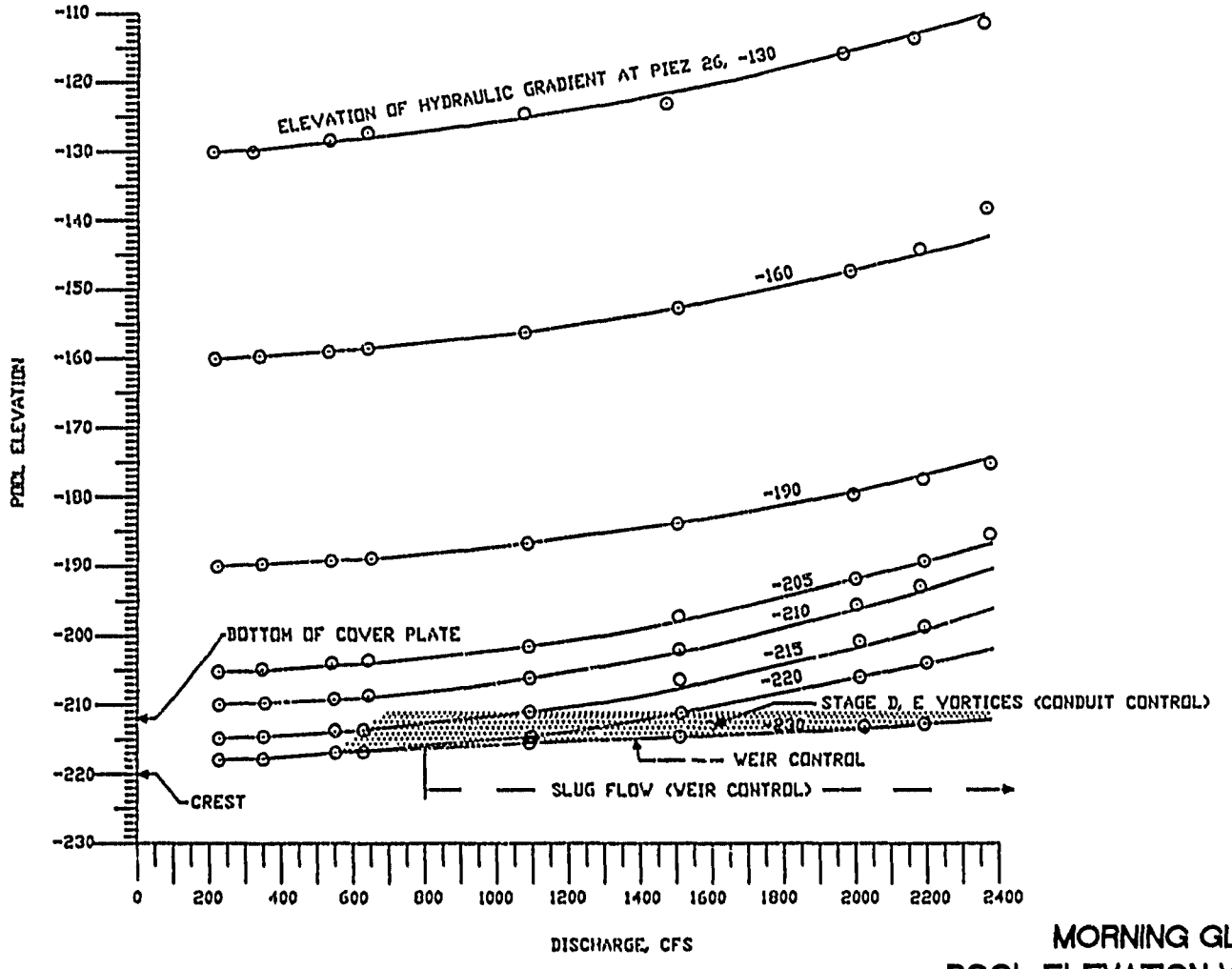

MORNING GLORY INTAKE
POOL ELEVATION VERSUS DISCHARGE

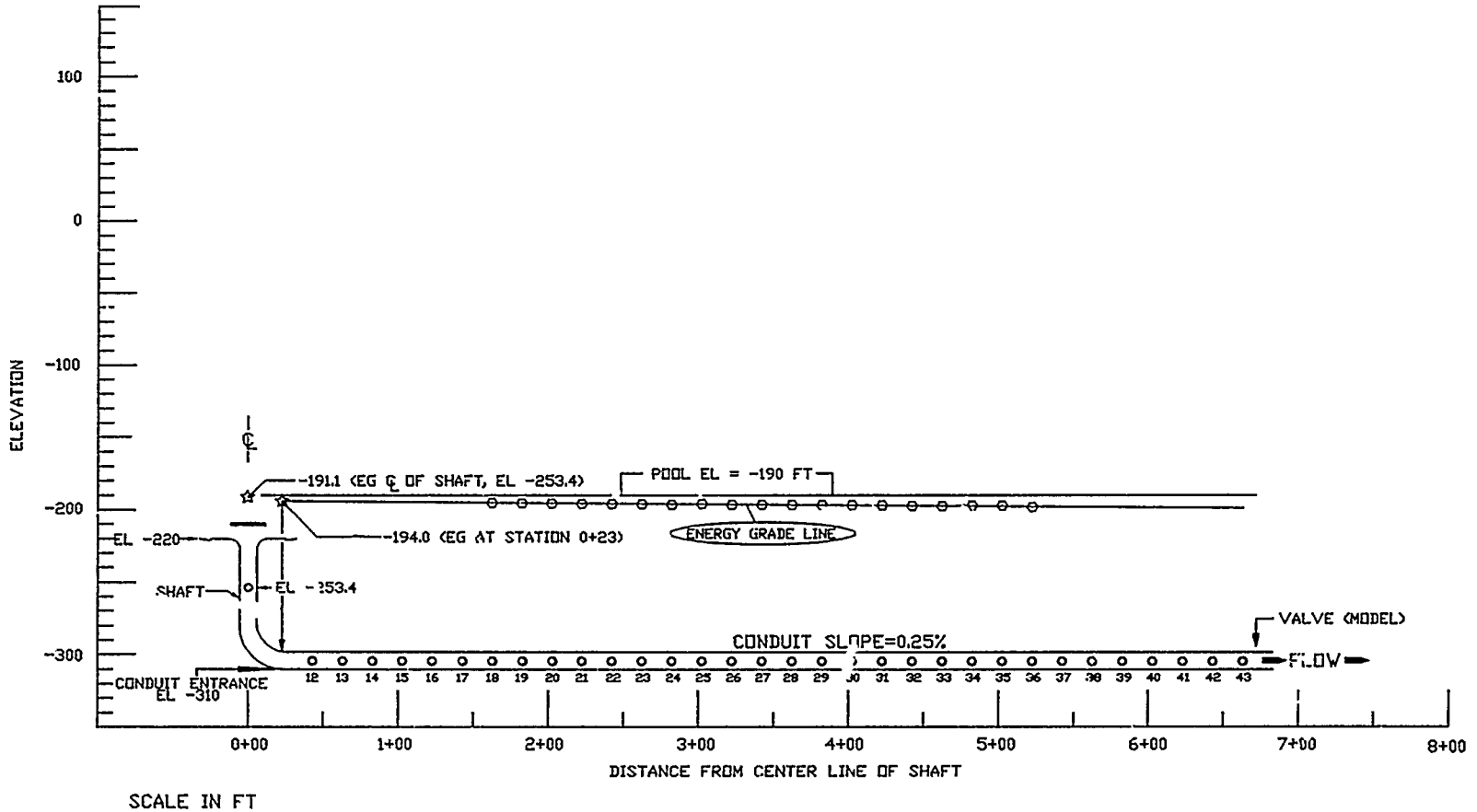

SCALE IN FT

0 80 160 240

o = PIEZOMETER TAP

NOTE: PIEZOMETERS 12 THROUGH 43 LOCATED ON 20-FT CENTERS
PIEZOMETERS ARE LOCATED ALONG CENTER-LINE ELEVATION OF CONDUIT

MORNING GLORY
ENERGY GRADIENT
DISCHARGE 2 000 CFS
POOL EL -190.0

PLATE 7

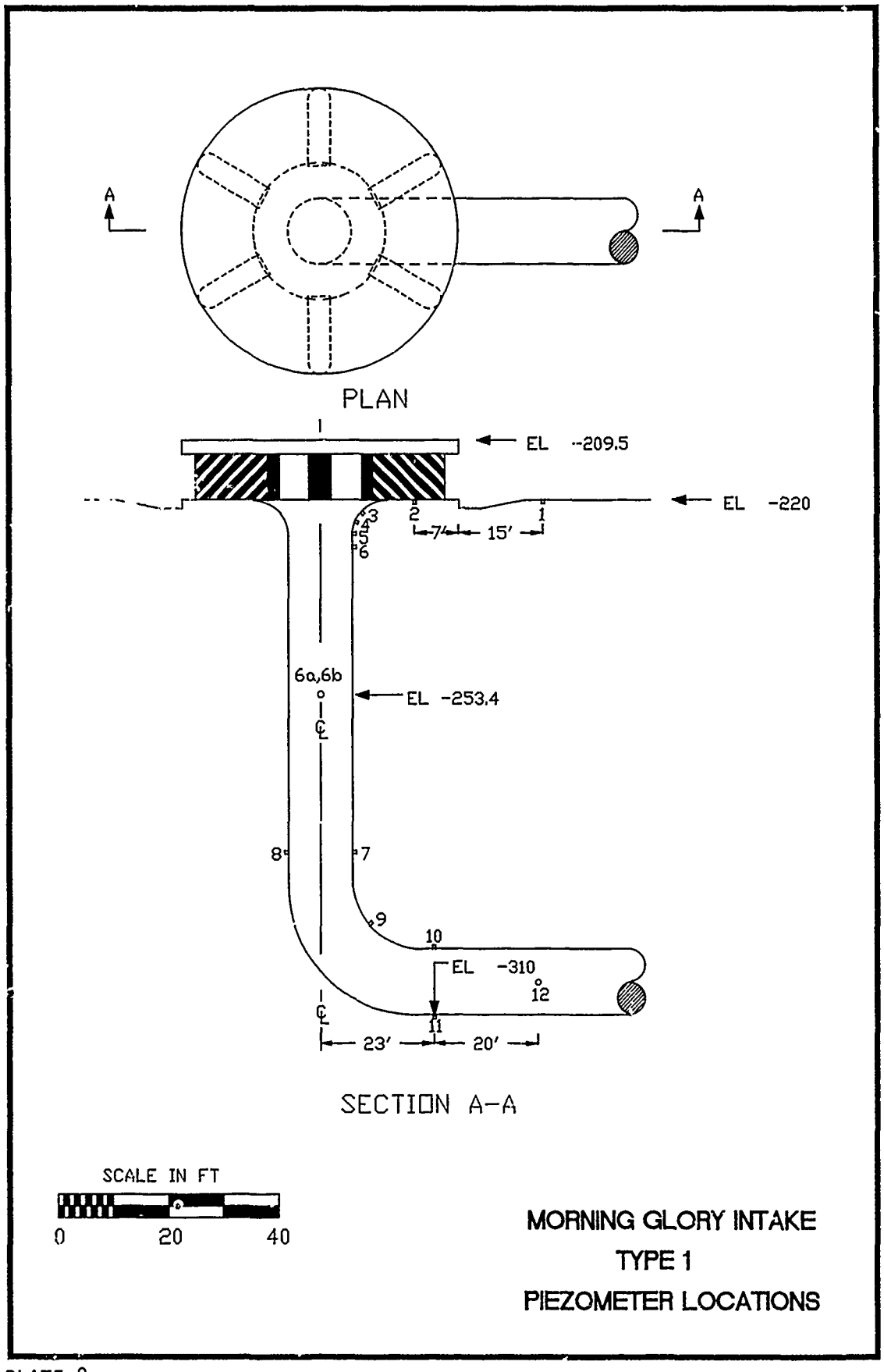

MORNING GLORY INTAKE
TYPE 1
PIEZOMETER LOCATIONS

PLATE 8

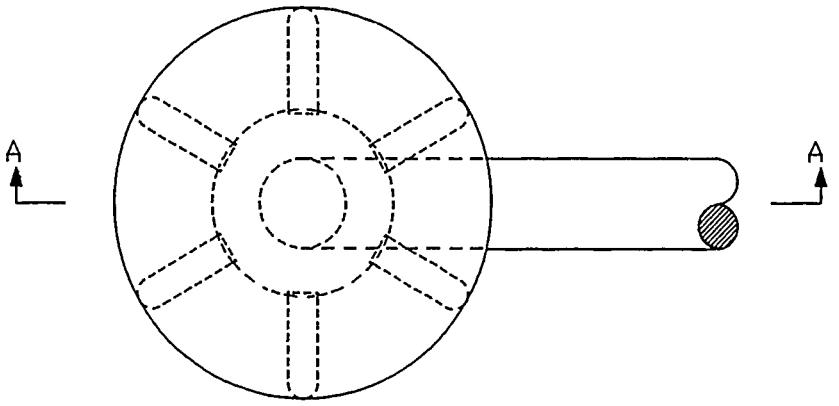

PLAN

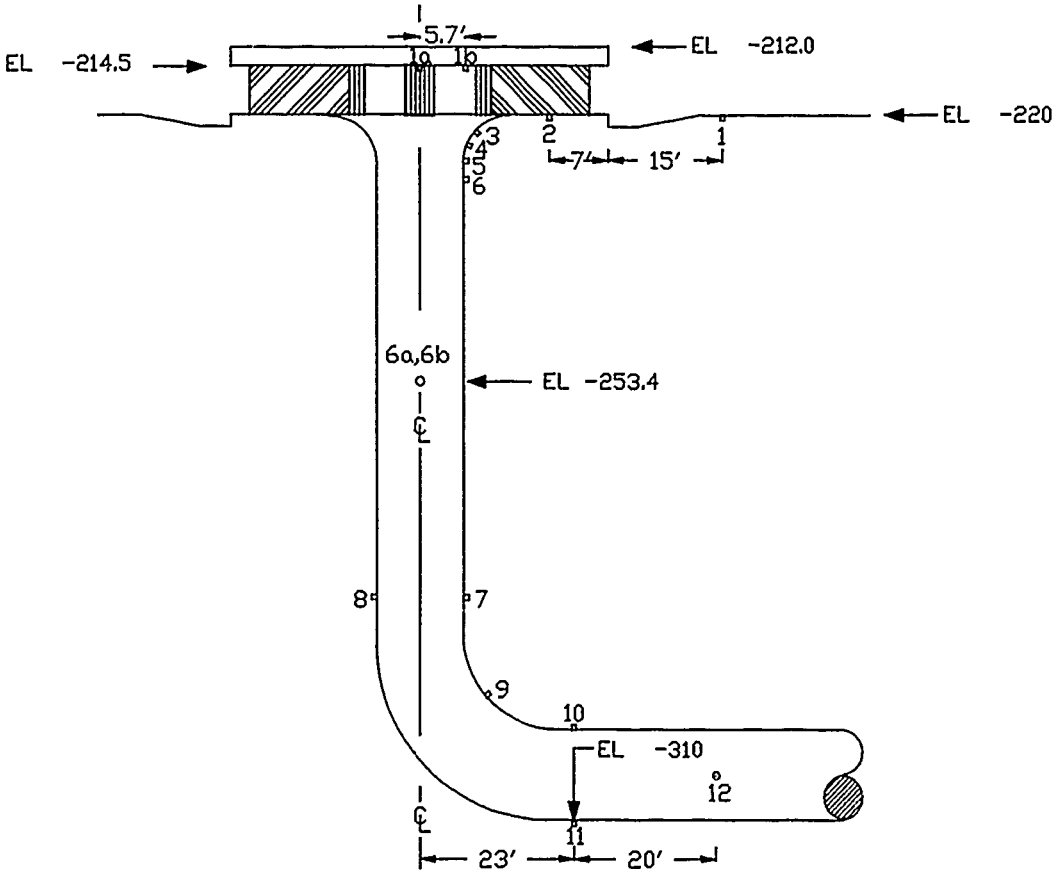

SECTION A-A

SCALE IN FT

0 20 40

MORNING GLORY INTAKE
TYPE 2
PIEZOMETER LOCATIONS
IN SHAFT AND ELBOW

PLATE 9

PLATE 10

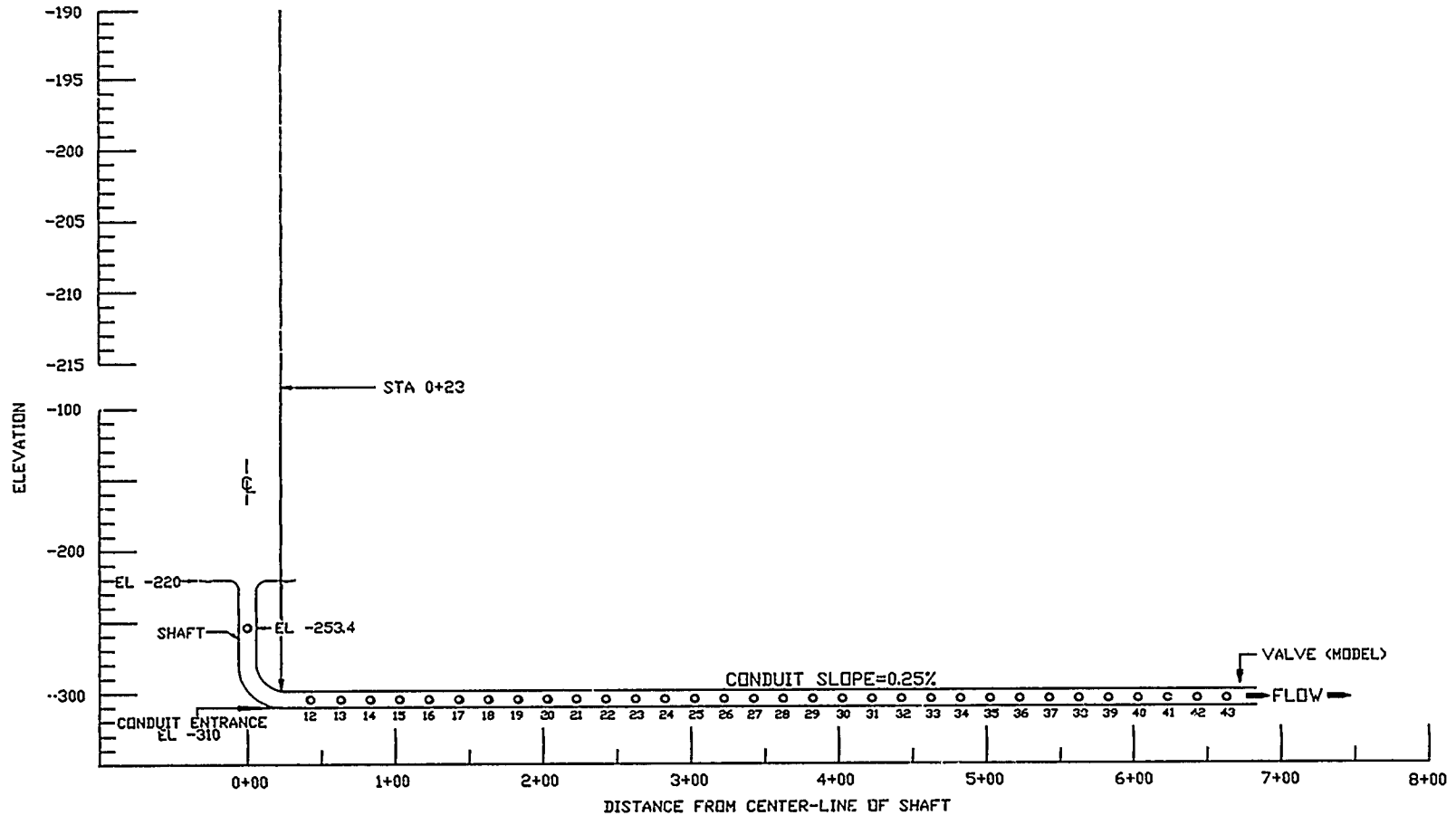

SCALE IN FT

0 80 160 240

o = PIEZOMETER TAP

NOTE: PIEZOMETERS 12 THROUGH 43 LOCATED ON 20 FT CENTERS
PIEZOMETERS ARE LOCATED ALONG CENTER-LINE ELEVATION OF CONDUIT

MORNING GLORY INTAKE PIEZOMETER LOCATIONS IN CONDUIT TYPE 2

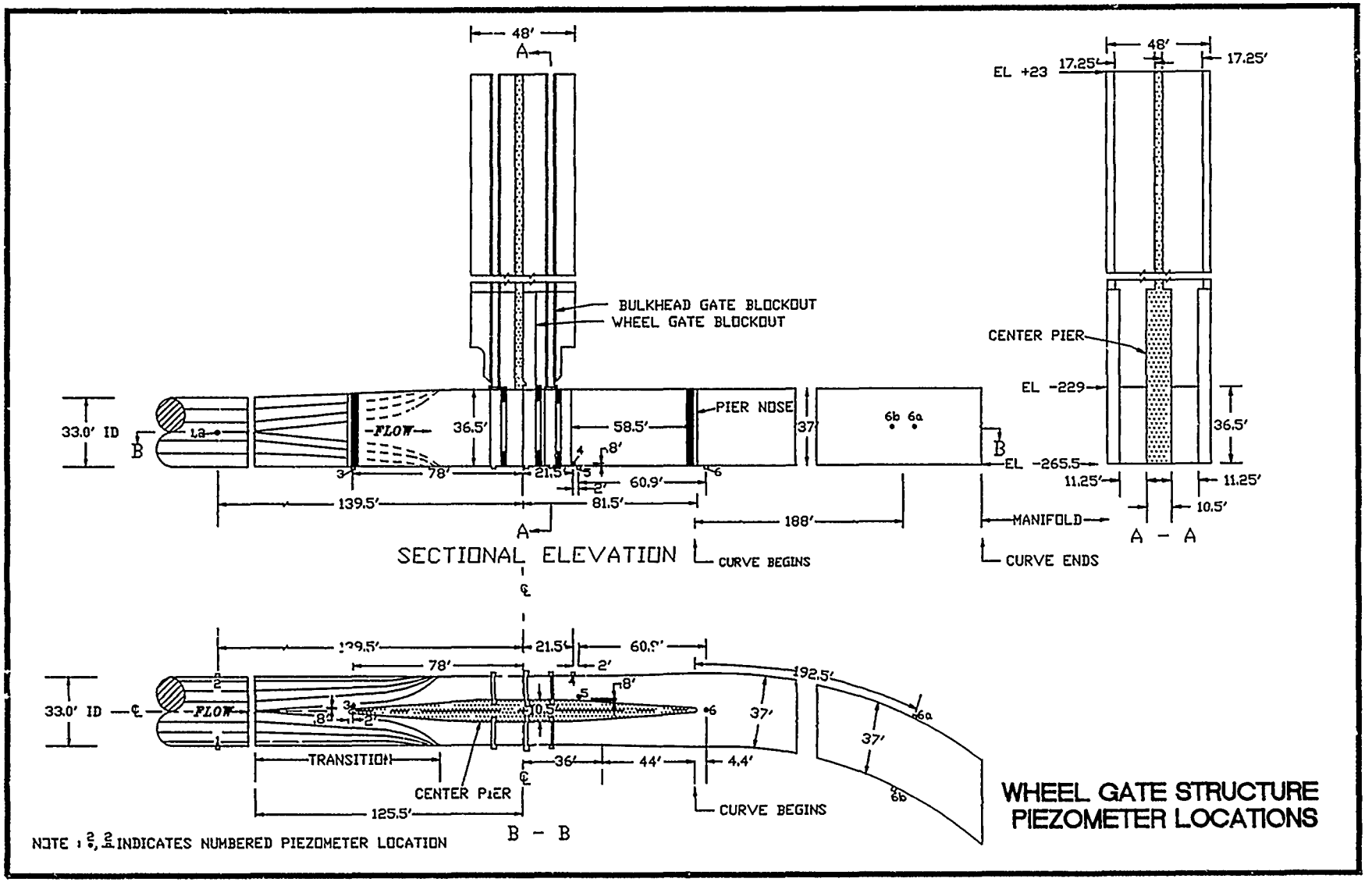

WHEEL GATE STRUCTURE PIEZOMETER LOCATIONS

PLATE 11

PLATE 12

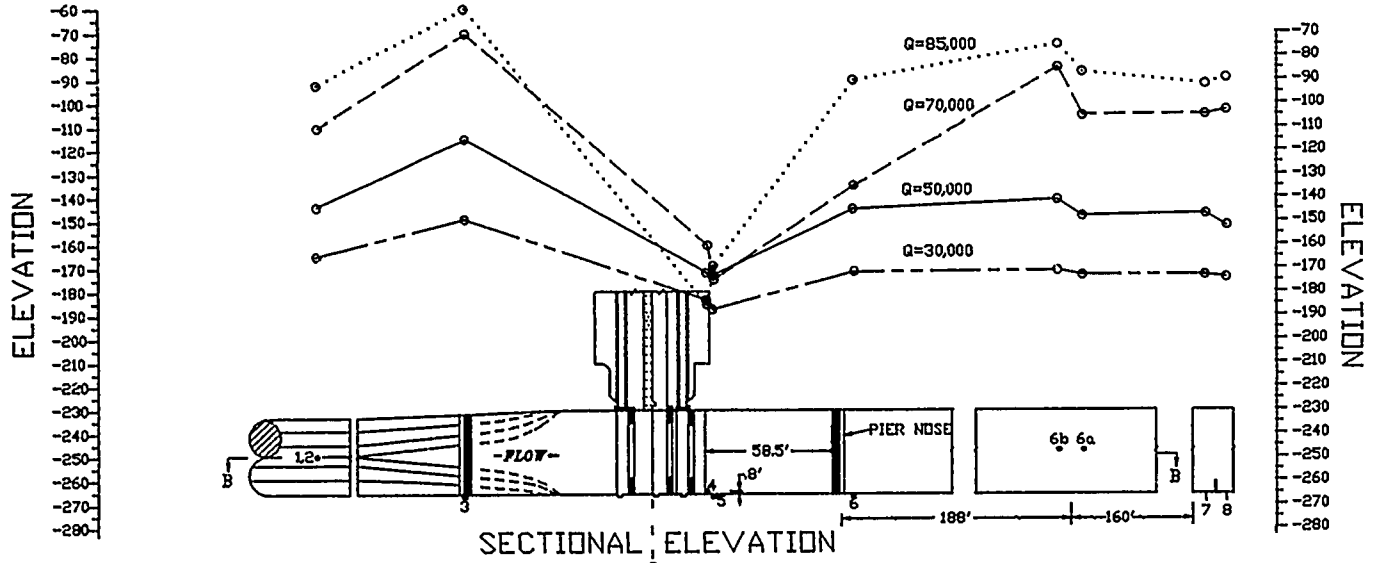

NOTE : ⊙ INDICATES NUMBERED PIEZOMETER LOCATION

WHEEL GATE STRUCTURE
HYDRAULIC GRADIENTS
RESERVOIR WATER-SURFACE EL -190.0

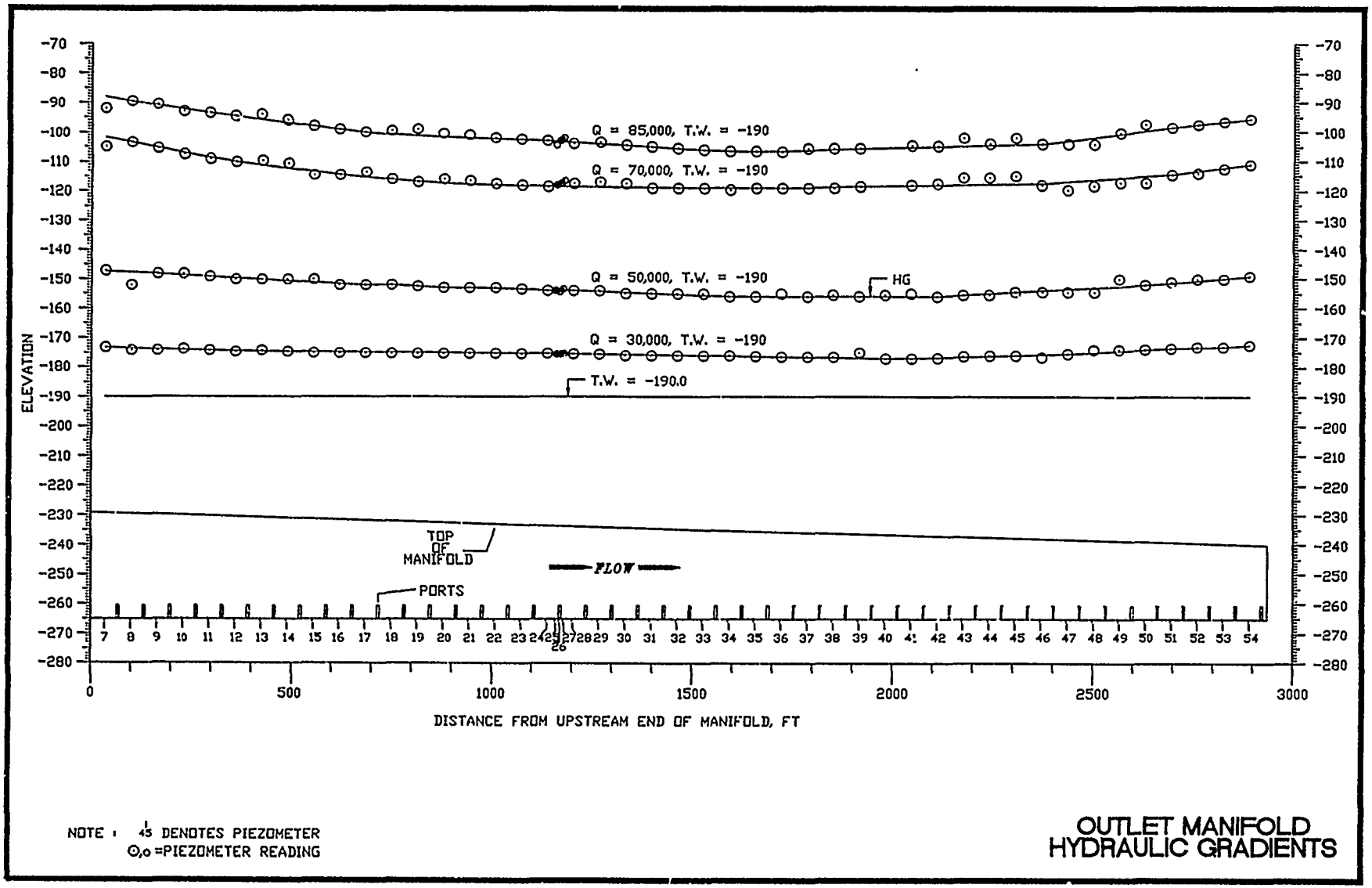

OUTLET MANIFOLD HYDRAULIC GRADIENTS

PLATE 13

PLATE 14

V_e =36.5 FT/SEC, $\frac{V_e^2}{2g}$ = 20.7'

H_e = −190 − −126.3 = 63.7'

$K_e = \frac{H_e}{\frac{V_e^2}{2g}} = \frac{63.7'}{20.7'} = 3.08$

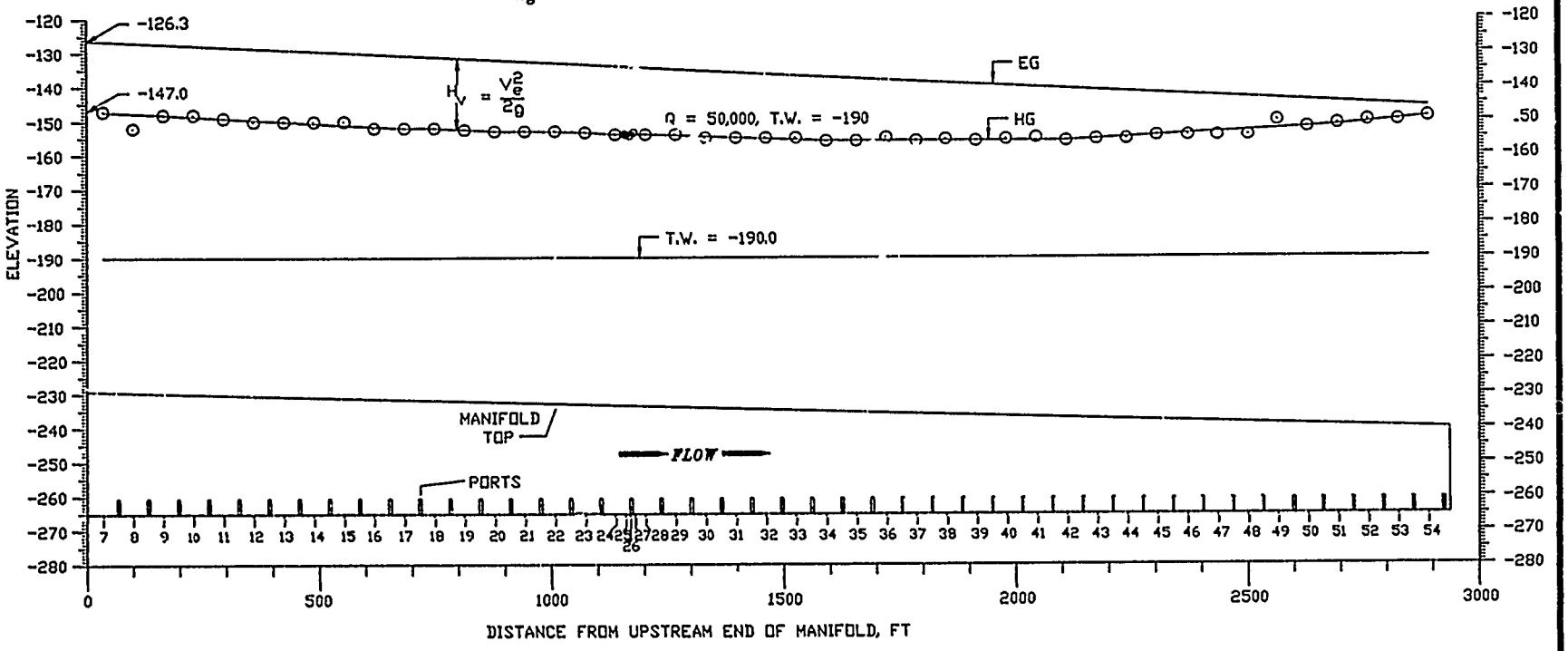

NOTE : $\frac{1}{45}$ DENOTES PIEZOMETER
O,o =PIEZOMETER READING

OUTLET MANIFOLD ENERGY AND HYDRAULIC GRADIENTS

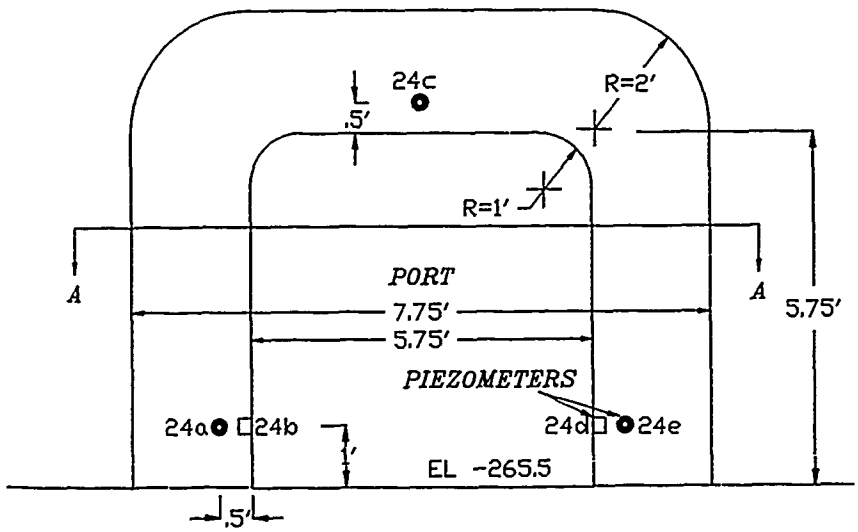

ELEVATION

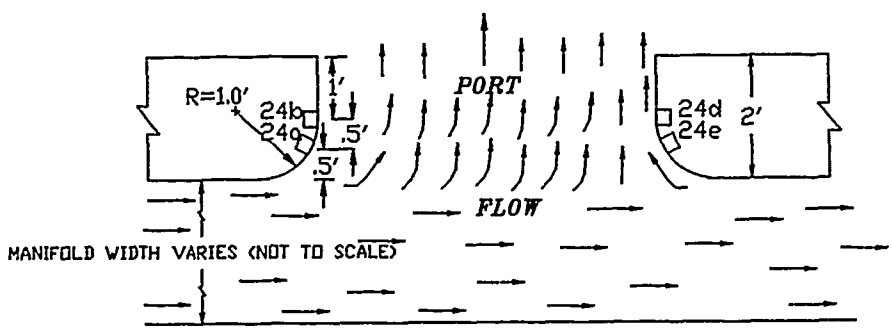

SECTION A – A

HYDRAULIC PRESSURES

		DISCHARGE							
		30,000 CFS		50,000 CFS		70,000 CFS		85,000 CFS	
PIEZOMETER NUMBER	PIEZOMETER ELEVATION	HYDRAULIC GRADIENT ELEVATION	PRESSURE FT	HYDRAULIC GRADIENT ELEVATION	PRESSURE FT	HYDRAULIC GRADIENT ELEVATION	PRESSURE FT	HYDRAULIC GRADIENT ELEVATION	PRESSURE FT
24a	-264.5	-187.8	76.7	-188.5	76.0	-190.8	73.7	-189.5	75.0
24b	-264.5	-187.8	76.7	-188.5	76.0	-190.9	73.6	-189.5	75.0
24c	-259.25	-187.0	72.25	-187.0	72.25	-194.5	64.75	-187.5	71.75
24d	-264.5	-170.8	93.7	-151.0	113.5	-96.0	168.5	-65.5	199.0
24e	-264.5	-167.0	97.5	-138.5	126.0	-87.0	177.5	-45.5	219.0

HYDRAULIC PRESSURES
MANIFOLD PORT 18

PIEZOMETERS 24a THROUGH 24e
RESERVOIR WATER-SURFACE EL -190

PLATE 16

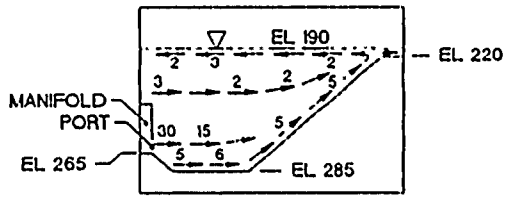

SECTION A-A

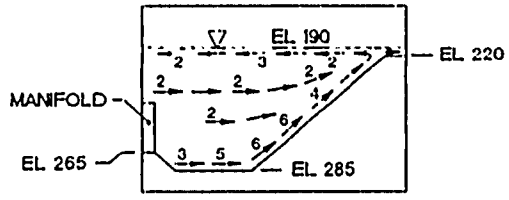

SECTION B-B

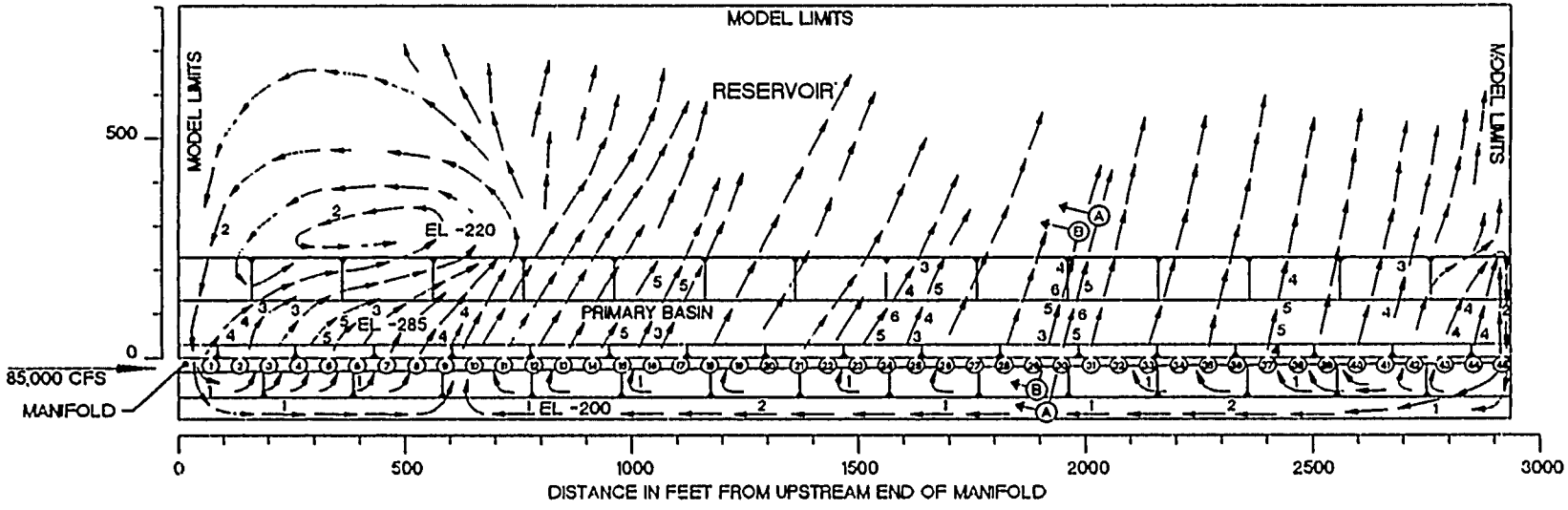

PLAN

NOTE:
- 6 MAGNITUDE OF VELOCITY, FT/SEC
- (30) LOCATION AND NUMBER OF PORT
- VELOCITIES MEASURED 2 FT ABOVE BOTTOM IN PLAN VIEW
- VELOCITIES IN SECTIONS A-A AND B-B WERE MEASURED IN PLANES PARALLEL TO FLOW EXITING PORT NO. 30. SECTION A-A IS A PLANE LOCATED IN THE CENTER OF FLOW. SECTION B-B IS A PLANE LOCATED BETWEEN FLOWS EXITING PORTS 29 AND 30.

MANIFOLD OUTLET VELOCITIES

DISCHARGE 30,000 CFS
WATER SURFACE EL -190.0

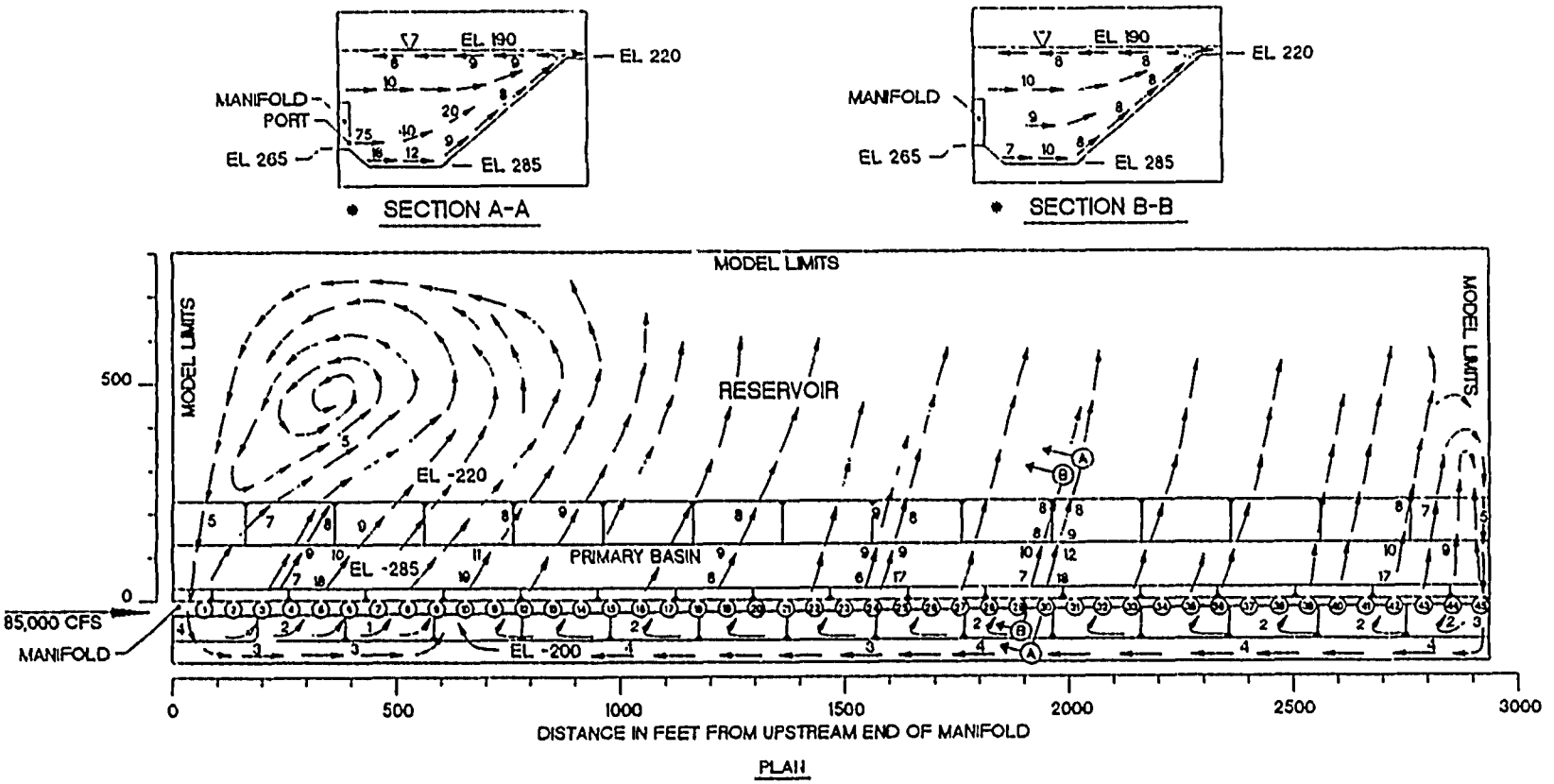

NOTE:
- 6 MAGNITUDE OF VELOCITY, FT/SEC
- (30) LOCATION AND NUMBER OF PORT
- VELOCITIES MEASURED 2 FT ABOVE BOTTOM IN PLAN VIEW
- VELOCITIES IN SECTIONS A-A AND B-B WERE MEASURED IN PLANES PARALLEL TO FLOW EXITING PORT NO. 30. SECTION A-A IS A PLANE LOCATED IN THE CENTER OF FLOW. SECTION B-B IS A PLANE LOCATED BETWEEN FLOWS EXITING PORTS 29 AND 30

MANIFOLD OUTLET VELOCITIES

DISCHARGE 85,000 CFS
WATER SURFACE EL -190.0

PLATE 17